LIFE-CYCLE COST ANALYSIS AND PROBABILISTIC COST ESTIMATING IN ENGINEERING DESIGN USING AN AIR DUCT DESIGN CASE STUDY

A Thesis Submitted to the College of

Graduate Studies and Research

in Partial Fulfillment of the Requirements

for the Degree of Doctor of Philosophy

in the Department of Mechanical Engineering

University of Saskatchewan

Saskatoon

By

Yaw Asiedu

Spring 2000

Permission to Use

In presenting this thesis in partial fulfillment of the requirements for the Degree of Doctor of Philosophy from the University of Saskatchewan, I agree that the Libraries of this University may make it freely available for inspection. I further agree that permission for copying of this thesis in any manner, in whole or in part, for scholarly purposes may be granted by my supervisors, Professors Robert W. Besant and Peihua Gu, the Head of the Department of Mechanical Engineering, or the Dean of the College of Engineering. It is understood that any copying, publication or use of this thesis or parts thereof for financial gain shall not be allowed without my written permission. It is also understood that due recognition shall be given to me and to the University of Saskatchewan in any scholarly use which may be made of any material in my thesis.

Requests for permission to copy or to make other use of material in this thesis in whole or part should be addressed to:

Head of the Department of Mechanical Engineering

University of Saskatchewan

57 Campus Drive

Saskatoon, Saskatchewan

S7N 5A9

Abstract

Although the issue of uncertainties in cost model parameters has been recognized as an important aspect of life-cycle cost analysis, it is often ignored or not well treated in cost estimating. A simulation approach employing kernel estimation techniques and their asymptotic properties in the development of the probability distribution functions (PDFs) of cost estimates is proposed. This eliminates the guess work inherent in current simulation based cost estimating procedures, reduces the amount of data sampled and makes it easier to specify the accuracy desired in the estimated distribution.

Building energy costs can be reduced considerably if air duct systems are designed for the least life-cycle cost. The IPS-Method, a simple approach to HVAC air duct design is suggested. The Diameter and Enhanced Friction Charts are also developed. These are charts that implicitly incorporate the LCC and are better than the existing Friction Chart for the selection of duct sizes. Through illustrative examples, the ease and effectiveness of these are demonstrated.

For more complex designs, a Segregated Genetic Algorithm (SGA) is recommend. A sample problem with variable time-of-day operating conditions and utility rates is used to illustrate its capabilities. The results are compared to those obtained using weighted average flow rates and utility rates to show the life-cycle cost savings possible by using this approach. Although life-cycle cost savings may be only between 0.4% and 8.3% for some simple designs, much larger savings may occur with more complex designs and operating constraints. The SGA is combined with probabilistic cost estimating to optimize HVAC air duct systems with uncertainties in the model parameters. The

designs based on the SGA method tended to be less sensitive to typical variations in the component physical parameters and, therefore, are expected to result in lower balancing and operating costs.

Acknowledgments

My sincere thanks to Professors R. W. Besant and P. Gu for their invaluable guidance during the course of my studies without which this work would not have been possible. I also wish to express my appreciation to the members of my advisory committee, Dr.R. Burton, Dr. R. Billinton, Dr. W. Szyszkowski and the external examiner Dr. D. Strong, for their comments and suggestions.

Financial support from the Natural Sciences and Engineering Research Council of Canada (NSERC) and Atomic Energy Canada Limited (AECL) is also acknowledged and appreciated.

Dedication

Dedicated to my family: Dad, B.B., Sister, Afua Frema, Brothers;

Amagyei, Baffour, Wiredu, and Nana Yaw and more importantly,

to the memory of my Mom, Amma Asomanin.

Thanks for being there for me.

Table of Contents

List of Tables

List of Figures

List of Notations

Acronyms

ABC	Activity Based Costing
ASHRAE	American Society of Heating Refrigerating and Air-Conditioning Engineers
CER	Cost Estimating Relationship
EDF	Empirical distribution function
GA	Genetic Algorithm
HVAC	Heating Ventilating and Air-Conditioning
LCC	Life-Cycle Cost
pdf	Probability density function
PDF	Probability distribution function
PWEF	Present worth escalation factor
SGA	Segregated Genetic Algorithm

English Symbols

A_i	Area of duct connected to section ι of fitting; $\iota = b, s, c$ (b: branch; s: straight; c: common) (m^2)
B_{y_k}	Bias limit of parameter y_k
B_Y	Total absolute bias
C	CER with dependent and/or independent parameters
C'	CER with only independent parameters
$\sum C$	Summation of dynamic friction loss coefficients for duct fittings

d_x	Size of duct section x (m)
d_x^{max}	Maximum allowable size for duct section x (m)
d_x^{min}	Minimum allowable size for duct section x (m)
D	Duct diameter (m)
D_c	Equivalent by cost diameter (m)
D_e	Equivalent circular duct of a rectangular duct (m)
D_h	Hydraulic diameter (m)
D_v	Equivalent-by-velocity diameter (m)
$\lceil D \rceil$	Smallest standard duct size $>D$ (m)
$\lfloor D \rfloor$	Largest standard duct size $<D$ (m)
E	Present worth owning and operating cost -LCC ($)
E_c	Unit electrical energy cost (cost/kWh)
$E_{c,g}$	Unit electrical energy cost in operation mode g (cost/kWh)
E_d	Energy demand cost (cost/kW)
E_p	First year energy cost ($)
E_s	Initial Cost ($)
f	Friction factor
f_C	Frictional factor of circular duct
f_R	Frictional factor of a rectangular duct
$f(x)$	Probability density function
$F(x)$	Probability distribution function
$F^{-1}(p)$	Inverse probability distribution function

$\hat{F}_n(x)$	Kernel distribution function
FF	Fitness function
G	Number of different system operation modes
h	Smoothing factor
h_n	The bandwidth or smoothing parameter for the kernel estimator
h_{opt}	Optimal smoothing parameter.
H	Duct height (m)
i	Interest rate (%)
I	Set of duct sections in path ι
$I_{(\cdot)}$	Indicator function
j	Escalation rate (%)
L	Duct length (m)
m	Amortization period (years)
M	Measure of global fit of kernel quantile estimate
n'	Stopping rule for single quantile estimate
$\overline{n}$	Data points for exploratory studies to determine the optimal smoothing factor
n_s	Stopping condition for estimating a single quantile
n_Ω	Stopping condition for a set Ω of quantiles to be estimated
N	Number of independent parameters in a CER
N'	Number of dependent parameters in a CER

p	*pth* quantile of $F(x)$
p_1	Lower limit of quantile function on the interval $[p_1,p_2]$
p_2	Upper limit of quantile function on the interval $[p_1,p_2]$
P_{fan}	Fan total pressure (Pa)
$P_{t,g}$	Path pressure during operation mode g (Pa)
p_{n1}	Probability value to determine the lower bound of $\hat{Q}(p)$
p_{n2}	Probability value to determine the upper bound of $\hat{Q}(p)$
$\hat{P}$	Maximum allowable path pressure imbalance
P_g^s	Maximum subsystem path pressure during operation mode g
$q(p)$	Quantile density function
Q	Duct flow rate (m^3/s)
$Q(p)$	Quantile function
$Q_n(p)$	Empirical quantile function
Q_{fan}	Fan airflow rate (m^3/s)
$Q_{fan,g}$	Fan flow rate during operation mode g (m^3/s)
$\hat{Q}(p)$	Kernel quantile estimate based on jackknifed sample
$\hat{Q}_n(p)$	Kernel quantile function
$Q''(p)$	Second derivative of quantile function
Re	Reynolds number.
S_s	Set of paths in a (sub)system s

S_d	Unit duct cost (cost/m^2)
S_{y_k}	Standard deviation of parameter y_k
SD	Set of standard duct sizes
t	*Student t* at 95% confidence level
T	Operational time (hours/year)
u (<1)	Factor reflecting the relative importance of pressure imbalance
$U(Y)$	Uncertainty in Y
V	Air flow velocity in duct (m/sec)
V_C	Air flow velocity in circular duct (m/sec)
V_R	Air flow velocity in rectangular duct (m/sec)
V_x^{max}	Maximum allowable velocity for duct section x (m)
V_x^{min}	Minimum allowable velocity for duct section x (m)
w	Penalty weighting parameter
W	Duct width (m)
x	Index (number) of the duct section
X	Total number of duct sections in the system
X_l	An instance of a random variable
$X_{l,n}$	n^{th} order statistic of the a set of random variables
y	Parameter in expression to determine Y
Y	Derived engineering quantity

Greek Symbols

∂_x Duct occurrence density

Ω Set of quantiles to be estimated

ρ Air density(kg/m^3)

β Bias error

ϕ Precision error

θ_k Sensitivity of parameter y_k.

ε Absolute roughness factor (m)

υ Kinematic viscosity of the air (m^2/s)

κ Number of chromosomes used in tournament selection

σ Standard deviation of a random variable

λ_C Friction parameter of circular duct

η_f Fan total efficiency (%)

η_m Motor drive efficiency (%)

λ_R Friction parameter of rectangular duct

ψ_g Fraction of time system operates in mode g

ζ Quantile for a predetermined confidence interval >0

Subscripts

ι Duct path index

C Circular

g Index of duct system operation mode

k Index of parameter in expression to determine Y

n Number of independent identically distributed random numbers

R Rectangular

x Index of duct section

y_k k^{th} parameter in expression to determine Y

1 Introduction

1.1 Life-Cycle Cost Analysis

To improve the design of products[1] and reduce design changes, costs and time to market, life-cycle engineering has emerged as an effective approach to design. The principal and unique aspect of life-cycle engineering is that the complete life-cycle of the product is treated in each phase of the product development [Keys 1990]. Life-cycle engineering goes beyond the life of the product itself and simultaneously considers the issues of the manufacturing process and the product service systems. There are three coordinated life-cycles that are considered in life-cycle product design namely, product, process and logistic support. Figure 1.1 illustrates these parallel life-cycles which are initiated when the need for the product is first recognized. Each life-cycle comprise three phases; acquisition, utilization and retirement/recycling phase. In time, these phases of the individual life-cycles may coincide with or overlap one another.

The life-cycle of a product begins with the identification of the need and extends through design, production, product use, support and finally, disposal. The process life-

[1] "Product" in this thesis shall be used to refer to engineering systems as simple as a bearing to complex ones like a power plant.

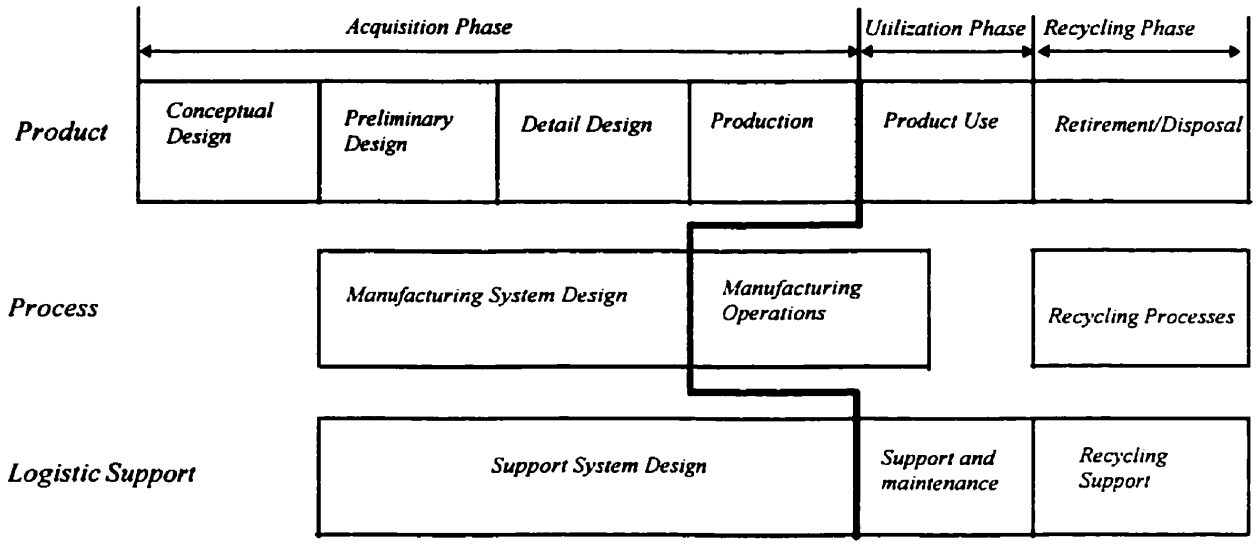

Figure 1.1: Parallel Life-Cycles in Product Development.

cycle begins with the definition of the production task by the preliminary product design [Kriwet et al. 1995]. This entails production planning, plant layout, equipment selection, process planning and other similar activities. The third life-cycle, logistic support, is also initiated at the preliminary design phase and includes, the development of the support for the design and production stages, consumer support and maintenance during the product usage and support for the product recycling.

In suggesting a life-cycle engineering approach to design, Alting [1993] identified a number of issues that needed to be addressed. These are, ease of manufacture, environmental protection, working conditions, resource optimization, life-cycle cost and product properties. This thesis focuses on life-cycle cost.

The life-cycles shown in Figure 1.1 include the main steps in the processes in the life of the product from conception to disposal which may or may not recycle part or all of the product. Raw material and energy inputs will be required along with human labor.

Waste materials may be disposed of during several of the steps including manufacturing, use and retirement or disposal. Energy inputs and waste energy dissipation and maintenance requirements will occur at each physical step but, they may be most significant during product use. In life-cycle engineering, these energy and maintenance inputs may be just as important as the materials. So they must be considered.

In order to compare the importance of materials and energy which go into a product and its use, a common metric or unit system is needed. The money or dollar value of energy, labor and materials provides the common system of units needed, provided the time value of materials, products, labor and money is included.

The life-cycle cost of a product is made up of the costs to the manufacturer, user and society. This is depicted in Figure 1.2. The total cost of any product from its earliest concept through its retirement will eventually be borne by the user and will have a direct bearing on the marketability of that product [Wilson 1986]. As purchasers, we pay for the resources required to produce and market the product and as owners of the product, we pay for the resources required to deploy, operate and dispose of the product.

Studies reported in [Dowlatshahi 1992] and by other researchers in design suggest that the design of the product influences between 70% and 85% of the total cost of products, which often involve large energy and maintenance costs throughout their life-cycle. Designers are therefore in a position to substantially reduce the life-cycle cost of the products they design. The reduction of life-cycle costs has been the prime motivation for the development of methodologies such as Design for Manufacturability, Design for Assembly (DFA), Design for Producibility, Design for Maintainability and Design for

Quality, in the general research area of Design for "X" (where "X" is the objective; manufacturability, producibility, etc. to be optimized).

	COMPANY COST	USERS COST	SOCIETY COST
DESIGN	MARKET RECOGNITION DEVELOPMENT		
PRODUCTION	MATERIALS ENERGY FACILITIES WAGES, SALARIES etc.		WASTE POLLUTION HEALTH DAMAGES
USAGE	TRANSPORTATION STORAGE WASTE BREAKAGE WARRANTY SERVICE	TRANSPORTATION STORAGE ENERGY MATERIALS MAINTENANCE	PACKAGING WASTE POLLUTION HEALTH DAMAGES
DISPOSAL/ RECYCLING		DISPOSAL/ RECYCLING DUES	WASTE DISPOSAL POLLUTION HEALTH DAMAGES

Figure 1.2: Life-Cycle Stages and Costs[2].

While the aforementioned methodologies have on the most part proven successful in reducing cost, the design evaluation criterion in most of these methodologies is not cost. Costs are implicit in each process or material used in the design, manufacturing, use and retiring/recycling of a product. Although it is not commonly done, costs can even be assigned to factors that are not easily measured such as environmental pollution and climate change. Thus cost should be the common currency for life-cycle engineering. The life-cycle cost of the product is specified when all the costs of the product are taken to a common instant in time (e.g. the present) by considering the time variation of money. Life-Cycle Cost (LCC) analysis provides a framework for specifying the estimated total cost of developing, producing, using and retiring a particular item.

[2] Adapted from [Atling 1993].

Cost can be employed as an evaluation criterion in design in two ways. It can be used either in a Design-to-Cost or Design-for-Cost context. Design-for-Cost is the conscious use of engineering process technology to reduce life-cycle cost while Design-to-Cost obtains a design satisfying the functional requirements for a given cost target [Dean and Unal 1992].

Typically, design and economic justifications have been considered as two separate undertakings. Though they both have the common goal of arriving at a competitive product, their goals are often diametrically opposite to each other - the goal of designing the best product possible is often contrary to the goal of cost minimization [Noble and Tanchoco 1990]. LCC concept was initially applied by the U.S. Department of Defense (DoD). Its importance in defense procurements was stimulated by findings that operational and support costs for typical weapon systems accounted for as much as 75% of the total cost [Gupta 1983]. Previously, most of the methodologies developed by the DoD were not intended for use for design but for procurement purposes. It was not until the early 1970s that the concept of integrating product design and economic modeling was suggested by Pugh [1974]. The importance of cost modeling in the design stage has since been advocated by many others.

Recognizing the need for more extensive application of engineering economy methodologies in the planning and control of systems for the production of goods and services, the U.S. National Science Foundation sponsored a joint academe-industry conference in 1984 [Fleischer and Khoshnevis 1986, Fabrycky 1987], where thirty-four research opportunities were identified and ranked. The two research areas receiving the

highest scores were "economic evaluation of design trade-offs over the life-cycle" and "CAD-CAE (Computer Aided Design-Computer Aided Estimating)".

Designers are not the only ones who might be interested in the cost of the products they design. Management certainly has a vested interest in the cost of products and often have professional estimators employed for this purpose. These professional estimators might have little or no design experience and may or may not be an integral part of the design process. Normally, the estimator will be satisfied if he/she obtains a reasonable estimate [Weirda 1988]. Cost estimators rarely focus on why a system has a certain cost. The designer on the other hand will not be satisfied with just an estimate. Seeing the cost estimate, designers search for an understanding of why a product costs what it does and for more cost-effective alternatives bearing in mind that, certain costs like the cost of the design process, might be beyond his/her control and that there are uncertainties in each future cost estimate.

The most important task for the designer therefore is to determine the relationship between cost and design decisions and to be able to assess the uncertainties associated with his/her cost estimates. In this regard, LCC analysis should not be seen as an approach for determining the cost of the system per se but as an aid to design decision making and that through early implementation, it can not only influence the final design but can contribute to cost reductions during each step in the process. Two broad issues can be identified in life-cycle cost analysis: cost estimating and developing design tools based on cost information and thus, the general approach to life-cycle cost analysis can be summarized in the following steps:

1. Identify the costs involved.
2. Develop relationships for each cost as a function of economic and design parameters and determine how design parameters affect these costs. Note, economic parameters can not be influenced by the design.
3. Develop design methodologies or procedures based on this knowledge.
4. Incorporate uncertainty in (2) and (3) above.

The following sections discuss some of the issues that have to be included in life-cycle costing and present the objective of this thesis. An HVAC air duct system would be used as an example to illustrate how the four steps above can be implemented. Most of the material in this chapter has been published in [Asiedu and Gu 1998].

1.2 Cost Estimating Models

Just as the design process may produce lower level functional requirements through functional decomposition to enable design solutions to be easily developed, it is imperative that a cost decomposition[3] be performed. This permits the allocation of cost functions/models to the various categories to allow for the easy calculation of the total cost. Such a decomposition is known as a Cost Breakdown Structure (CBS) and an example is shown in Figure 1.3. This is by no means the most comprehensive and

[3]An alternative approach is the concept of function costing presented in [French 1990]. This is based on the principle that many functions can be quantified and the costs associated with a function are often simply related to the quantity or qualities [French 1990]. This approach decomposes the product by function and quantifies the cost of each function.

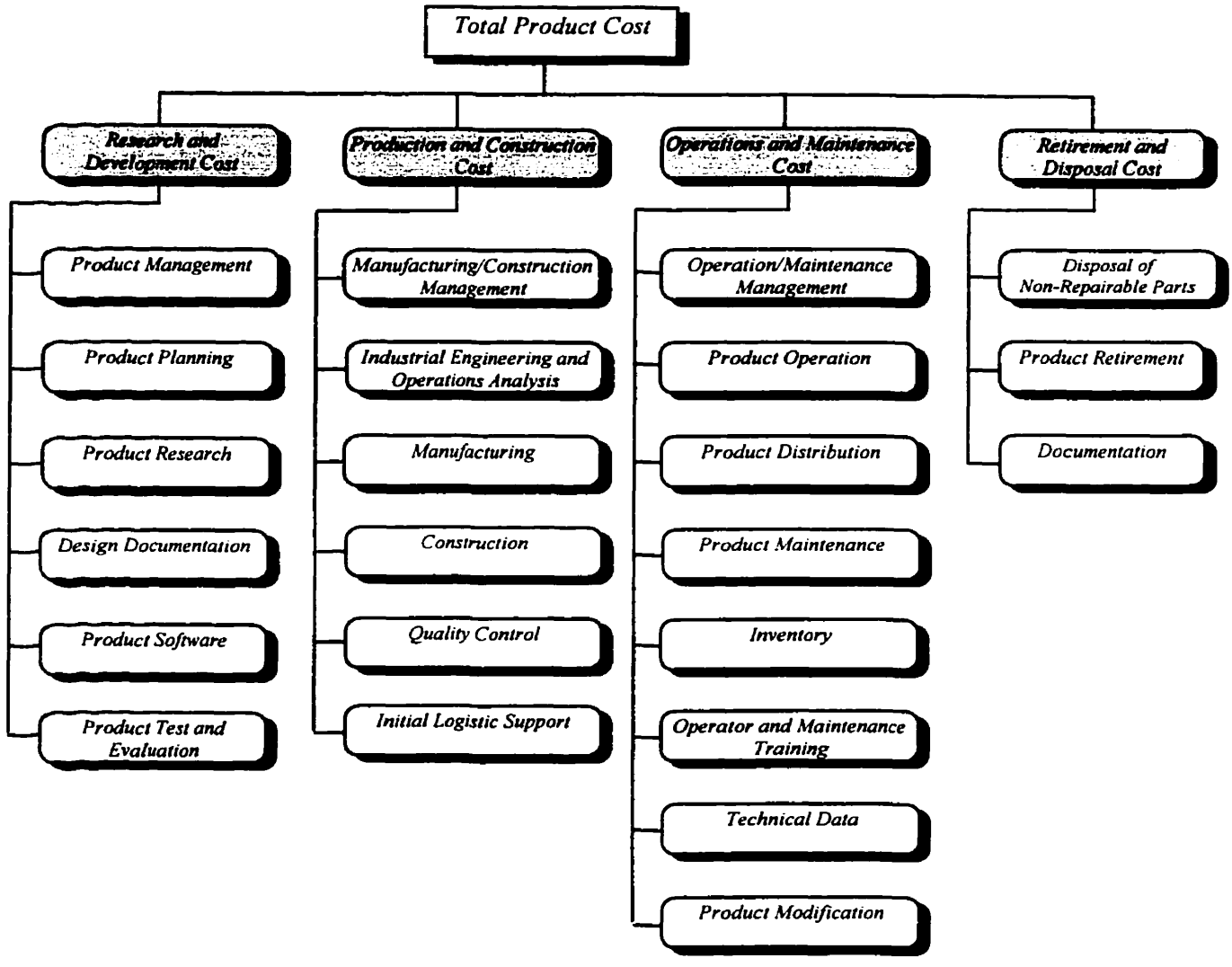

Figure 1.3: Cost Breakdown Structure [Fabrycky and Blanchard 1991].

representative of all products or any product for that matter. The level of cost breakdown and categories considered will depend on the design phase in which the model is to be used, the kind of information to be extracted from the model, the data available as input to the model and the product being designed/purchased.

Depending on the stage of the analysis and the level of detail expected, an LCC model may be a simple series of Cost Estimation Relationships (CERs) or a set of computer subroutines. LCC analysis during the conceptual or preliminary design phases may require the use of accounting techniques and the model may be rather simple in construction [Fabrycky and Blanchard 1991]. On the other hand, life-cycle cost analysis done during the detail design stage may be more elaborate.

Estimating models used in industry can be broadly classified as parametric models, analogous models (estimating by analogy) and detailed models. These are explained below.

Parametric Models

Cost estimating with a parametric model is based on predicting a product's (or component's) cost either in total or for various activities, e.g. design or manufacture, by the use of regression analysis based on historical cost and technical information. A simple CER is the relation between the cost of buildings and floor area. Thus each type of building in a city (e.g. houses, strip malls, schools, office buildings etc.) will have somewhat uniform costs per unit floor area. Parametric estimating can involve considerable effort because of the systematic collection and revision process required to keep the CERs updated, but once this data is available, estimates can be produced rapidly [Greves and Schreiber 1993]. Fad and Summers [1988] suggest that it be used throughout the design process. In addition, parametric models that have been developed to facilitate this process are now available in commercial software. The most widely used is the Lockheed Martin PRICE system. This is used by establishments such as the

British Aerospace Corporation [Daschbach and Apgar 1988], the European Space Agency [Greves and Schreiber 1993] and NASA [Dean 1989]. Parametric estimating is not very good for estimating the cost of products that utilize new technologies. These are best done using an analogous or a detailed model.

Analogous Models

Cost estimating made by analogy identifies a similar product or component and adjusts its costs for differences between it and the target product [Shields and Young 1991]. The effectiveness of this method depends on an ability to identify correctly the differences between the case in hand and those deemed to be comparable [Greves and Schreiber 1993]. The main disadvantage of estimating by analogy is the high degree of judgment required. Expert judgment and complete familiarity with the product and processes are required to identify and deal with similarities and make adjustments for perceived differences. This approach tends to be very good for new products where a low-cost effort is needed to get a cost estimate.

Detailed Models

A detailed model uses estimates of labor time and typical rates along with material quantities and prices to estimate the direct costs of a product or activity [Shields and Young 1991]. An allocation rate is then used to allow for indirect/overhead costs. It is the most time consuming and costly approach and requires a very detailed knowledge of the product and processes. It is, however, the most accurate costing method. In principle it is a simple method, determine the time needed to perform an activity and the hourly

rates for the man and/or machine, then multiply times and rates to get the costs. Time standards can be industry standards, in-house standards or based on the estimates of experts. This approach is flexible and can be used for many different products. The information used is basic information and can therefore be used for numerous related applications. The other estimating techniques demand one or more existing products that resemble the new product in some way. The main difficulties of the method include [Weirda 1988]:

1. determining or collecting typical standard times,
2. determining the hourly rates and keeping them up to date,
3. managing large amounts of information,
4. doing a large number of simple, but tedious, calculations, and
5. knowing how to use the information accurately.

1.3 Accuracy and Uncertainty in Cost Estimating

In a competitive situation, if a company's estimates of its cost for a product is unrealistically low (i.e. underestimated), it will risk a financial loss for that product. On the other hand, an overestimate of costs may cause the company to lose orders because its predicted price is high. High accuracy in cost estimating is, therefore, essential to the survival of an organization. Good cost estimates are not only important for external use (e.g. pricing and contract bidding) but also for internal use (e.g. for cost control and budgeting). The relationships between the over- and underestimates and the cost of

products can be represented by the Freiman curve shown in Figure 1.4. This graph shows that:

1. the greater the underestimate, the greater the actual expenditure,
2. the greater the overestimate the greater the actual expenditure, and
3. the most realistic estimate results in the most economical project cost.

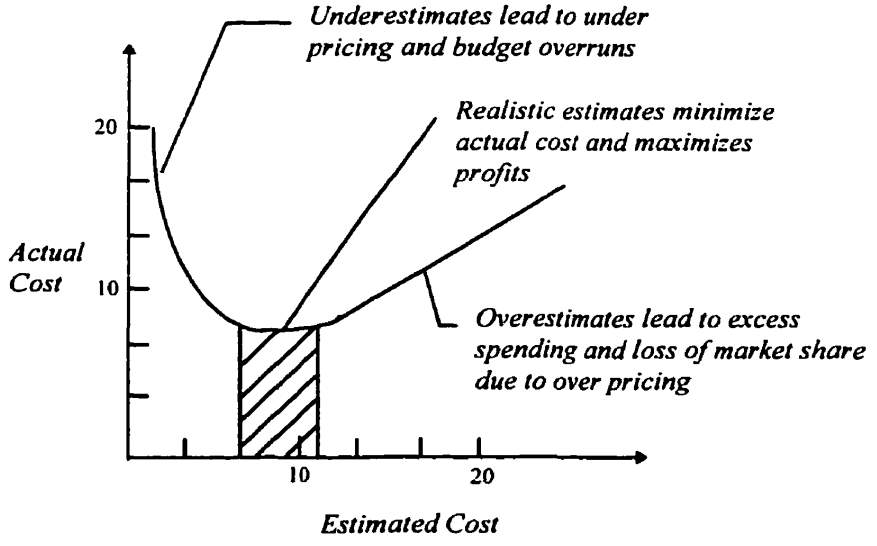

Figure 1.4: The Freiman Curve [Daschbach and Apgar 1988].

When costs are underestimated, initial plans for staffing, scheduling, machine processing, tooling, etc. leads to production or cost goals not being achieved. Though plans are established to realize the underestimated costs, it becomes increasingly difficult for cost targets to be met as the project progresses. In response, there is reorganization, replanning and possibly the addition of personnel and equipment [Daschbach and Apgar 1988]. These additional resources incur costs that were not originally budgeted for and result in increased total project or product cost. On the other hand, when costs are

overestimated, rather than resulting in greater profits, the overestimate often creates an example of Parkinson's law - the money is available; therefore, it must be spent [Daschbach and Apgar 1988]. Unless there is firm management control, there is a self fulfilling prophesy and it will be virtually impossible to reduce cost.

One approach that has been suggested to improve cost estimates is Activity Based Costing (ABC). ABC differs from traditional cost accounting methodologies in the way that the overhead cost is allocated. Overhead, sometimes called hidden factory cost, include design and production documentation, equipment depreciation, engineering changes, rework of defective products, product inspection and quality control and repair. Generally, this is allocated based on the direct labor cost and in a few instances on direct material cost. As companies automate production processes, the amount of direct labor decreases and the overhead costs rises approaching 50% of the total production costs at many companies while direct labor is as low as 5% [Huthwaite 1989]. This increased overhead head cost is due primarily to the machinery that replace the humans. The low fraction of labor cost compared to overhead costs and total cost has led to distortions in product costing. There is a move to track overhead costs to the processes that drive them by employing ABC. ABC allocates costs to products based on each product's consumption of activities. Activities can be classified into four general hierarchies. These are, unit, batch, product and factory level activities. The measure of the demand of an activity is known as the cost driver. The unit price of a cost driver is known as the consumption intensity. The cost of an activity is thus given by the product of the total amount of the cost driver used by the activity and the consumption intensity.

There have been suggestions that ABC also encourages better product designs [Huthwaite 1989, Kaplan 1989, Brooks et al. 1993] and that ABC should be used in cost analysis during design if designers expect to develop cost competitive products. ABC can not resolve all the problems confronting designers and in certain instances, like single product and Just-in-Time (JIT) settings, ABC does not offer much advantage over traditional costing systems.

In practice, regardless of how the overhead cost is treated, it is highly improbable for the actual cost of a product to be exactly as estimated. That is, uncertainty is associated with any cost estimate and it is necessary in cost estimating to also assess this uncertainty associated with the cost estimates and to include this uncertainty with the cost estimate. This issue is discussed further below.

1.3.1 Certainty, Risk, Uncertainty and Dependency in Cost Estimating

Cost estimates are decisions about future costs and like all decisions, cost estimates can be classified as those made under certainty, risk or uncertainty. The simplest of the states of nature is one that has a probability of occurring equal to one (i.e. complete certainty). This seldom exists in nature or in competitive society, rather some state outcomes have higher probabilities than others. For example, labor costs, production rates or material costs may be stable or constant in the short term. In certain instances, it is expedient to make these assumptions to simplify the analysis.

A decision under risk is one in which each action may result in more than one outcome or end state where each end state or outcome has a known probability and the sum of these probabilities equals one. These probabilities are usually subjective as actual

measurements are either impossible or too expensive to establish. A decision under uncertainty is one in which each action may result in more than one outcome or end state, but each end state or outcome has an unknown probability [Jelen and Black 1983].

In the foregoing definitions, a distinction was drawn between decisions made under risk and those made under uncertainty. However, under the subjective interpretation of probability, it is always possible to assess probabilities for the possible events, or states [Ravindran et al. 1987]. Hence, the risk versus uncertainty dichotomy is nonexistent and any decision-making problem in which the states of a system is not known for certain is said to be decision making under uncertainty [Ravindran et al. 1987] and risk is generally defined as the exposure to the possibility of economic or financial loss or gain, physical damage or injury, or delay, as a consequence of the uncertainty associated with pursuing a particular course of action [Cooper and Chapman 1987].

Let Equation (1.1) be a cost estimating relationship, CER, of any functional form.

$$C = f(c_1, c_2 \cdots c_N) \tag{1.1}$$

Deterministic cost models treat the cost parameters, c_1, c_2, ..., c_N, as fixed and known with certainty. It is assumed that average values of the parameters in the cost models are sufficient for the analysis. Although this assumption simplifies the evaluation of the cost, this is satisfactory only for the simplest of design problems. Furthermore, the accuracy of a LCC estimate is inversely proportional to the span of time between the estimate and when the activity actually occurs, the stage of the design process, the extent of product definition and the type and depth of the analysis being undertaken. Physical laws, which depend on well-ordered cause and effect relationships are unlike economic laws which

depend on the reaction of people [Ostwald 1974]. Accordingly, the state of uncertainty is more applicable in cost estimating. Assessing the uncertainties associated with cost estimates is important because of the effects that wrong cost estimates can have on profit margins. This is more so in dealing with projects with each phase of its life-cycle spanning several years such as nuclear power stations and large bridge constructions, projects involving large amounts of money or with a cost element being a large portion of the total cost.

To include uncertainty in estimating C, a contingency amount can be added to the deterministic cost estimate or the parameters can be treated as interval, random or fuzzy variables. Interval variables are not considered adequate because that presupposes that the values in the range are all equally likely. Treating the parameters as random or fuzzy variables does not preclude the use of interval variables. Interval variables can be defined as a uniform distribution or a fuzzy number with a constant membership function. While fuzzy variables can be used in cost models for computerized decision making, it is not worthwhile to provide cost information to designers or managers in the form of fuzzy variables. Probabilistic models treat these parameters as random variables in the statistical sense and this is what is done in this thesis.

There are fundamentally two ways to develop probabilistic cost estimates once the uncertain variables have been assigned probability density functions (pdfs): simulation[4] and analytical. Monte Carlo simulation has been accepted by estimating researchers as superior to analytical methods for determining cost distributions. Given the pdfs of the input variables, random values for the independent variables can be generated and used

[4]Unless specifically stated, simulation can be assumed to mean Monte Carlo simulation in this thesis,.

to calculate the resulting value(s) for the output variable(s) (i.e. C). When this is repeated a number of times, a probability distribution function (PDF) and/or pdf for the output/dependent variable can be developed or determined. As with all simulations, the problem is in being able to tell when enough replications have been made. Current research employing simulation often do not incorporate good procedures for terminating the simulation. The number of replications is often arbitrarily chosen before the start of the simulation (e.g. Bras and Emblemsvag 1995 & Zhi 1993). A better approach is to monitor the convergence of certain parameters. The most commonly used parameters are based on the first four central moments. These are the mean, standard deviation, kurtosis and skewness. This does not necessarily eliminate the tendency to stop the simulation either too soon or too late. Furthermore, as in [Uher 1996], the distributions that are plotted after the simulation has been stopped may have moments that are different from the sample moments that were used to monitor the convergence of the simulation. A further shortcoming of this approach is the fact that it is very difficult to translate a desired accuracy in the cost estimates to the required accuracy in the moments.

One other assumption made about CER parameters is the independence of these parameters. That is, the value of one parameter is presumed not to be influenced by any other parameter in the CER. Perhaps the lack of attention paid to this issue is due to the over-reliance on single value or deterministic cost estimating models. In such cases, the problem is trivial. However, if these parameters are treated as random variables, then it is imperative that the correlations (measure of (inter)dependence) between the parameters be considered since ignoring them, were they exist, may have very disastrous consequences.

1.4 HVAC Air Duct Systems

Heating, ventilating and air-conditioning (HVAC) systems are necessary to provide control of space temperature, humidity, air contaminants including odors, toxic gases, volatile organic compounds and aerosols, differential pressurization and air motion in buildings [Herbert 1990]. Most HVAC systems are designed for human comfort and safety. However, many industrial applications have objectives other than human comfort. If in the process of satisfying the industrial demands and human safety, human comfort can be achieved, the design will be that much the better. There are two kinds of HVAC distribution systems: air ducts and piping. Air ducts are used to convey air to and from desired locations [Herbert 1990]. Air ducts include supply air, return-relief air, exhaust air, and air conveying systems. Piping is used to convey steam and condensate, heating hot water, chilled water, brine, cooling tower water, refrigerants and other heat-transfer fluids [Herbert 1990]. Energy is required to force the fluids through these systems and is provided by fans (air ducts) and pumps (piping). The amount of energy needed for distribution purposes should be considered when these systems are designed. This thesis, however, deals only with the air duct distribution system.

The function of a duct system is to provide a means to transmit air to and from the air handling equipment. The primary task of the duct designer is to design duct systems that will fulfill this function in a practical, economical, and energy-conserving manner within the prescribed limits of available space, friction loss, sound levels, and heat and leakage losses and/or gains [Grimm 1990]. This is an area of design in which LCC analysis can be useful. Studies show that these systems are one of the major electrical energy consumers in industrial and commercial buildings [Tsal et al. 1988a]. Energy cost of

fans used in air duct systems can account for 15-20% of electrical energy used in commercial buildings (this figure is even higher in industrial buildings) and a significant fraction of the building interior space is reserved for the air handling. The life-cycle cost of air handling in buildings is always important even though it is seldom investigated for the least life-cycle cost. Among the opportunities that exist for the reduction of these life-cycle costs are:

1. improved contaminant removal,
2. reduced airflows, and
3. improved ducting design.

The effectiveness of contaminant, thermal energy and water vapor removal strongly depends on the location and jet momentum of the supply air to a room as well as the location of the return grilles [Irwin et al. 1998]. Compared to well mixed spaces, contaminant removal effectiveness for most interior spaces are less than 100% [Heiselberg 1996] suggesting that good opportunities exist to improve these designs by improved interior airflow patterns which include some aspects of displacement ventilation. Reduction of airflow rates while still maintaining good interior air quality may, in some applications, be achieved by using some radiant ceiling cooling or slightly reduced supply air temperatures [Kirkpatrick and Elleson 1996]. The life-cycle cost effectiveness of these two options need more research because there are several special and temporal variables that vary for each application.

The third option is to improve the life-cycle cost of the ducting systems in buildings. Ducting systems are complex in terms of their layout within a building with terminal flow rate requirements that vary from room-to-room and over time in each room but they

are usually well defined in terms of airflow rates and ducting layout. Since designers of ducting systems are faced with a large number of constraints and requirements, as well as some choices for layout, they have most frequently used rules of thumb (e.g. Equal Friction and Static Regain methods) rather than trying to optimize the life-cycle costs (e.g. T-Method). A study on the ducting system in the Agriculture Building of the University of Saskatchewan, discussed in [Carriere et al. 1998] showed that there could be as much as a 30% cost saving when life-cycle optimizing procedures are used in HVAC air duct design.

Some of the methodologies that have been employed for HVAC duct design and their shortcomings are discussed in Chapter 2.

1.5 Objective and Scope of Thesis

This thesis includes the application of life-cycle cost principles to the design of an engineering system and the estimation of life-cycle cost under economic uncertainty. The HVAC air duct design problem is used as an illustrative example. In this regard, the objectives of this research are:

1. Develop methodologies for the estimation of LCC under uncertainty and the specifications of the uncertainties associated with cost estimates,
2. Investigate the development of simple life-cycle cost based design methodologies for HVAC air duct design,
3. Demonstrate the use of genetic algorithm optimization techniques in the design of complex HVAC air duct systems for minimum life-cycle cost,

4. Investigate the impact of parameter uncertainty in HVAC air duct design optimization, and
5. Show the robustness of the final design to typical variations of some key design parameters for the system components.

Current work in cost estimating employing simulation often do not incorporate proper procedures for terminating the simulation. The number of replications is often arbitrarily chosen before the start of the simulation. As has already been mentioned, a better approach is to monitor the convergence of the moments. In Section 1.3.1, some of the problems associated with current approaches were mentioned. An approach that will overcome these difficulties would be proposed in this thesis. This approach employs kernel estimation techniques and their asymptotic properties in the development of the PDFs of the cost estimates. The approach is illustrated with an example.

With regard to the optimal design of an HVAC air duct system, two design approaches are suggested. The first approach to air duct design is a simple design methodology that eliminates the need to condense and expand the air duct system which is required in the T-Method, a duct design methodology recommended by ASHRAE. There are three stages involved in this approach: **I**nitial Sizing, **P**ressure Augmentation and Size Augmentation, hence the name IPS-Method. As an extension of the IPS-Method, the Enhanced Friction Chart and Diameter Chart are developed. These charts can be used as a guide in selecting the size of a duct.

In the second approach, a genetic algorithm is used for the design of HVAC air duct systems. Genetic Algorithms are in the class of optimization methods known as Evolutionary Algorithms. These are 0-order methods (all they need is an evaluation of

the objective function), they can handle non-linear problems, defined on discrete, continuous or mixed search spaces and may be unconstrained or constrained. This approach has the capability to handle only standard duct sizes, complex objective functions and to incorporate other problem specific constraints. Furthermore, it tends to be faster than other operations research methods that have been used in the past for duct design.

As the parameters in cost models are mostly uncertain, when they are used as objective functions for a design, the design optimization should incorporate these uncertainties if possible. The genetic algorithm and the probabilistic cost estimating methodologies are combined to determine the optimal duct sizes under uncertainty, i.e. stochastic optimization of the HVAC air duct system.

The outline of the thesis is as follows. A more detailed review of pertinent literature is discussed in the next chapter. The simulation approach to cost estimating is discussed in the Chapter 3. This will present a discussion on kernel estimators, their asymptotic properties and their use in a simulation based probabilistic cost estimating. The principles of random number generation are not discussed in this thesis. The material in this chapter appears in [Asiedu et al. 1999c] and is currently under review by a journal. Chapter 4 discusses the theory of the methodologies developed for the HVAC air duct sizing problem which are the IPS-Method, the Diameter and Enhanced Friction charts and the use of Genetic Algorithms for air duct design. The material in this chapter appear in [Asiedu et al. 1999a & b]. The paper, Asiedu et al. [1999b], is currently under review.

Chapters 5 and 6 will cover the case studies. Chapter 5 will deal with an air duct design example and Chapter 6 will discuss a probabilistic cost estimating example, stochastic/probabilistic optimization of the HVAC air duct system and the effect variations in the physical parameters have on designs based on various design methodologies. The conclusions and possible extensions of the thesis are covered in Chapter 7.

2 Literature Review

2.1 A Review of Cost Models and Estimating Methodologies

The growing demand on producers to develop products that are inexpensive to acquire, use and dispose off has necessitated that the life-cycle cost of products be considered during the design of the product. Efforts have been made toward providing the designer with cost information during the design. A survey by Gupta and Chow [1985] of the life-cycle cost analysis literature found about 300 publications. In recent years, a large number of papers have been written. Since a complete review of all of this material is impractical, a number of pertinent papers in which the cost models are related to engineering design are reviewed. The review is divided into deterministic and probabilistic models.

2.1.1 Deterministic models

Prior to the 1970s, the concept of integrating product design and economic modeling had received little attention. Pugh [1974] was among the first to make mention of providing economic information to the designer. The importance of cost modeling in the design stage has also been reported by various authorities such as Boothroyd and Dewhurst [1983a], Ehrlenspiel [1987], Wierda [1988], and Alting [1993]. The models

reviewed herein illustrate how models have been developed for the various stages of the design process in an attempt to provide the designer with cost information.

As part of a Design for Manufacture research program at the University of Rhode Island, a number of computer based models for estimating the cost of fabricating parts have been developed [Dewhurst 1988]. The objective of these studies was to provide methods with which the designer or design team can quickly obtain information on costs before detailed design takes place [Boothroyd 1994]. Cost studies have been completed for machined, injection-molded parts, die-cast parts and sheet-metal stampings parts [Dewhurst and Blum 1989, Dewhurst 1988, Dewhurst and Boothroyd 1988, Boothroyd and Rodovanovic 1989, Zenger and Dewhurst 1988].

Models for the estimation of the cost of fabrication have also been developed by others. Knight [1991] developed a methodology for determining the cost for processing parts manufactured by sintering from powder metals, Dixon and Poli [1995] developed methodologies for injection molding, stamping and die casting. Most of these models for early cost estimating results from a detailed study of each process to identify the main cost drivers. From these studies, simplified but realistic, cost estimating procedures were developed which can then be used to quantify the effect of early design decision on manufacturing costs [Knight 1991].

In a series of papers, Boothroyd and Dewhurst [1983a, 1983b, 1984a, 1984b] presented models for calculating the cost of assembly of products using robots, automatic machines, and manually. These have been formalized into computer programs. The programs can show whether a particular product is likely to cost less if assembled manually, automatically or by a robot. The cost in all cases is based on determining the

time needed to assemble the products by the particular method and a cost rate plus the cost of the equipment used.

Service Mode Analysis (SMA), as an evaluation of the most important service costs in design for serviceability was developed by Gershenson and Ishii [1993]. Its use is discussed in Marks et al. [1993] and Ishii [1995]. SMA focuses on the service needs in estimating life-cycle ownership cost. Their computer software infers the labor operations necessary for various service operations, identifies cost drivers and indicates areas for improvement. The current implementation utilizes a semantic network representation known as "linker" for the design layout. Given a set of cost driving service modes, and their frequencies of occurrence, the program can compute the total life-cycle service costs. While the semantic representation of the design is very comprehensive, the model does not include random failures.

Emblemsvag and Bras [1994] illustrated how an ABC based deterministic cost model can be used in the decision making process to obtain an overall cost efficient design. The recycling of the product at the end of its useful life is what is considered here. The recycling phase is broken down into a hierarchy of activities. Then for a particular design, a determination is made of the activities that it will require and the cost is calculated. Though this model is suppose to help designers make decisions, the model, as presented in this paper, can only be used to make decisions at the product level.

A more complete model was discussed in [Johnson 1990]. The LCC model is composed of elements to calculate RDT&E (Research, Development, Testing and Evaluation) cost, production cost, DOC (Direct Operation Cost), IOC (Indirect Operating

Cost) and an existing conceptual design and analysis code, the Flight Optimization Systems (FLOPS)

FLOPS is a multidisciplinary system of computer programs for the conceptual and preliminary design and evaluation of advanced aircraft concepts. FLOPS may be used to analyze a point design, parametrically vary certain design variables, or optimize a configuration with respect to design variables using nonlinear programming techniques. The addition of the LCC module to the conceptual design system allows cost to become an additional design parameter, making it possible to specify life-cycle cost, acquisition cost, direct operating cost, total operating cost or return on investment as the parameter to be optimized. This is illustrated specifically for aircraft design.

The preceding material illustrates the wide range of models that have been developed for different phases of the product life-cycle. With the exception of the model discussed in [Johnson 1990], there has not be any attempt to incorporate all the models for the various stages of the product life-cycle into a single model. However, this is not the main shortcoming of the models discussed above. Deterministic models do not incorporate uncertainties that occur in practice.

2.1.2 Probabilistic Models

In probabilistic cost estimating, given the uncertainty distribution for each cost parameter and the correlation between the cost parameters when they exist and are being considered, their probability density functions must be combined according to the functional form of the Cost Estimation Relationship (CER) to generate the overall

Probability Distribution Function (PDF) for the cost estimate. Fundamentally, there are two ways to do this; simulation and analytical. A number of simulation and analytical methodologies that have been developed to solve cost estimating problems are reviewed.

2.1.2.1 Analytical Models

Analytical methods use the method of moments to determine the PDF of cost estimates. The moments method allows the approximation of the moments of a CER from knowledge of the moments of the component cost elements by using series expansions.

A procedure described by McNichols [1983] assumes that the desired PDF is a member of the generalized beta family of distributions. Given the functional form of the CER, the moments of the cost parameters can be used to generate the moments of the distribution. This is done by first approximating the cost using a first or second order Taylor series expansion assuming the parameters in the CER are independent. The coefficients of the terms of the expansion can be expressed as functions of the moments of the parameters of the CER which are in turn related to the moments of the desired cost estimate.

The approach to stochastic cost estimating discussed by Tzemos and Dippold [1986] is similar to that above. In this paper, the Gram-Charlier series expansion is used to approximate the distribution of the cost estimate. Using the Gram-Charlier approximation, an a priori knowledge of the final distribution's functional form need not be known but the cost model input parameters must be independent. The Gram-Charlier

method approximates the final cost distribution with a series expansion of the standardized normal frequency distribution and their derivatives. The moments (cumulants) of the input cost parameters are used to form the coefficients of the terms of the expansion.

The results obtained from the above analytical methods are restricted to independent and continuous cost model input parameters. For complex systems with many variables, the difficulty in dealing with complex non-linear cost functions, where one parameter may be correlated with another input parameter, and requirements placed on the functional form of a pdf (e.g. continuity, differentiability etc.) makes the use of the above analytical probability cost estimating methods impractical.

Point estimates of distributions are methodologies that can be used to obtain approximate probability values for a number of discrete points in the range of the density function. Even though its application in cost estimation is yet to be seen, this is an approach that can be used to handle correlated variables.

Rosenblueth [1975] first introduced the point estimate method by requiring the equivalency of the first three statistical moments of two random variables and their point -wise approximation. The method was then generalized to functions of several symmetrical random variables. The number of points estimates of Rosenblueth's method is 2^N, where N is the number of random variables. As an illustration, for a function of three random variables (N=3), Rosenblueth's point distributions are at the corners of a 3-dimensional cube, and hence, the number of point estimates is 2^3=8.

The difficulty of obtaining point estimates in Rosenblueth's method increases exponentially with N. To address this issue, Lind [1983] and Harr [1989] developed

methods requiring $2N$ point estimates. In practice, the variables encountered could be skewed and/or correlated random variables. Panchalingam and Harr [1994] provides a method that also accommodate correlated and skewed random variables in uncertainty analyses.

The shortcoming of the point estimate methods is that, the number of points depends on the number of parameters(variables), N. To get a more accurate distribution, a CER that has a large number of parameters is required. This might explain why it is not used in cost estimating where the number of parameters in the CERs are few.

A method of modeling uncertainty in cost estimating based on a simple extension of the central limit theorem is proposed in [Flood 1997]. The approach is applicable irrespective of the form of the probability density functions (pdfs) describing the uncertainty in individual cost items. While most cost distribution functions cannot be approximated by any of the standard distributions (such as the Gaussian, Beta, or gamma distributions), it could be constructed as a composite from several primitive functions. Such composites are termed mixture functions. In Flood [1997], the pdf of each cost item is constructed as a Gaussian mixture function. These are then combined into a single total cost density function by means of an extension of the central limit theorem. There is the question of how to determine an appropriate set of amplitude adjusted Gaussian functions which, when added together, will result in an acceptable approximation of the pdf of a cost item. Furthermore, this procedure can only be applied to sums of cost elements. It is not clear how it can be extended to other functional forms of CERs.

2.1.2.2 Simulation Models

Simulation has been accepted by the estimating community as superior to analytical methods for determining cost distributions [Uher 1996]. Given the probability distribution functions of input variables, random values for the independent variables can be generated and the resulting value(s) for the output variable(s) calculated. When this is repeated a number of times, a probability distribution function for the dependent variables can be developed. This is the basic approach to simulation based cost estimation. The implementation may vary in terms of the way the sampling is done (e.g. Monte Carlo or Latin Hypercube), how the simulation is terminated and the kind of distribution (empirical or histogram) plotted once the simulation has been terminated. Unfortunately, there is very little variation in the numerous publications employing simulation for cost estimation. A number of representative works are presented in this section.

Bras and Emblemsvag [1995] extend their work in [Emblemsvag and Bras 1994] to include uncertainties. The crux in developing an ABC model is to identify the activities that will be present in the life cycle of a product and assign reliable cost drivers and associated consumption intensities to the activities. Probability distributions are assigned to the numbers used in the calculations, representing the inherent uncertainty in the model. The effect of the uncertainty on the cost model behavior are found by employing the Monte Carlo simulation technique. The additional use of detailed process action charts and sensitivity charts allows the influence of the uncertainty to be traced through the cost model to specific product and process parameters.

A similar approach is employed in [Zhi 1993]. The only difference is that traditional cost accounting techniques are employed instead of ABC. Furthermore, the distributions plotted were empirical distributions.

Like many simulation models, the number of replications in both of the above studies was selected arbitrarily before the start of the simulation. Uher [1996], has shown that arbitrarily fixing the number of replications a priori is inappropriate. A better approach is to monitor the convergence of certain parameters. The most commonly used parameters are based on the first four central moments. These are the mean, standard deviation, kurtosis and skewness. When the number of replications was fixed at 5000, the moments showed less than a 1/100% change beyond the 1000^{th} iteration, indicating that most of the computations yielded no improvements in the cost estimate.

With regards to the treatment of dependencies, if the individual cost rates are normally or lognormally distributed, then the specification of the correlation coefficients of the variables are enough to describe the relationships and the correlated random variables can be easily generated. The problem is not that straight forward when the random variables are of different forms. Most publications have preferred to make the assumption of normality or lognormality when treating dependencies. This simplifying assumption is limited in its applicability and is not always necessary. An algorithm for generating approximate correlated vectors of random numbers for any set of continuous, strictly increasing distribution functions is presented by Lurie and Goldberg [1998]. Their algorithm requires that the user at least specify the marginal distributions and the correlation matrix.

2.2 A Review of HVAC Air Duct Design Methodologies

There are a number of design methodologies that are currently recommended by the American Society of Refrigeration, Heating and Air-Conditioning Engineers (ASHRAE) for use in duct design. These are: the Equal Friction Method, Static Regain Method and the T-Method [ASHRAE 1997]. The Equal Friction and Static Regain methods are non-optimizing methods that rely on heuristics which do not explicitly take into account prevailing local economic conditions. The Equal Friction method requires ducts to be sized so that there is a constant pressure loss per unit length of each duct in the system. The objective of the Static Regain design method is to reduce air velocity at each junction in the direction of flow so that the increase in static pressure of each transition balances with the pressure losses in the following section. These approaches result in designs that are workable but not necessarily cost efficient. The T-Method is a deterministic optimizing method that is gaining acceptability in the HVAC community. It consists of 3 main steps, system condensation, fan selection and system expansion. In the first step, the entire duct system is replaced with a single duct section having the same pressure drop and economic characteristics. An optimal fan pressure is selected in the second step. This pressure is then distributed through out the system in the third stage (a detailed discussion and illustration of this method can be found in [Tsal et al. 1988a&b]). This method, although currently the most widely used optimization approach in air duct design, does not treat the constraint dealing with standard duct sizes very well. This constraint is relaxed throughout the design procedure and incorporated at the very end through the use of a heuristic. For a ducting system with a large number of components, this does not ensure that the T-Method design is optimal. Also, the process

of system condensation and expansion requires a lot of computations which can cause complications in large systems. Another shortcoming of the T-Method is that it was designed for a specific objective function (i.e. minimum life-cycle cost) with fixed input parameters (unit energy cost, duct flow rates, etc.) and currently cannot be used to optimize a system that has for example, time variable duct flow rates or utility rates. The final design using the T-Method may be very sensitive to small variations in some input parameters and more expensive to balance for the design airflow rates to each space than is necessary.

2.3 Summary

While most researchers recognize the need for a LCC model for product design decision making, the models developed have been restricted to specific processes, simple operations, or one phase of the life cycle.

One issue that has been largely ignored in cost estimating models is uncertainties in the parameters. As cost is uncertain in many aspects, it is imperative that any life-cycle model incorporate the treatment of uncertainties. Although these parameters and costs may not be independent, the few probabilistic cost models that have been developed have simply ignored the problem of dependence or treated it casually. In cases where there is reason to believe that dependency exist, it is better to make explicit assumptions about the degree of correlation (dependency) between variables or equations than to ignore it and thereby assume it is zero. However, it should be mentioned that the

achievement of an LCC analysis including uncertainty and dependencies could result in cost ineffectiveness, i.e. the savings from this will not be worth the effort to achieve it.

Among the three design methodologies recommended by [ASHRAE 1997], only the T-Method is a life-cycle cost optimization procedure. However, it requires the condensation and expansion of the system. For very large systems, this may introduce complications. It can also not be used for systems where the parameters in the objective functions or constraints may be stochastic or uncertain, or with time variable duct flow rates or utility rates without making a number of simplifying assumptions.

In the next chapter, a methodology for cost estimating when economic conditions are uncertain is developed and the issue of dependency addressed. The duct design methodologies are, however, discussed in Chapter 4.

3 Probabilistic Cost Estimating

3.1 Simulation Based Cost Estimating

Let Equation (3.1) be a cost estimating relationship (CER) which is dependent on the cost parameters $c_1, c_2, \ldots, c_N$.

$$C = f(c_1, c_2 \cdots c_N) \tag{3.1}$$

To incorporate uncertainty in cost estimating, the cost parameters $c_1, c_2, \ldots, c_N$, are assumed to be random variables in the probabilistic sense. This is termed, probabilistic or stochastic cost estimating. An example of a CER is the expression for calculating the life-cycle cost of HVAC air duct systems given in Equation (3.2) where the model is explained in detail in Chapter 4.

$$C = f(Q, \Delta P, E_d, E_c, T, \eta_f, \eta_m, PWEF, E_s) = Q\Delta P\left[\frac{(E_d + E_c T)}{10^3 \eta_f \eta_m}\right] PWEF + E_s \tag{3.2}$$

In probabilistic cost estimating, three types of studies are considered:

1. Determine the probability density function (pdf) which describes the uncertainty inherent in each cost model parameter ($c_1, c_2, \ldots,$ and c_N) using available historic information or expert knowledge,

2. For independent cost parameters, combine the probability density functions for each cost parameter obtained in 1 above according to the functional form of C to generate an overall pdf and/or probability distribution function (PDF), and
3. For interdependent cost parameters, determine the dependencies or correlations between the cost parameters and include these dependencies in the development of the overall pdf and/or PDF.

The problem mentioned in (1) above is not treated in this thesis. Rather, a probability distribution is assigned to every cost parameter for which there exists uncertainty and problems (2) and (3) considered to determine the probability function for the total cost.

Determining the probability function of a given cost estimate can be considered a matter of selecting a distribution from a family of distributions. If the form of the family of distributions for the cost estimate is known from experience, then the problem reduces to that of just determining the necessary parameters for the distribution. In general, the form of the distribution is not known. Nonparametric methods are therefore the most appropriate techniques for determining the form of the distribution. The most commonly used is the histogram.

The rest of this chapter discusses one such method known as kernel estimators and a simulation procedure to produce PDFs for a predetermined degree of accuracy in the cost estimate. The assumption required in this method is simply that the distribution be continuous. The approach is first developed for the case of independent parameters (problem (2)) and then its possible extension to that of coupled or interdependent parameters (problem (3)) discussed.

3.2 Kernel Estimators

Given a sequence $X_1, X_2,...,X_n$ of independent and identically distributed random variables with continuous probability distribution function $F(x)$ and probability density function $f(x)$ on the real line, $-\infty<x<\infty$. Let $X_{1,n}\leq X_{2,n}\leq....\leq X_{n,n}$ be the order statistics of the X_is. For $0<p<1$, let the *pth* quantile of $F(x)$ be defined as $Q(p)=\inf\{x: F(x)\geq p\}=F^{-1}(p)$. For each n, a natural estimator of $F(x)$ is the well-known empirical distribution function (EDF) $F_n(x)$, defined as

$$F_n(x) = \frac{number\ of\ X_i's \leq x}{n} = \frac{1}{n}\sum_{i=1}^{n} I_{(X_i \leq x)} \tag{3.3}$$

where

$I_{(.)}$ is the indicator function.

Likewise, the *pth* quantile can be estimated using

$$Q_n(p) = \inf\{x: F_n(x) \geq p\} = \sum_{i=1}^{n} X_{in} I_{\left(\frac{i-1}{n}<p\leq\frac{i}{n}\right)}\ . \tag{3.4}$$

According to the Glivenko-Cantelli theorem, the EDF converges to the "true" distribution function with a probability of one [Winter 1973]. Also, the difference between the *pth* sample and true quantiles, $Q_n(p)-Q(p)$, is asymptotically normally distributed with zero mean and variance $[q(p)]^2p(1-p)/n$ (where $q(p)=Q'(p)$, is the quantile density function) [Cheng 1995]. Other asymptotic properties of these estimators have been studied by a number of authors who also showed that these can be extended to smoothed/perturbed versions of the above estimators. The asymptotic normality property of the quantile function is explored further in Section 3.2.2. In statistical models where it is known or reasonable to assume that $F(x)$ is smooth, it is common to use smoothed

random functions as estimators of $F(x)$ and $Q(p)$. The best known of these estimators are kernel estimators. The kernel estimates of the distribution and quantile functions are defined respectively as

$$\hat{F}_n(x) = \frac{1}{n}\sum_{i=1}^{n} K\left(\frac{x - X_i}{h_n}\right) \tag{3.5}$$

and

$$\hat{Q}_n(p) = \frac{1}{nh_n}\sum_{i=1}^{n} k\left(\frac{i/n - p}{h_n}\right) X_{i,n} \tag{3.6}$$

where $h_n \to 0$ as $n \to \infty$ and $K(t) = \int_{-\infty}^{t} k(t)dt$ is a suitable distribution function. There are other definitions for the kernel quantile estimator. Yang [1995] introduced the kernel quantile estimator defined by Equation (3.6). While Equation (3.6) is very simple, it is not always easy to use. Kernel estimators like most nonparametric methods have a drawback in the choice of the bandwidth (smoothing parameter) h_n. A wrong choice of this parameter will either under- or over-smooth the representation of the true distribution. The next section discusses how this choice can be made.

3.2.1 Selection of Smoothing Parameter

Because it is easier for cost estimators to specify the accuracy required for the quantile function, it is suggested that the PDF be estimated by inverting the estimate of the quantile function. The optimal choice of h_n, h_{opt}, depends on both the sample size and the underlying distribution, the latter being what has to be determined. Usually, h_{opt} is chosen to minimize the asymptotic mean squared error of the estimate. For all fixed

$p \in (0,1)$, apart from $p \approx 0.5$ when $F(x)$ is symmetric, the asymptotically optimal bandwidth is given by [Sheather and Marron 1990],

$$h_{opt} \approx \alpha(K) \cdot \beta(Q) \cdot n^{-1/5} \tag{3.7}$$

where

$$\alpha(K) = \left[2 \int_{-\infty}^{\infty} uk(u)K(u)du \Big/ \left\{ \int_{-\infty}^{\infty} u^2 k(u)du \right\}^2 \right]^{1/3}$$

$$\beta(Q) = \left[Q'(p) / Q''(p) \right]^{2/5}.$$

When $F(x)$ is symmetrical, there is no single bandwidth that minimizes the asymptotic mean squared error of $\hat{Q}_{0.5}$. Any $h = \gamma n^{-m}$ $(0 < m \leq 1/2)$ will produce a good estimate [Sheather and Marron 1990].

The value of h_{opt} in Equation (3.7) depends on the first and second derivatives of the quantile function. Thus estimates of $Q'(p)$ and $Q''(p)$ using the data are needed for the determination of h_{opt}. Unfortunately, that will also involve the determination of two smoothing parameters. Sheather and Marron [1990] discuss in detail how this can be done. Alternative methods of obtaining data based bandwidths can be found in [Zelterman 1990] and [Yang 1995]. These two approaches can be used to select an h_n for a smooth estimate of the entire quantile function on an interval $[p_1, p_2]$, $0 < p_1 < p_2 < 1$.

All the aforementioned approaches are very elaborate and computationally and/or mathematically complex. Apart from extreme quantiles, there may be little difference between kernel quantile estimates and the sample quantiles. Given the well know distribution-free inference procedures (e.g., easily constructed confidence intervals) associated with the sample quantile, as well as the ease with which it can be calculated,

it will often be a reasonable choice as a quantile estimator [Sheather and Marron 1990], if it is not desirable to expend too much effort in determining h_n. That is, if there is no simple rule to determine h_n, then it will be easier to sample extra data to improve the sample quantile estimate than to obtain a good bandwidth for a limited data set when using kernel estimators. Simulation studies suggest that, $h_n=\gamma n^{-m}$ $(0<m\leq 1/2)$ will be appropriate. Azzalini [1981] suggests $m=1/3$ and Zelterman [1990], $m=0.4153$. Additionally, the optimum choice of γ ranges between σ and 2σ ($\sigma^2=p(1-p)$), for a large number of distributions when estimating the long tail [Azzalini 1981]. However, a compromise value of $\gamma=1.3\sigma$ is satisfactory. When estimating the quantiles not in the long tail region, $\gamma=0.5\sigma$ is more appropriate [Azzalini 1981]. For convenience, $\gamma=(1.3+0.5)\sigma/2=0.9\sigma$ could be used giving $h_n=0.9\sigma n^{-1/3}$ for the entire quantile function. However, because of the manner in which the data would be sampled in this thesis, the approach of Zelterman [1990] can be used for an exploratory study with an initial set of $\bar{n}$ data points to determine $b=\gamma/\sigma$ and then calculate subsequent h_ns using

$$h_n = b\sigma n^{-1/3}. \tag{3.8}$$

Following Zelterman [1990], the measure of global fit, M, of the kernel estimate $\hat{Q}(p)$, of p is defined as

$$M = \sum_{i=1}^{n} i(n-i+1)\left(\hat{Q}(i/(n+1)) - Q(i/(n+1))\right)^2. \tag{3.9}$$

If $\hat{Q}_i$ denotes the estimator of $Q_n(i/(n+1))$ for the jackknifed sample of size $n-1$ in which X_{in} has been omitted, then the cross-validated estimate of $b_{\bar{n}}$ is defined as the $b_{\bar{n}}$ that minimizes,

$$\tilde{M} = \sum_{i=1}^{n} i(n-i+1)\left(\hat{Q}_i - X_{in}\right)^2 - \sum_{i=1}^{n} i(n-i+1)\left(\hat{Q}(i/(n+1)) - X_{in}\right)^2 \qquad (3.10)$$

subject to $0.5 \le b_{\bar{n}} \le 2.0$. The range $0.5 \le b_{\bar{n}} \le 2.0$, is motivated by [Azzalini 1981].

3.2.2 Confidence Intervals

If the kernel and the underlying distribution satisfy the regularity conditions (A1-A4), then the asymptotic normality of $\hat{Q}_n(p)$ is assured.

A1) The characteristic function corresponding to $k(x)$ is absolutely integrable.

A2) The density function $f(x)$ is bounded and uniformly continuous.

A3) $n^{-1/2}[E(\hat{F}_n(x)) - F(x)] \to 0$ as $n \to \infty$ (this is fulfilled if, for instance, $k(-x)=k(x)$, $\int_{-\infty}^{\infty} x^2 k(x)dx < \infty$, $F(x)$ has a bounded second derivative and $n^{1/2}h_n^2 \to 0$ as $n \to \infty$).

A4) $nh_n^2 \to \infty$ as $n \to \infty$.

Although a large number of kernel functions, including the Epanechnikov kernel which will be defined and used in Chapter 6, satisfy these conditions, they are a bit restrictive. Condition A1 requires the kernel k, to be uniformly continuous. This excludes kernels such as the uniform and step function kernels which are quite appropriate in practice. Secondly, A3 and A4 require that for every constant $\gamma > 0$ and n large enough, $n^{-1/2} < \gamma h_n < n^{-1/4}$. This excludes sequences which may converge to zero in the range $[0,0(n^{-1/2})]$, thus leaving many statistically interesting cases uncovered. Sun and Ralescu [1993] specified more generalized regularity conditions on the underlying distribution and kernel and are given below.

Conditions on the underlying PDF F:

B1) i. f is differentiable with bounded derivative f' on the support of F and $f(Q(p))>0$.

ii. f' is continuous in a neighborhood of $Q(p)$ and $f'(Q(p)) \neq 0$.

or

B2) i. f is bounded and $f(Q(p))>0$.

ii. f is continuous in a neighborhood of $Q(p)$.

Conditions on kernels k:

C1) $\int_{-\infty}^{\infty} xk(x)dx = 0$ and $\int_{-\infty}^{\infty} x^2 k(x)dx < \infty$

or

C2) $\int_{-\infty}^{\infty} |x|k(x)dx < \infty$ but $\int_{-\infty}^{\infty} xk(x)dx \neq 0$

Ralescu and Sun [1993] showed that

1. If f and k satisfy B1 and C1, then the condition $\lim_{n\to\infty} n^{1/4} h_n = 0$, is necessary and sufficient for

$$n^{1/2} f(Q(p))[\hat{Q}_n(p) - Q(p)] \xrightarrow{D} N(0, p(1-p)). \qquad (3.11)$$

2. Under conditions B2 and C2, Equation (3.11) holds if and only if $\lim_{n\to\infty} n^{1/2} h_n = 0$.

Thus for $0<\alpha<1$, and z denoting the $100(1-\alpha/2)\%$ quantile of the standard normal distribution function, a $100(1-\alpha)\%$ confidence interval for $\hat{Q}(p)$ can be constructed using

$$I_n = \left[\hat{Q}_n(p) - \frac{z\sigma}{n^{1/2} f(Q(p))}, \hat{Q}_n(p) + \frac{z\sigma}{n^{1/2} f(Q(p))} \right] \tag{3.12}$$

where $f(Q(p))$ denotes the density quantile function and $\sigma^2=p(1-p)$ has confidence coefficient converging to α as $n\to\infty$. Unfortunately, $f(Q(p))$ is unknown and has to be estimated. This complicates the approach. An alternative is to consider a pair of sequences $p_{n1}<p<p_{n2}$ such that as $n\to\infty$, $p_{n1}\approx p-z\sigma n^{-1/2}$ and $p_{n2}\approx p+z\sigma n^{-1/2}$ [Ralescu and Sun 1993]. Equation (3.13) then gives the confidence interval.

$$\begin{aligned} \hat{I}_n &= \left[\hat{Q}_n(p_{n1}), \hat{Q}_n(p_{n2}) \right] \\ &= \left[\hat{Q}_n(p - z\sigma n^{-1/2}), \hat{Q}_n(p + z\sigma n^{-1/2}) \right]. \end{aligned} \tag{3.13}$$

As is apparent from the above, the advantage of this approach is that $f(Q(p))$ does not need to be estimated.

3.2.3 Stopping Rule

The approach suggested in this thesis for the determination of the PDF of cost model outputs is based on the statistical techniques discussed above. As stated earlier, what is required is a simulation approach that permits the sampling of just enough data points for the desired accuracy and also that the PDF is going to be estimated by inverting the estimate of the quantile function. This is done because it is easier to specify the desired accuracy in terms of deviations of the cost estimates than in terms of probabilities. From the discussion above, in estimating a quantile for a predetermined confidence interval $\zeta>0$, it is reasonable to use the stopping rule n_s given by

$$n_s = \inf\left\{ n \geq 1, \hat{Q}_n(p + z\sigma n^{-1/2}) - \hat{Q}_n(p - z\sigma n^{-1/2}) \leq \zeta \right\}. \tag{3.14}$$

In estimating a set of quantiles Ω, to describe the entire distribution, this can be applied to the quantiles simultaneously. This leads to the stopping rule n_Ω given by

$$n_\Omega = \inf\left\{ n \geq 1, \sup_{p \in \Omega} \left[\hat{Q}_n(p + z\sigma n^{-1/2}) - \hat{Q}_n(p - z\sigma n^{-1/2}) \right] \leq \zeta \right\}. \qquad (3.15)$$

It might not be computationally efficient to apply the above tests each time a new random sample is obtained. The data can be sampled in batches of a reasonable size n' and the test applied each time a batch of data is sampled. Furthermore, it should be noted that ζ does not need to be the same for all the quantiles. It can be expressed as a percentage of the quantile. This is a reasonable approach given the fact that cost contingencies are normally specified in this manner and the quantile function is an increasing function. Once sampling has been stopped, other statistical functions (density function, quantile density function etc.) and population parameters (mean, variance, skewness, kurtosis etc.) can be estimated from the data.

3.3 Treating Statistical Dependence

In the preceding development of the simulation procedure for cost estimating, it was assumed that the random cost variables were independent. That is, it was assumed that the value of one parameter was not influenced by any other parameters in the CER. This might not be so in practice. There may exist interdependencies amongst parameters and it is imperative that the degree of interdependence between the parameters be considered since ignoring it could lead to results of little practical value.

Measures of association assign a numerical value to the degree of association or strength of relationship between variables. Two variables are associated if they are not independent. Many different kinds of measures of association between two or more variables have been proposed and their values may need to be interpreted differently [Gibbons 1993]. The most commonly used measure of association for two variables is the *correlation coefficient*. It is calculated as the ratio of the covariance between the two variables to the product of the respective standard deviations. The value of this coefficient always lies between -1 and +1. While the independence of variables implies a zero value, the converse does not generally apply. It does apply for jointly normal variables, and sometimes for others [Kendall and Stuart 1961] that can be closely approximated by the normal distribution. Herein lies the difficulty in interpreting the correlation coefficient as a general measure of interdependence. In fact, it is essentially a coefficient of linear interdependence. That is, it should be used only when there are reasons to believe that the dependency between two variables can be described by a linear relationship. In general, the problem of correlation is too complex to be fully accounted for in a single coefficient. In practical work, except in normal or near-normal variation, the correlation coefficient is not recommend for use as a measure of interdependence [Kendall and Stuart 1961].

The foregoing discussion not withstanding, it is not easy to specify these correlation coefficients. Dependencies for a set of variables can be specified through the correlation coefficients in the form of a correlation matrix. A correlation matrix is any symmetric, positive semi-definite matrix having unit diagonal elements and the non-diagonal elements equal to the pairwise correlation between the variables. In many practical

situations, not enough data is available to accurately compute a correlation matrix and the correlations are frequently derived from expert opinion, usually the combined opinions of many experts [Lurie and Goldberg 1998]. This might result in an inconsistent correlation matrix, i.e. one that is not positive semi-definite. This inconsistency can also occur if the pairwise correlations are estimated empirically but are not all based on the same set of observations [Lurie and Goldberg 1998]. Lurie and Goldberg [1998] have developed an approach to rectify such inconsistencies should they exist. The approach first checks for these mathematical consistency (positive semi-definiteness), and adjusts the matrix if necessary to achieve a matrix as close as possible to the original correlation matrix and is also positive semi-definite.

It is obvious that the use of the correlation coefficient to incorporate dependency is not that simple and straight forward. However, there are times when there is the need for this to be done and it is better to make explicit assumptions about the degree of correlation (dependency) between variables or equations than to ignore it and thereby assume it is zero. To incorporate dependency in the simulation based cost estimating approach discussed above, what is needed is the ability to generate correlated random variables. Methodologies exist for that purpose. If the individual cost variables are normally or lognormally distributed, then the specification of the correlation coefficients permits an easy and exact generation of the correlated random variables. The problem is not that straight forward when the random variables are of different forms. An algorithm for generating approximate correlated vectors of random numbers for any set of continuous, strictly increasing distribution functions is presented in Lurie and Goldberg [1998]. This algorithm requires that the user at least specify the marginal distributions

and the correlation matrix. Once the random numbers are generated, the procedure for determining the PDF of the cost estimate is just as discussed earlier.

Given the limitations of the correlation coefficient and the problems associated with specifying these coefficients, it might be better to stress the development of CERs that consist of only independent variables. This is motivated by the fact that, given any CER C, with N correlated variables, it is always possible to designate N' variables as independent variables and express the remaining N-N' dependent variables in terms of the N' independent variables. Replacing these in C would give a new CER, C', which will be a function of only the new independent variables.

3.4 Summary

In this chapter, some of the issues that have been overlooked in attempts to quantify the uncertainties associated with cost estimates through simulation were identified. A simulation approach employing kernel estimation techniques and their asymptotic properties in the development of the PDFs of cost estimates was proposed. This approach to cost estimating will provide information about the cost estimate that is invaluable in decision making. It is anticipated that employing this approach will eliminate some of the guess work in simulation based cost estimating procedures and also reduce the amount of data sampled. The approach will also make it easier for

estimators to specify the required accuracy desired in the estimated distribution. To illustrate this approach, a probabilistic cost estimating problem is treated in Chapter 6 of this thesis.

The incorporation of life-cycle cost analysis into the design of an HVAC air duct system is shown in the next chapter.

4 Life-Cycle Cost Based Methodologies for Air Duct Design

4.1 Introduction

They are four steps to LCC analysis. These are

1. Identify the costs involved.
2. Develop relationships for each cost as a function of economic and design parameters and determine how design parameters affect these costs (by definition, economic parameters can not be influenced by the design).
3. Develop design methodologies or procedures based on this knowledge.
4. Incorporate uncertainty in (2) and (3) above.

In the following sections, the implementation of the aforementioned aspects of LCC analysis in the case of an HVAC air duct design is illustrated. The duct design problem and its associated cost model are described next. Then the development of a number of methodologies that explicitly incorporate cost information in duct system design are described. The theory behind the IPS-Method of duct design and how it can be extended to develop charts for duct design are discussed first. The latter part of this chapter is dedicated to the discussion of Genetic Algorithms and its application to air duct design.

4.2 The Air Duct Sizing Problem

In designing an air duct system, the designer usually starts off with a duct system layout and air flow rates in each duct section. What is required is to select the materials for the ducts and fittings, duct sizes and fan(s). A schematic for a very simple HVAC air duct system is shown in Figure 4.1 (the flow rates are not indicated). This system has four duct sections or elements numbered 1 through 4 and 2 airflow paths comprised of sections (4 and 3), and (4, 2 and 1). Duct elements 4, 3 and 1 are specified round ducts and duct 2 is rectangular.

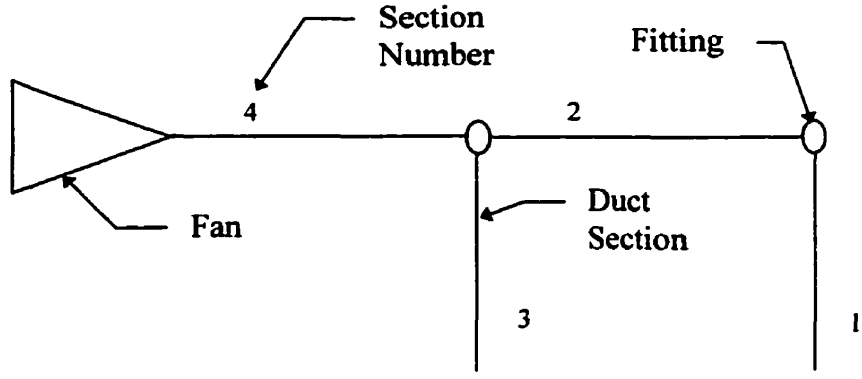

Figure 4.1: A Simple Duct System.

The duct size optimization problem can be stated as follows:

$$\textbf{Minimize} \quad E = E_p(PWEF) + E_s \tag{4.1}$$

Subject to

pressure balancing for each flow path

$$\sum_{x \in I} \Delta P_x = P_{fan} \qquad \text{for } \iota \in S_s \qquad (4.2)$$

size and flow limitations

$$d_x^{\min} \le d_x \le d_x^{\max} \qquad \text{for } x=1,2,\ldots,X \qquad (4.3)$$

$$d_x \in SD \qquad \text{for } x=1,2,\ldots,X \qquad (4.4)$$

$$V_x^{\min} \le V_x \le V_x^{\max} \qquad \text{for } x=1,2,\ldots,X \qquad (4.5)$$

where

E = Present worth owning and operating cost (LCC)

E_p = First year energy cost

E_s = Initial Cost

$PWEF$ = Present worth escalation factor

ΔP_x = Total pressure losses in duct section x

P_{fan} = Total fan pressure

S_s = Set of paths in a (sub)system s

I = Set of duct sections in path ι

SD = Set of standard duct sizes

X = Total number of duct sections in the system

x = Index (number) of the duct section

d_x = Size of duct section x

$d_x^{\min}$ = Minimum allowable size for duct section x

d_x^{max} = Maximum allowable size for duct section x

V_x^{max} = Maximum allowable velocity for duct section x

V_x^{min} = Minimum allowable velocity for duct section x.

The set of constraints above is not exhaustive. Other problem specific constraints might exist. Generally, the pressure balancing constraints, Equation (4.2), are the most difficult constraints to satisfy. It is virtually impossible to achieve equal path pressure losses in an HVAC air duct system without the use of dampers. HVAC air duct designers, therefore, aim for a design that has an acceptable level of path pressure imbalance. Furthermore, Equation (4.4) requires that the duct sizes assume values from a fixed set of sizes. This makes the use of methods such as Lagrange multipliers and projected gradient that require that the decision variables be continuous, inappropriate. The issues of material selection and duct leakage are not treated in this thesis.

4.2.1 The Air Duct System Cost Model

The Life-Cycle Cost (LCC) of a duct system comprise the initial cost and the operating cost. This is expressed in Equation (4.1). The initial cost, E_s, includes, fan, materials, handling and installation labor, shop drawings, shipping and a mark up for overhead, maintenance and insurance. The annual operating cost, E_p, is usually the energy cost.

The energy cost is determined by

$$E_p = \frac{Q_{fan}\left(E_d + E_c T\right) P_{fan}}{10^3 \eta_f \eta_m} \tag{4.6}$$

where

Q_{fan} = Fan airflow rate (m^3/s)

E_c = Unit electrical energy cost (cost/kWh)

E_d = Energy demand cost (cost/kW)

T = Operational time (hours/year)

P_{fan} = Fan total pressure (Pa)

η_m = Motor drive efficiency

η_f = Fan total efficiency.

The present worth escalation factor is calculated as follows:

$$PWEF = \begin{cases} \dfrac{\left[(1+j)/(1+i)\right]^m - 1}{1-\left[(1+i)/(1+j)\right]} & if\ i \neq j \\ i & if\ i = j \end{cases} \qquad (4.7)$$

where

m = Amortization period (years)

i = Interest rate

j = Escalation rate.

The initial cost of a duct section is given by the following equations:

for round ducts,

$$E_s = S_d \pi L D \qquad (4.8)$$

where

D = Duct diameter (m)

L = Duct length (m)

S_d = Unit duct cost ($cost/m^2$),

for rectangular ducts,

$$E_s = 2S_d(H+W)L \tag{4.9}$$

where

H = Duct height (m)

W = Duct width (m).

If the equivalent by cost diameter D_c is defined to be equal to D for round ducts and $\frac{2(H+W)}{\pi}$ for rectangular ducts, then Equations (4.8) and (4.9) can be rewritten as

$$E_s = S_d \pi L D_c . \tag{4.10}$$

By combining Equations (4.1), (4.6)-(4.10), the total life-cycle cost can be rewritten as

$$E = \sum_{x=1}^{X}\left(Q_x \Delta P_x \left[\frac{\left(E_d + E_c T\right)}{10^3 \eta_f \eta_m} \right] PWEF + S_d \pi L_x D_{cx} \right). \tag{4.11}$$

4.3 The IPS-Method of Duct Design

For each individual duct section in an HVAC air duct system, the first term on the right hand side of Equation (4.11) is the cost of the energy needed to overcome the frictional forces in that duct section and the second term is the initial cost of that duct. This can be represented by Figure 4.2. Increasing the duct size results in a decrease in the energy cost and an increase in the initial cost of that duct section. Thus the optimal duct size (the duct size corresponding to the minimum point of the Total Cost line in Figure 4.2) can be found by optimizing the following function for each individual duct (for clarity the subscripts on the right hand side of the equation have been dropped):

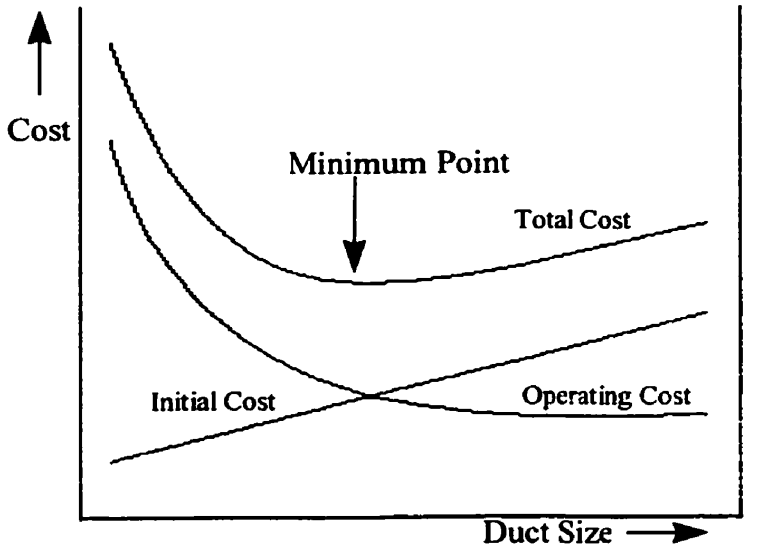

Figure 4.2: Cost Structure of Air Duct Section.

$$E_x = Q\Delta P \frac{Z}{10^3} + S_d \pi L D_c \tag{4.12}$$

with

$$\Delta P = \left(\frac{fL}{D_h} + \sum C \right) \frac{V^2 \rho}{2} \tag{4.13}$$

and

$$Z = \frac{\left(E_d + E_c T\right) PWEF}{\eta_f \eta_m}, \tag{4.14}$$

where

f = Friction factor[1]

D_h = Hydraulic friction diameter (m).

[1] See Appendix A for how the friction factor is calculated.

$\sum C$ = Summation of dynamic friction loss coefficient for duct fittings within the duct section.

For a circular duct section, Equation (4.12) can be rewritten as

$$E_x = \frac{8\times10^{-3}Q^3Z\rho}{\pi^2}\left(\frac{fL}{D^5}+\frac{\sum C}{D^4}\right)+\pi S_d LD. \tag{4.15}$$

The optimal duct size can thus be found by differentiating Equation (4.15) with respect to D giving

$$\frac{\delta E_x}{\delta D} = -\frac{8\times10^{-3}Q^3Z\rho}{\pi^2}\left(\frac{5fL}{D^6}+\frac{4\sum C}{D^5}\right)+\pi S_d L \tag{4.16}$$

where f and ΣC are assumed to be constant.

Equating the above equation to zero gives

$$D^5 = \frac{8\rho}{\pi^3}\left(\frac{Z}{10^3 S_d}\right)\left(\frac{Q^3}{L}\right)\lambda_C \tag{4.17}$$

where

$$\lambda_C = \frac{5fL}{D}+4\sum C. \tag{4.18}$$

This implies an iterative solution because D is on both sides of Equation (4.17) when ΣC is significant.

For a rectangular duct, Equation (4.12) becomes

$$E_x = \frac{10^{-3}Q^3Z\rho}{W^2}\left(\frac{fL}{4H^2W}+\frac{fL}{4H^3}+\frac{\sum C}{2H^2}\right)+2S_d(H+W)L. \tag{4.19}$$

If the dimension of one side has already be fixed, the optimal dimension of the other side of the duct can be determined by following a procedure similar to that above. In this thesis, it is assumed that the height is fixed. This leads to an optimal width given by

$$W^3 = \frac{\rho}{2}\frac{Z}{10^3 S_d}\frac{Q^3}{LH^2}\lambda_R \tag{4.20}$$

where

$$\lambda_R = \frac{fL}{2H} + \frac{3fL}{4W} + \sum C. \tag{4.21}$$

H and W in Equations (4.19)-(4.21) and all other expressions involving these two parameters would have to be switched in cases where the width is fixed and the height needs to be determined.

The duct section property, λ_C or λ_R, is defined as the *Friction Parameter* and $Z/(1000S_d)$ m^2/kW, as the *Economic Factor*. In the development of Equations (4.17) and (4.20), it was assumed that f and ΣC were independent of D or W. In reality, this is not so. However, the error introduced by this assumption is no worse than the uncertainty associated with the calculation or determination of f or ΣC. Uncertainties in f and ΣC will be discussed in more detail in Chapter 6. It was also assumed that each duct existed in isolation thus making the pressure balancing constraints redundant. The duct dimensions given by Equations (4.17) and (4.20) are therefore not optimal with respect to the entire duct system which require that the pressure balancing constraints be satisfied.

4.3.1 The Design Procedure

In this section, a three-stage approach to duct system design based on the discussions of the preceding section is presented. For clarity, the explanation is done using a circular duct. Everything discussed here can be applied to rectangular ducts with the appropriate parameters and equations.

As noted above, the size of the duct that will achieve the optimal pressure drop in each duct section is given by Equation (4.17). Unfortunately, this value also depends on λ_C (Equation (4.18)) which in turn depends on D. That is, D can not be determined unless λ_C is known, and λ_C can not be determined until D has been determined. This interdependency calls for an iterative approach to the determination of D. Any initial value of λ_C can be selected and used to calculate D using Equation (4.17). Equation (4.18) can then be used in conjunction with tables of dynamic loss coefficients to determine λ_C. This process is repeated till the value of D converges. Normally, only standard size ducts are used, hence D can be said to have converged if successive Ds fall within the same interval of standard duct sizes. A choice between the two standard duct sizes $\lceil D \rceil$ (the smallest standard duct size $>D$) and $\lfloor D \rfloor$ (the largest standard duct size $<D$) will have to be made. This is done by computing the cost associated with each duct size using Equation (4.15) and selecting the size that gives us the lower cost. If at any time during the process outlined, it is determined that the duct size will violate a constraint other than the pressure balancing constraint, the procedure can be stopped and the duct size set to an appropriate fixed value.

In applying this approach to a duct system, one problem that will be encountered is the fact that dynamic loss coefficients at junctions depend not only on the size of the duct under consideration but also on the other duct sections attached to the that fitting. Thus, sizing of the ducts should be done simultaneously. However, if assumptions about the relationship between the sizes of the ducts at any junction are made, then the whole system becomes de-coupled and the duct sizes can be determined by applying this procedure to each duct separately. This is the approach adopted in the sample problems in Chapter 5. If the system consists of more than one sub-system, each sub-system should be treated separately.

As indicated in Equation (4.2), a constraint on the air duct design problem is the balancing of the pressure drops among each of the flow paths. The procedure outlined above requires that this be relaxed while determining the sizes of the ducts. It is therefore conceivable that the duct sizes determined will not satisfy the pressure balancing constraints. If such a situation arises, the sizes of the ducts must be modified to ensure a correct and acceptable design. The process of pressure balancing has been seen as an art depending mostly on the skills of the person doing the design (no systematic approach to this process other than trial and error, has been found in the literature). Using the approach above to determine the initial duct sizes, it is possible to approach the issue of pressure balancing in a systematic manner. Before discussing this, it will be expedient to introduce a number of terms

Dominant Path = the path with the highest path pressure loss.

Dominant Section = a duct section on the dominant path.

Path Pressure Differential = the difference between the dominant path pressure loss and the pressure loss of any other path.

Duct Occurrence Density is defined as

$$\partial_x = \frac{Number\ of\ paths\ with\ duct\ section\ x\ common}{Total\ number\ of\ paths}. \qquad (4.22)$$

In order to balance the path pressure losses, a system pressure has to be selected and then the sizes of the ducts changed accordingly to approach this pressure. There are three options when it comes to the selection of the system pressure. The selected system pressure can be equal to

1. the lowest path pressure loss,
2. the highest path pressure loss or
3. a pressure in between the lowest and highest path pressure losses.

A system pressure loss equal to the highest path pressure loss is recommended. The reason for this is that, to ensure that all the path pressures are balanced, the duct sizes of the other ducts, will have to be reduced - a process termed, *Pressure Augmentation*. This will in turn reduce the initial cost of those ducts. On the other hand, if a system pressure corresponding to the lowest path pressure loss was chosen, then to ensure a pressure balance, certain duct sizes will have to be increased. This would cause the initial cost to increase and may involve the relaxation of some maximum duct size constraints. For a system pressure in between the two points, certain duct sizes will have to be reduced and others increased. Thus there will be an increase in the initial cost of certain ducts while others will decrease in initial cost. The overall consequence of the changes can not therefore be predicted easily.

There are two things that can happen as pressure balancing proceeds. Either a point is reached were the pressures of the non-dominant paths can no longer be changed without violating other system constraints or a new dominant path with a path pressure higher loss higher than the system pressure emerges. In the first case, there will be a need to reduce the system pressure by increasing the sizes of some dominant sections - a process termed, *Size Augmentation.* In the second case, unless the resulting path pressures are acceptable to the designer, any change that results in a new dominant path will have to be reversed.

With the foregoing discussion in mind, a new algorithm for optimal duct sizing has been developed. The aim is to attempt to balance the system without increasing the initial system pressure. However, when this is not possible, the algorithm permits an increase in the system pressure in order to balance the system. The algorithm given below is divided into three separate stages, ***Initial Duct Sizing, Pressure Augmentation and Size Augmentation***, hence the name, **IPS-Method.**

Initial Duct Sizing

1. Size each duct using the iterative procedure outlined above.
2. Calculate the path pressure loss for each path.
3. If the path pressure losses are not balanced within a specified tolerance, select the highest path pressure loss as the system pressure and go to the Pressure Augmentation stage, otherwise select the fan and stop.

Pressure Augmentation

1. Identify the dominant path and sections.
2. Rank each path. Paths with higher path pressure differentials must be ranked higher. Do not include the dominant path in this ranking.
3. Rank the non-dominant duct sections according to the duct occurrence density (Equation (4.22)) in descending order. Do not include a duct if its size can not be reduced any further.
4. Select the path at the top of the path list created in Step 2. If there is no path in the path list go to Step 9.
5. Select the duct from the path that is ranked highest in the duct list created in Step 3. If no such duct section exists, take the path off the path list and go to Step 2.
6. Reduce the size of the duct.
7. Calculate the path pressure losses.
8. If the change in Step 6 results in an unacceptable design (i.e. violation of a constraint, a higher maximum pressure differential or a change in the dominant path resulting in an increase in the system pressure without an accompanying satisfactory path pressure distribution), reverse the change and take that duct off the duct list onto a temporary duct list and go to Step 4.
9. If the pressure distribution is satisfactory, stop and select the fan. Otherwise, if there are no more paths on the path list and no ducts on the temporary duct lists go to the Size Augmentation stage. Go to step 2.

Size Augmentation

1. Rank the dominant sections according to the duct occurrence density in ascending order. However, do not include any duct with δ=1 and those with sizes that can not be increased any further
2. Select the duct ranked highest in the duct list created in Step 1. If no ducts sections exist, stop. That is the best design possible. Select the fan.
3. Increase the size of the duct.
4. Calculate the path pressure losses.
5. If the change in Step 3 results in a violation of a constraint or a higher maximum pressure differential, reverse the change and take that duct off the duct list and go to Step 2.
6. If the pressure distribution is satisfactory stop and select the fan. Otherwise, go to Step 1 of the Pressure Augmentation stage.

It is conceivable that the algorithm's exit from Step 2 of the Size Augmentation stage will result in a final design that will have a maximum pressure differential that is more than desired. To verify if this is the best possible pressure distribution, the procedure can be repeated with Step 8 of the Pressure Augmentation stage replaced with Step 8A below.

8A. If the change in Step 6 results in an unacceptable design (i.e. violation of a constraint or a higher maximum pressure differential) reverse the change and take that duct off the duct list and put it onto a temporary duct list. If the highest path pressure loss is more than the current system pressure, set the system pressure to this value. Go to Step 4.

This will permit the exploration of the possibility of increasing the system pressure in order to achieve a better pressure distribution in the system. When there is the need to make a distinction, the algorithm with Step 8 shall be referred to as the *Standard IPS* and that with Step 8A as the *Revised IPS*.

4.4 Diameter and Enhanced Friction Charts

The Friction Chart is a chart that gives the pressure loss per unit length in straight circular ducts for different flow rate/diameter and flow rate/velocity combinations. This can be used for selecting the sizes of ducts during design. ASHRAE [1997] recommends that for an economical design, the duct sizes should be selected with frictional losses within the dark band of Figure 4.3. This recommendation has no explicit economic justification because no costs are included in the analysis. In this section, the development of charts that explicitly incorporate economic information is discussed.

For a straight circular duct section with no fittings, Equation (4.17) reduces to

$$D^6 = \frac{40 \times \rho}{\pi^3}\left(\frac{Z}{10^3 S_d}\right)Q^3 f \,. \tag{4.23}$$

A procedure akin to that discussed in Section 4.3.1 can therefore be used to determine D and consequently $\Delta P/L$, for various values of the economic factor and flow rate. The information can then be used to develop charts that can be used to read off the value of D that satisfies Equation (4.23) once the economic factor and flow rate are known. Figure 4.4 is what is termed the *Diameter Chart* and Figure 4.5 is the *Enhanced Friction*

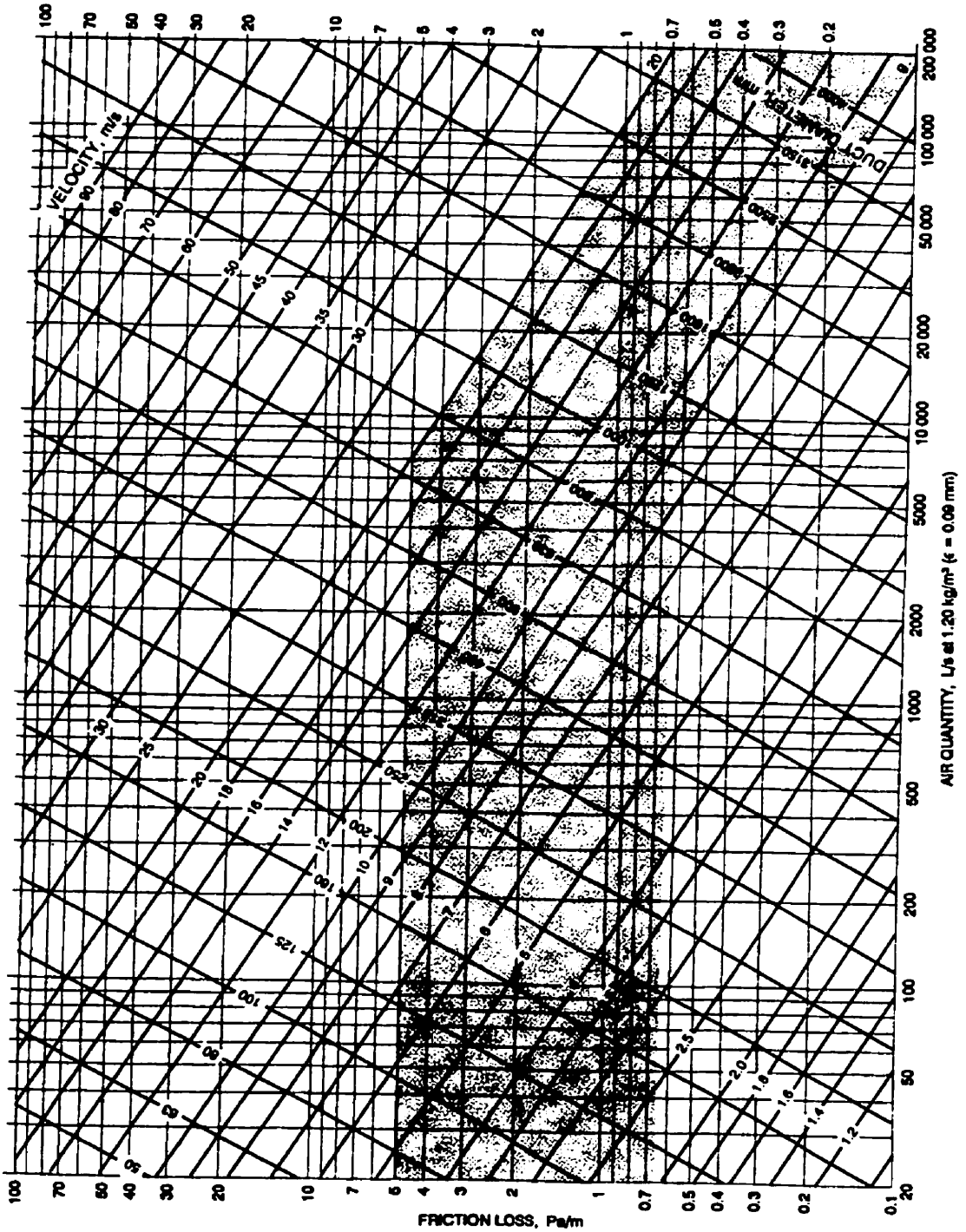

Figure 4.3: Friction Chart (ε=0.09mm).

Chart (these are for air with ρ=1.2kg/m^3 and duct surface roughness ε=0.09mm). The use of Figure 4.4 is straight forward. To use the Enhanced Friction Chart for a duct design problem, first, calculate the economic factor for the duct section and identify that line on the chart. The duct diameter is then selected so that the flow rate, the economic factor and the diameter lines intersect. Since most ducts in real design problems will have additional losses, it may be better to use an economic factor line that is slightly lower (i.e. has a higher value) than that initially calculated. For example, if the dynamic losses are expected to account for a quarter of all the losses and the economic factor is determined to be 2, then the revised economic factor of 2x(1+0.25)=2.5 may be used.

For a straight rectangular duct section with no fittings Equation (4.20) reduces to

$$W^4 = \frac{\rho}{8}\left(\frac{Z}{10^3 S_d}\right)\frac{Q^3 f(2W+3H)}{H^3}. \tag{4.24}$$

Unlike Equation (4.23) for the round duct, it is not easy to incorporate this information in the form of a chart because of the dependence of the width on the height or vice versa. However in designing rectangular sections, the equivalent round duct could be selected and then the dimensions of the rectangular duct approximated using Equation (4.25)[2] providing $D_e >> 2H/\pi$.

$$D_e = 1.476 \times \left(\frac{W^4 H^3}{2W+3H}\right)^{1/6} \tag{4.25}$$

This function is not analytic and therefore an iterative method should be used to determine the corresponding dimensions of the rectangular duct.

[2] The complete derivation of Equation (4.25) is given in Appendix B.

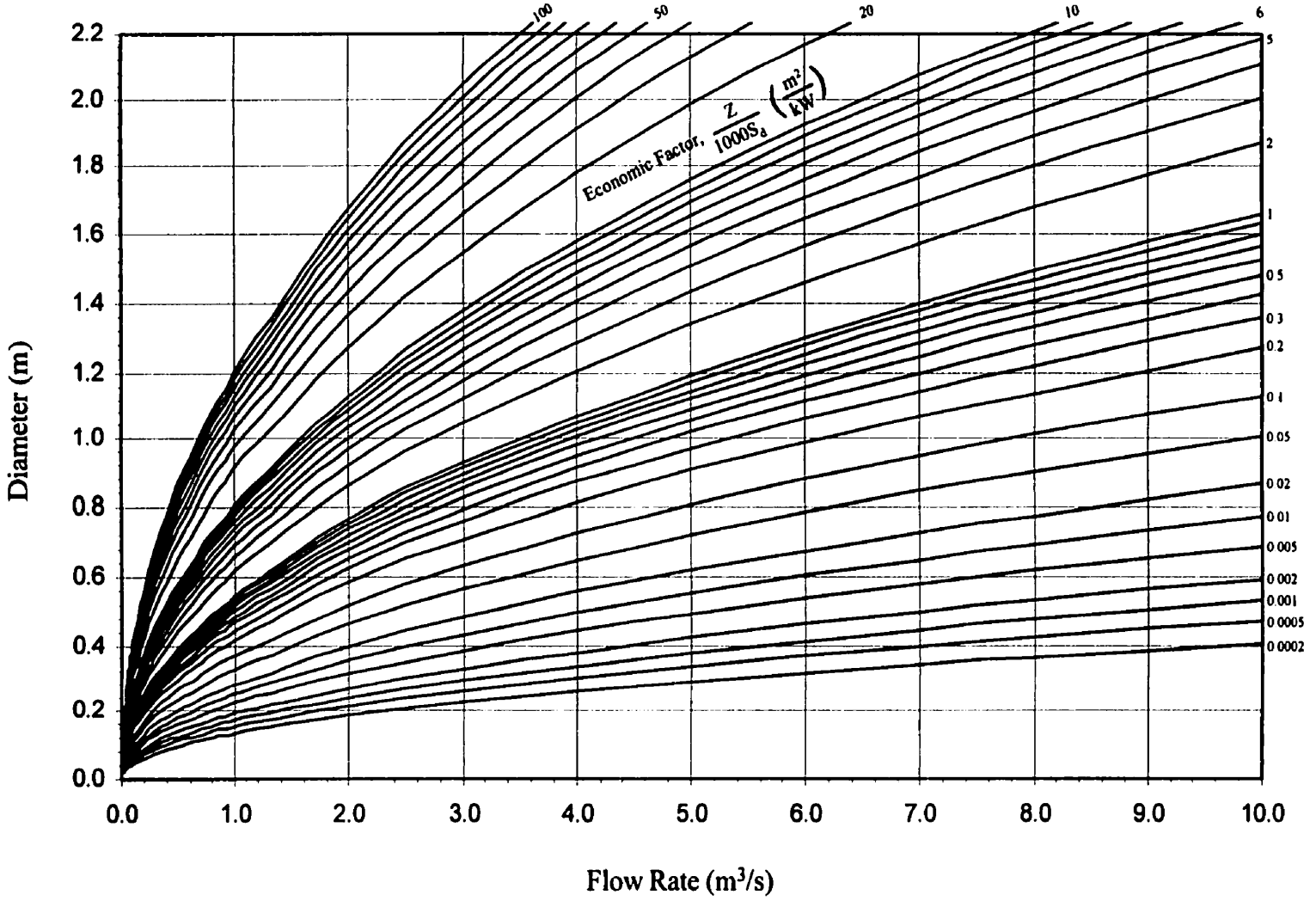

Figure 4.4: Diameter Chart (ε=0.09mm and ρ=1.2 kg/m^3).

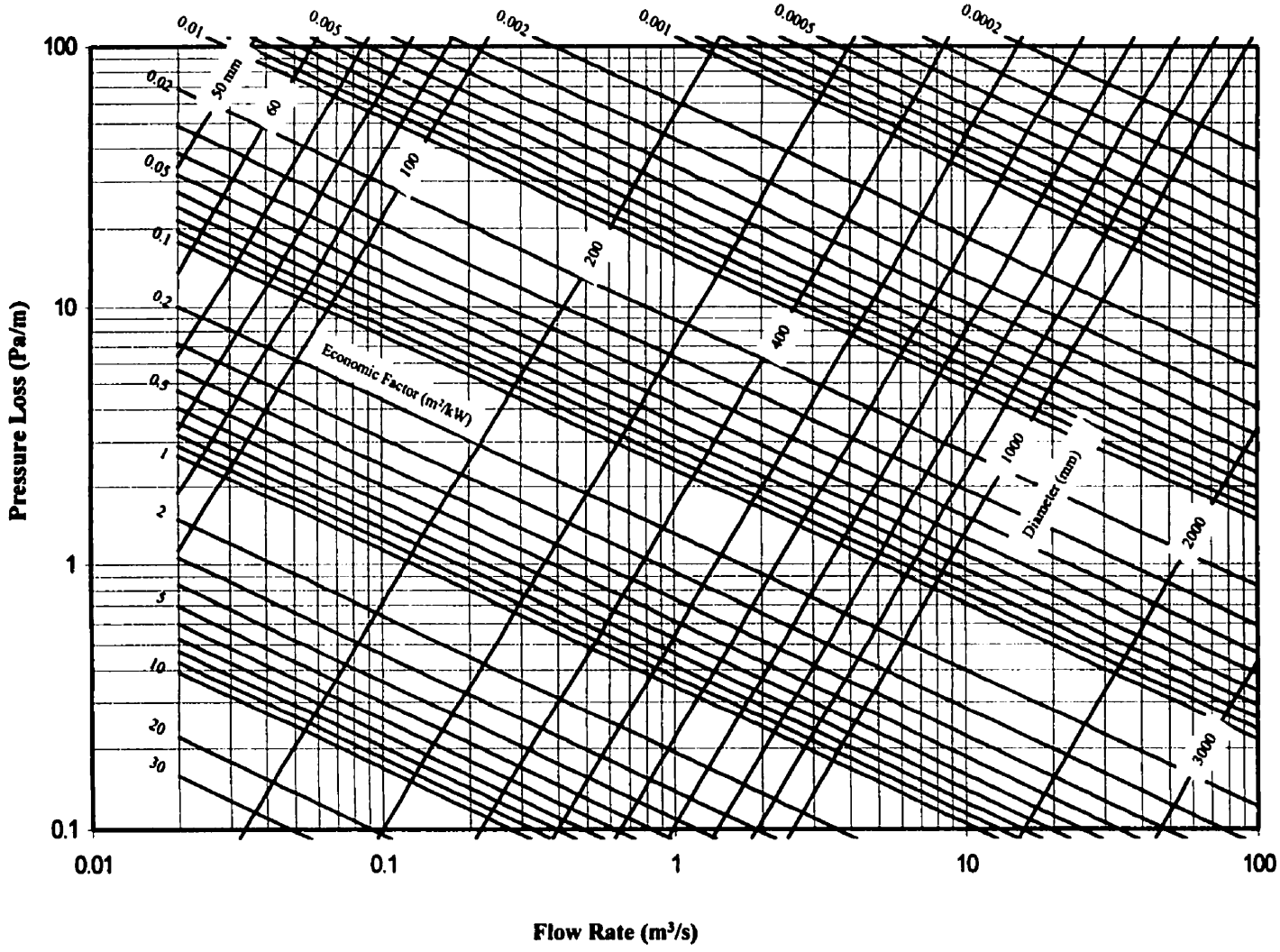

Figure 4.5: Enhanced Friction Chart (ε=0.09mm and ρ=1.2 kg/m^3).

The significant difference between the chart in Figure 4.5 and that provided by ASHRAE [1997] (Figure 4.3) is the extra capabilities incorporated into Figure 4.5 by replacing the velocity lines of the standard friction chart with the economic factor lines. In using the standard friction chart to size a duct, only the flow rate of the duct section is explicitly considered. For instance, if a duct with a flow rate of $0.1m^3/s$ (100 L/s) is to be sized using the friction chart in [ASHRAE 1997], it is recommended that a duct size between approximately 165 and 210mm be selected irrespective of the values of the economic parameters, i.e. cost of materials and energy, fan efficiency, operation time, etc. The size selected will depend on the expertise of the designer who, to some degree, may inherently take into consideration the aforementioned economic parameters in the process. Evidently, different designers may arrive at different duct sizes given the same problem. The new charts developed removes this inconsistency while incorporating the economic parameters explicitly in the sizing of the duct. With the Enhanced Friction Chart or Diameter Chart, once the flow rate and economic factor are fixed, the size is also fixed (this is subject to minor errors caused by the reading of the diameter from the chart). For example, if a duct with a flow rate of $0.1m^3/s$ is sized using the new charts, the size would be 180mm, 150mm, and 100mm for economic factors of $1m^2/kW$, $0.2m^2/kW$ and $0.03m^2/kW$ respectively.

4.4.1 Uncertainty in Duct Size

The values of the optimal duct size given by Equations (4.23) is based on the assumption that the parameters on the right hand side of the equation are known for

certain or can be measured accurately. As discussed in Chapter 3, there exist some degree of uncertainty with the parameters in cost models and consequently on expressions based on the models, for example, Equation (4.23). It is often necessary to determine these uncertainties. While simulation can be used in conjunction with Equation (4.23) to determine the uncertainty in the optimal diameter given by that equation, the time required for this can not be justified for reasons given at the end of this section. However, there is a simpler procedure that can be adopted.

In [ASME 1985], methods to estimate measurement uncertainty and effects of individual measurement uncertainties on test results are presented. It specifies procedures for the evaluation of uncertainties in individual test measurements, arising from both random errors and fixed errors and for the propagation of these errors into the uncertainty of the test result. This treatment of uncertainty assumes that measurement uncertainties are caused by two sources; random or precision errors and fixed, systematic or bias errors. Random errors behave in a random manner and are assumed to have a Gaussian distribution. Bias errors, on the other hand, are fixed but still unknown until they can be established by calibration and may be either positive or negative. That is, the total error is a measure given by

$$E = \beta + \phi \tag{4.26}$$

where

ϕ = Precision error

β = Bias error.

Most quantities in engineering are not measured directly but rather derived from other measured quantities through a mathematical function. The uncertainty of a derived result

$Y=T(y_1, y_2, ..., y_N)$ where $y_1, y_2,...$ and y_N, are assumed independent, can be obtained by using

$$U(Y) = \left[B_Y^2 + (tS_Y)^2\right]^{1/2} \tag{4.27}$$

with

$$B_Y^2 = \sum_{k=1}^{N}\left(\theta_k B_{y_k}\right)^2$$

$$S_Y^2 = \sum_{k=1}^{N}\left(\theta_k S_{y_k}\right)^2$$

$$\theta_k = \frac{\partial Y}{\partial y_k}$$

where

$U(Y)$ = Uncertainty in Y

B_{y_k} = Bias limit of parameter y_k

B_Y = Total absolute bias

S_{y_k} = Standard deviation of parameter y_k

t = *Student t* at 95% confidence level (=2.0 for 30 or more samples)

θ_k = Sensitivity of parameter y_k.

In the case of a symmetrical bias ($\pm B$), Equation (4.27) gives an approximate 95% coverage for the uncertainty interval for the result. That is, there is a 95% chance that

$$Y_{actual} = Y \pm U(Y)\,. \tag{4.28}$$

Applying this to Equation (4.23) which is of the form

$$D = \left(\frac{40\times\rho}{\pi^3}\cdot\frac{Z}{10^3 S_d}\cdot Q^3 f\right)^{1/6} = T(Z, S_d, Q, f) \tag{4.29}$$

when uncertainties in Q, $f(\varepsilon, Re)$, $Z(E_d, E_c, T, PWEF, \eta_n, \eta_f)$ and S_d are considered and are assumed to be random, and normally and independently distributed gives

$$U(D)=\left[\left(\frac{\partial D}{\partial Q}^2 B_Q^2+\frac{\partial D}{\partial Z}^2 B_Z^2+\frac{\partial D}{\partial f}^2 B_f^2+\frac{\partial D}{\partial S_d}^2 B_{S_d}^2\right)+ +4\left(\frac{\partial D}{\partial Q}^2 S_Q^2+\frac{\partial D}{\partial Z}^2 S_z^2+\frac{\partial D}{\partial f}^2 S_f^2+\frac{\partial D}{\partial S_s}^2 S_{S_d}^2\right)\right]^{1/2}, \tag{4.30}$$

$$=\left[K^2\left(\frac{9B_Q^2}{Q^2}+\frac{B_Z^2}{Z^2}+\frac{B_f^2}{f^2}+\frac{B_{S_d}^2}{S_d^2}\right)+4K^2\left(\frac{9S_Q^2}{Q^2}+\frac{S_Z^2}{Z^2}+\frac{S_f^2}{f^2}+\frac{S_{S_d}^2}{S_d^2}\right)\right]^{1/2} \tag{4.31}$$

with

$$K=\frac{1}{6}\left(\frac{40\rho}{\pi^3}\cdot\frac{Z}{10^3 S_d}\cdot Q^3 f\right)^{1/6} \tag{4.32}$$

and the 95% uncertainty interval given by

$$D_{actual} = D \pm U(D)\,. \tag{4.33}$$

While this analysis provides a good way to assess uncertainties, it has a number of drawbacks and limitations that do not make it attractive for assessing the uncertainty associated with the optimal duct size given by Equations (4.23) and (4.29). These are:

1. The final duct size, which is attained after pressure balancing, that optimizes the overall system might not be the same as that given by Equation (4.23) (or (4.29)). Therefore, any parameter coverage probabilities given for the latter duct size might be meaningless for the former size.
2. Measurements of density, pressures, roughness factors, etc. are not taken when designing these duct systems. A value is assumed and the corresponding duct

sizes calculated. Thus, the only concern is the possibility that these quantities will deviate from their assumed values in the final installation and during its use.

3. The assumption of normality of the random errors is not appropriate for economic parameters which are often assumed to have forms that can not be approximated by the normal distribution.
4. The friction factor is not independent of the duct diameter, the parameter whose uncertainty is being measured.

Thus in applying the analysis in [ASME 1985] to problems such as an HVAC air duct sizing, the limitation of the results should be kept in mind. It is for these aforementioned reasons that the use of the foregoing results or the simulation procedure discussed in Chapter 3 is not recommended.

4.5 Genetic Algorithms for Air Duct Design

In the discussions above, a simple design methodology was suggested. Unlike the T-Method, this does not require the condensation and expansion of the air duct system during the design. A shortcoming of this approach and also of the T-Method, is that it is restricted to a specific type of objective function with fixed input parameters (unit energy cost, duct flow rates, etc.). Neither of these methods can be used to optimize a system that has, for example, time of day variable duct flow rates or utility rates, or in stochastic optimization of the HVAC air duct system without making a number of simplifying assumptions. In this section, a genetic algorithm approach to the design of HVAC air duct systems to address these shortcomings is suggested.

Genetic Algorithms are in the class of optimization methods known as evolutionary algorithms. These are 0-order methods; all they need is an evaluation of the objective function. They can handle non-linear problems, defined on discrete, continuous or mixed search spaces and may be unconstrained or constrained [Michalewicz et al. 1996]. This approach has the capability to handle standard duct sizes, complex objective functions and to incorporate other problem specific constraints.

Genetic Algorithms (GAs) are an optimization strategy in which points or states in the design space are analogous to organisms in a process of evolution by natural selection [Chapman et al. 1993]. Each candidate solution or state in the optimization problem is represented by a coded representation of design attributes that is analogous to a *chromosome*. Thus, a chromosome completely defines one functional design. The goodness of an individual design as a solution to the problem is evaluated as its *fitness*. Initially, GAs use problem knowledge to randomly generate a set (*population*) of functional designs. Operations such as *selection*, *crossover* and *mutation* are then performed on the designs to produce the next generation of designs with improved fitness. This process of creating new designs for a new generation is analogous to biological reproduction. The population of design alternatives evolves over a series of generations until a terminal criterion is met (i.e. until a good solution is obtained). Unlike most optimization algorithms, GAs work with a collection of design solutions rather than with a single solution with the search proceeding along different paths simultaneously. In this way, GAs can find optimal or relatively good sub-optimal solutions in a short computation time.

Most of the steps in the traditional GA can be implemented using a number of different algorithms. The choice of chromosomes for crossover and mutation, how these operations are done, and the product of these operations depend on the particular algorithm adopted by the designer. The basic mechanism of a GA is robust enough that within fairly wide margins, parameter settings (i.e. crossover and mutation probabilities, population size, etc.) are not critical. What is critical in the performance of a GA however, is the fitness function and the coding scheme used. In the next section, the fitness function and coding scheme used for the HVAC air duct system and the exact approach used for the GA implementation are discussed.

4.5.1 Coding Scheme

The power of the GA lies in it being able to find building blocks. Building blocks, are schemata of short defining length consisting of bits which work well together and tend to lead to improved performance when incorporated into individual solutions [Beasley et al. 1993]. A successful coding scheme is, therefore, one which encourages the formation of building blocks by ensuring that

1. related genes are close together on the chromosome, and
2. there is little interaction between genes.

Interaction between genes means that the contribution of a gene to the fitness of the chromosome depends on the value of other genes in the chromosome. In most applications, interactions cannot be eliminated.

Given the relationship between ducts in the same path, and "children" of a "parent" duct, the building of blocks can be encouraged by putting ducts in the same path together and children of the same parent relatively close to each other in the chromosome. It must be mentioned that since duct sections might be present across paths, it will not be possible to put all the ducts in each path together. The following is a procedure developed for arranging the genes in the chromosomes.

1. Identify all the duct paths in the system.
2. Arrange the paths such that the one with the most duct sections is at the top of the list and the one with the least number of sections is at the bottom of the list.
3. Starting from the path at the top of the list, assign the first duct section to the first gene, and the second to the second gene and so on until all the ducts in the path have been assigned gene positions.
4. Cross out any duct section that was assigned a gene position in step 3 from any other path.
5. Remove all paths that have no remaining duct sections from the list.
6. Starting from the path at the top of the list, select the first path with at least one duct section crossed out. If no such path exists, select the path at the top of the list. Assign the first duct to the first available gene, and the second to the second available gene and so on until all the ducts in the path have been assigned gene positions.
7. Repeat steps 4 through 6 until all of the ducts sections have been assigned gene positions.

If the system consists of both supply and return systems, steps 1-7 must be applied to each sub-systems separately. The next question that needs to be addressed is the value of the genes. This value should represent the true duct size in some manner. Two representations are discussed in Appendix C[3]. The representation adopted in this thesis assumes that the duct sizes are in a given interval and increase by jumps of a constant value at the end of each interval. A gene value can thus be transformed to a corresponding duct size by

$$\textit{Duct Size} = \textit{Lower Limit} + (\textit{Size Jump} \times \textit{Gene Value}). \qquad (4.34)$$

For example, let us consider the duct system in Figure 4.1, using this representation, and assuming that the *Lower Limit* equals 0.1m and the *Size Jump* equals 0.025m, for the chromosome shown in Figure 4.6, the duct sizes are, Duct 4, 0.125m; Duct 3, 0.175m; Duct 2, 0.225m; and Duct 1, 0.150m.

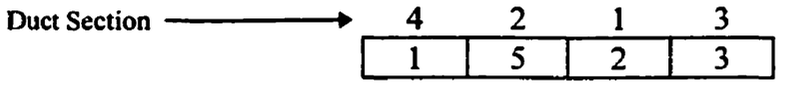

Figure 4.6: Sample Chromosome Based on Equation (4.34).

4.5.2 Evaluation of Candidate Solutions

The objective function can often be used to evaluate the fitness of chromosomes. In the case of the HVAC air duct design problem, the LCC of a given design may be used as the fitness function. Given the coding scheme adopted, it is possible to have infeasible solutions. There should therefore be a way to account for or penalize this in the fitness function. This problem could be eliminated by using chromosome representations and

[3] A brief description of the principles of Genetic Algorithms is also given in Appendix C.

operators to ensure that infeasible solutions are not generated in the first place. However, that is not the approach adopted in this thesis. Once it has be decided not to prevent the generation of infeasible solutions, they may be

1. discarded once they are generated,
2. repaired after they are generated or
3. given a fitness value that is less than the lowest fitness value for a feasible solution by the use of a penalty function.

The "death penalty" approach (1) simplifies the algorithm since infeasible solutions do not need to be evaluated. This method may work reasonably well when the feasible search space is convex and it constitutes a reasonable part of the whole search space. Otherwise such an approach has serious limitations. Sometimes, the values of genes can be changed to make an infeasible chromosome feasible (i.e., repaired). The problem with this approach is that in some problems the effort required to do this might be excessive. The most popular way of dealing with infeasible solutions is by penalizing chromosomes for being infeasible. Generally, penalty functions which represent the amount by which the constraints are violated are better than those which are based simply on the number of constraints violated [Beasley et al. 1993]. The problem with penalty functions is that more often than not, the feasible and infeasible regions are not precisely known. Thus there is the risk of specifying a penalty function that is either too severe or too lax. If the amount of penalty for being infeasible is too small, the search may yield infeasible solutions. On the other hand, the flaws of heavily penalizing infeasible designs is that it limits the exploration of the design space to feasible regions, precluding short cuts through the infeasible domain. One way around this is to use a variable penalty function.

This applies a very small penalty in the beginning of an algorithm run but increases the penalty with time or each generation. Another approach is to maintain two populations; one using a severe penalty and the other using a lax penalty with the two populations interacting. This is the so called *Segregated Genetic Algorithm* (SGA) [Michalewicz et al. 1996].

The segregated genetic algorithm is an attempt at desensitizing GA to the choice of the penalty parameters. The population is split into two coexisting and cooperating groups that differ in the way the fitness of their members are calculated. Each group uses a different value of the penalty parameter. Each of the groups corresponds to the best performing individuals with respect to one penalty parameter. The two groups interbreed, but they are segregated in terms of rank. Two advantages are expected. First, because the penalty parameters are different, the two groups will have distinct trajectories in the design space and secondly, because the two groups interbreed, they can help each other out of a local optima. The SGA is thus expected to be more robust than the GA with one fitness function.

This is the approach adopted for duct design in this thesis. However, it must be stated that the SGA is used only to treat the pressure balancing constraint. Constraints related to duct noise levels, architectural requirements, etc., just impose minimum and maximum duct size ranges on the ducts and these can be easily incorporated using the second method (i.e., repair of the chromosome).

In penalizing a design that does not satisfy the pressure balancing constraints, the amount of penalty is assumed to be directly proportional to the magnitude of the pressure imbalance in each path. The penalty function comprise 2 components; one assigns a

penalty based on the magnitude of the largest path pressure imbalance and the other assigns a penalty based on the magnitudes of all path pressure imbalances. In this thesis, for a system with say 5 paths, a design with 4 paths having a pressure imbalance of say, 5Pa each (for a total of 20Pa) is preferable to a design with only one path having a pressure imbalance of 20Pa. The second component of the penalty function is thus multiplied by a factor u (<1), to reflect this preference. The penalty function is thus defined as

$$PF = w\left[\sum_{g=1}^{G}\left(\sup_{\iota\in S_s}\left[\psi_g(P_g^s - P_{\iota,g})I_{(P_g^s - P_{\iota,g}>\hat{P})}\right] + \sum_{\iota\in S_s} u\cdot\psi_g(P_g^s - P_{\iota,g})I_{(P_g^s - P_{\iota,g}>\hat{P})}\right)\right] \quad (4.35)$$

G = Number of different system operation modes

w = Penalty weighting parameter

ψ_g = Fraction of time system operates in mode g

P_g^s = Maximum subsystem path pressure during operation mode g

$\hat{P}$ = Maximum allowable path pressure imbalance

$P_{\iota g}$ = Path pressure during operation mode g

$I_{(\cdot)}$ = Indicator function.

This function is for the general case where the system might have variable time of day duct flow rates and/or variable time of day utility rates. The first term is intended to account for the magnitude of the largest path pressure imbalance and the second term for the magnitudes of all path pressure imbalances.

The fitness function is therefore given by

$$FF = E_s + PF + \sum_{g=1}^{G} \frac{Q_{fan,g}\left(E_d + E_{c,g}\psi_g T\right)P_g^s}{10^3 \eta_f \eta_m} \tag{4.36}$$

where

$Q_{fan,g}$ = Fan flow rate during operation mode g

$E_{c,g}$ = Unit electrical energy cost in operation mode g.

The fitness function was selected to include both the objective and penalty functions. The smaller the fitness function, the better the design. This fitness function will be used in Chapter 5 as part of the segregated genetic algorithm in an illustrative example of designing a ducting system. In Chapter 6, the determination of the optimal duct design when the parameters in the above objective function are uncertain is illustrated.

4.5.3 Specific Implementation Algorithm

There are several implementation algorithms in the literature but the Segregated Genetic Algorithm (SGA) is used for the duct design problem in this thesis because it offers a way to handle infeasible chromosomes while avoiding the problems associated with selecting penalty parameters.

A typical implementation of the *SGA* will start with the generation of *2m* designs at random (*m* is any suitable large integer e.g. 100 or 500). These designs are then evaluated using two different penalty parameters ($w=w_1$ and $w=w_2$, with $w_1>>w_2$ in Equation (4.35)) to create two ranked lists. In ranking the chromosomes, duplicated individuals are pushed to the bottom (low rank) of the lists. This is a protection against

premature uniformization of the population. From the two lists of $2m$ ranked individuals, one single population of m individuals is built which mixes the relative influences of the two lists. The best individual of the list established using the highest penalty parameter, w_1 is first selected. Then the best individual of the other list (based on the lower penalty parameter, w_2), that has not yet been selected is chosen. The process is repeated alternatively on each list until m individuals have been selected. Then reproduction occurs as usual by application of linear ranking selection, crossover, mutation and swapping to the combined list, creating m offspring. They are added to the m parents and the entire process is repeated until the stopping criterion is met.

Most work in GA use a generation gap of 1, that is complete population replacement. The extreme opposite of this is the steady-state replacement. In this case, it is assumed that just as in real life, compared with the total population, only a small number of deaths and births occur at the same time. Thus at each generation, only a small number (typically two) individuals are replaced with offspring. The implementation of SGA in this thesis will be slightly different from that discussed above with regards to the generation gap policy. The steady-state replacement approach is used because an initial study conducted using the HVAC air duct design problem showed that it converges faster than the original SGA. In view of this, a κ-chromosome tournament shall be used to select the parents for mating (where κ is a small integer). In this approach, a predetermined number κ, of chromosomes are selected at random from the population

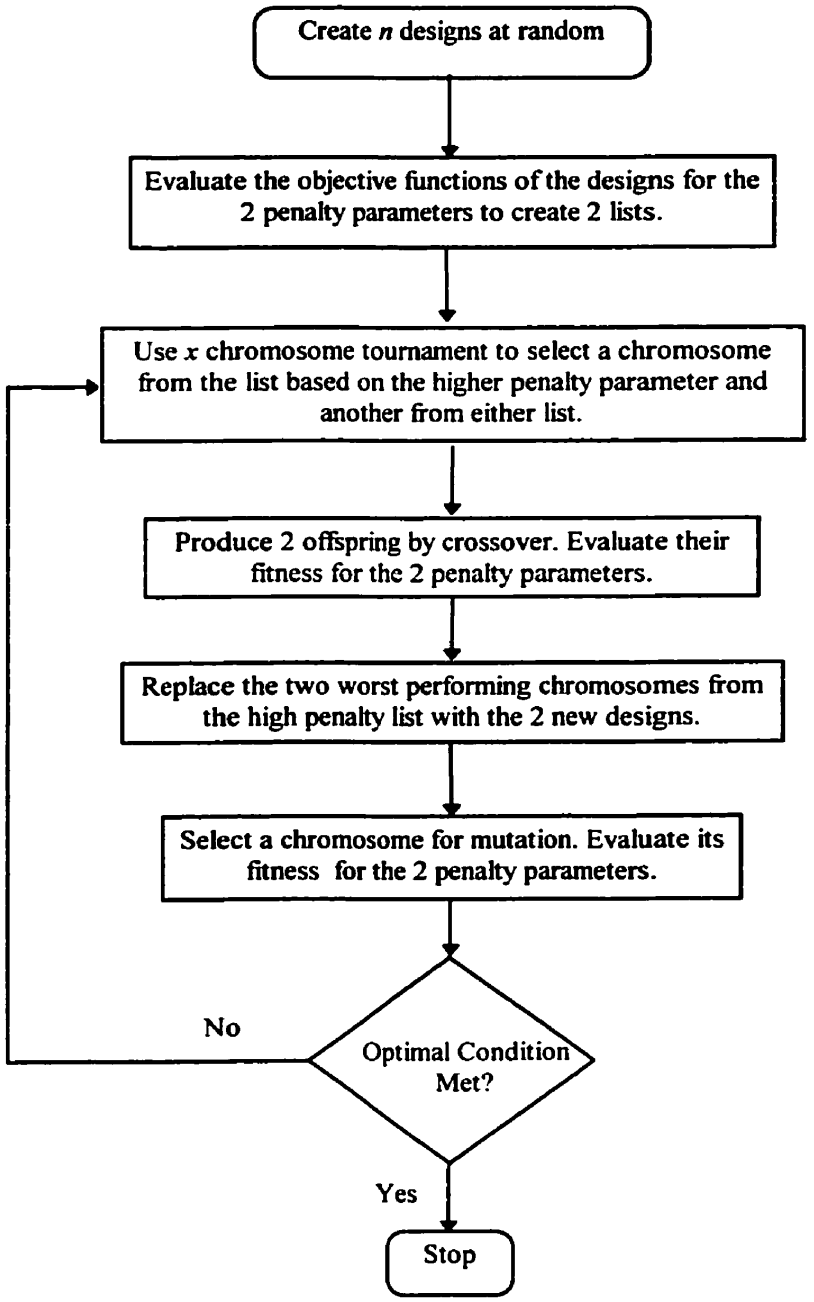

Figure 4.7: Flow Chart of Implemented Segregated Genetic Algorithm.

and the one with the best fitness function value is chosen. All the members are put back into the population and might take part in further tournaments. This eliminates the need to sort (rank) the population. Using this procedure, two parents are selected at each

generation to undergo crossover. One half of the time, the parents are selected from the list based on the high penalty parameter, and during the other half, to obtain the effect of interbreeding, a parent is selected from each list. The two worst performing chromosomes with respect to the fitness function with the higher penalty parameter are replaced with the two offspring. The complete algorithm is shown in Figure 4.7 The population size is represented by n (where $n=2m$).

4.6 Summary

In this chapter, the theory behind the IPS-Method of duct design and the Diameter and Enhanced Friction Charts was introduced. How genetic algorithms can be used to design more complex HVAC air duct systems was also shown. In the next chapter, a number of sample problems are used to illustrate the effectiveness of these methods. One of the appealing qualities of genetic algorithms is their ability to handle a wide range of objective functions. In Chapter 6, the use of the SGA to design an HVAC system when the objective function (LCC) has uncertain parameters is demonstrated through a sample problem.

5 HVAC Air Duct Design Case Studies

A number of methodologies and design aids that can be used for the design of an HVAC air duct system for minimum life-cycle cost were discussed in Chapter 3. These were the IPS-Method, Segregated Genetic Algorithm and the Enhanced Friction and Diameter Charts. This chapter presents a number of air duct design problems to illustrate the efficacy of these methodologies and design aids. All the sample problems are based on two duct system layouts. The first is a very simple design layout taken from [Tsal et al. 1988b] and the second is from [ASHRAE 1997] and is a more complicated duct design problem. The illustration of the IPS-Method is followed by a demonstration of the use of the Enhanced Friction and Diameter Charts. Later, a design problem with variable time of day load demands and utility rates is solved using a segregated genetic algorithm.

5.1 IPS-Method

5.1.1 Sample Problem 1

This problem is taken from [Tsal et al. 1988b]. The layout of the duct system is shown in Figure 5.1 and Table 5.1 shows the duct lengths and flow rates. Other general and economic parameters are also shown below. For this problem, it is assumed that the dynamic loss coefficients of the fittings are known constants independent of the flow rate and duct diameter.

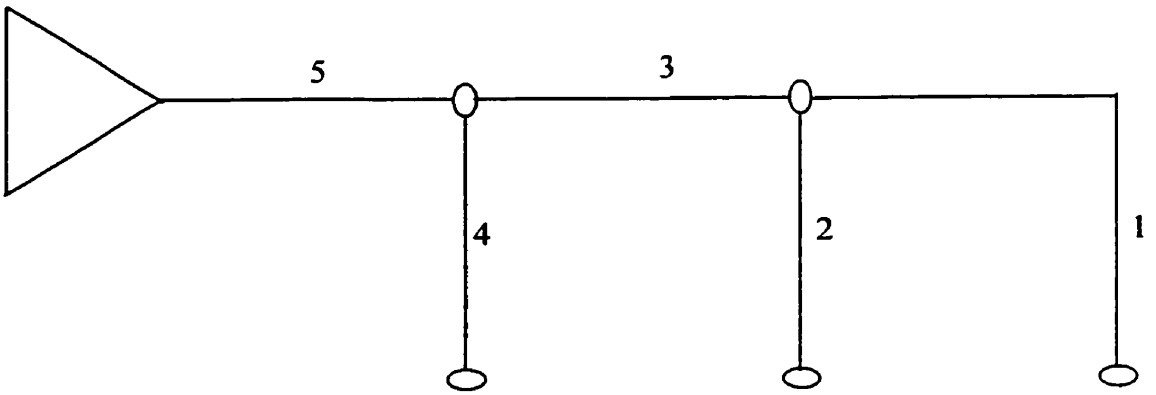

Figure 5.1: Five-Section Duct System.

General Data

Absolute Roughness	0.0003 m
Kinematic Viscosity	1.54×10^{-5} m^2/s
Air Density	1.2 kg/m^3
Fan Efficiency	0.75
Motor and Drive Efficiency	0.80
Total System Airflow	1.42 m^3/s

Economic Data

Energy Cost	2.03 c/kWh
Duct Cost	43.27 $/$m^2$
System Operation time	4400 hours/year
PWEF	8.61

Table 5.1: Duct Input Parameters.

Duct Section	Length (m)	Flow Rate (m^3/s)	Type	Dimension (m)	Extra Pressure Losses (Pa)	Dynamic Loss Coefficient
1	14	0.7	Rectangular	0.254*	25	0.8
2	12	0.22	Round	-	37.5	0.65
3	8	0.92	Round	0.33+	0	0.18
4	16	0.5	Round	-	0	0.65
5	19.81	1.42	Round	-	37.5	1.5

*Presized height of 254mm.
+Presized 330mm diameter duct.

5.1.1.1 Results and Discussions

Since the dynamic loss coefficients are assumed fixed, each duct can be sized individually. The procedure can be easily implemented in any computer worksheet package. Table 5.2 shows the implementation of the procedure for the sizing of the ducts. For the purpose of illustration, the calculation of the various values found in this table is shown for the first iteration for section 1.

Sample Calculation

Step One: Economic Factor

In a design with each duct made from the same material and employing the same manufacturing and assembly techniques, the economic factor is the same for all the duct sections and needs to be calculated only once. However, in cases were different materials and manufacturing and assembly techniques are being used, this would have to be calculated for each duct section. Using the input data for the sample problem gives,

$$\frac{Z}{1000 \times S_d} = \frac{(4400 \times 0.0203)8.61}{1000 \times 0.75 \times 0.8 \times 43.27} = 29.62 \times 10^{-3}\ \text{m}^2/\text{kW}. \qquad (5.1)$$

Table 5.2: Duct Size Determination.

Duct Section	λ_k	Duct Width/Diameter (m)	Duct Width/Diameter (in)	Reynolds Number	Friction Factor	λ_{k+1}	⌊D⌋ or ⌊W⌋ (in) k	⌊D⌋ or ⌊W⌋ (in) $k+1$
1	0.8	0.1754	6.9070	212000	0.0226	2.7713	-	6
2	0.65	0.1215	4.7830	153000	0.0256	3.1743	-	4
4	0.65	0.1877	7.3899	225000	0.0230	2.6077	-	7
5	1.5	0.3977	15.6571	302000	0.0195	2.4694	-	15
Second Iteration								
1	2.7713	0.2654	10.4508	175000	0.0218	2.2635	6	10
2	3.1743	0.1668	6.5682	111000	0.0244	2.4027	4	6
4	2.6077	0.2478	9.7568	170000	0.0220	2.0724	7	9
5	2.4694	0.4394	17.2987	273000	0.0192	2.3665	15	17
Third Iteration								
1	2.2635	0.2481	9.7689	181000	0.0219	2.3302	10	9
2	2.4027	0.1578	6.2124	117000	0.0245	2.5164	6	6
4	2.0724	0.2367	9.3186	179000	0.0222	2.1482	9	9
5	2.3665	0.4357	17.1520	275000	0.0192	2.3747	17	17
Fourth Iteration								
1	2.3302	0.2505	9.8639	180000	0.0219	2.3203	9	9

Step Two: Initial Value of λ (λ_R or λ_C)

The value of λ is indexed by the iteration number, k. The initial value of λ, λ_1 can be chosen either arbitrarily or through experienced guessing. An initial value equal to the

value of the fixed dynamic loss coefficients was used. Subsequent values of λ_k are taken from the λ_{k+1} column of the preceding iteration.

Step Three: Width or Diameter

The value of W is calculated using Equation (4.20) (for a circular duct, Equation (4.17) shall be used).

$$W = \left(0.6 \times 0.02962 \times \frac{0.7^3}{0.254^2 \times 14} \times 0.8\right)^{1/3} = 0.1754\text{m} \qquad (5.2)$$

Step Four: Friction Parameter

The value of λ_{k+1} is calculated using W from the previous step. As mentioned earlier, this will be the value of λ_k in the next iteration.

$$D_h = \frac{2(HW)}{(H+W)} = \frac{2(0.254 \times 0.1754)}{(0.254+0.1754)} = 0.2075\text{m} \qquad (5.3)$$

$$\text{Re} = \left(\frac{0.2075}{1.54\text{x}10^{-5}}\right)\left(\frac{0.7}{0.1754 \times 0.254}\right) = 212000 \qquad (5.4)$$

$$f = 0.11\left(\frac{0.0003}{0.2075} + \frac{68}{212000}\right)^{0.25} = 0.0226 \qquad (5.5)$$

$$\lambda_R = 0.0226 \times 14\left(\frac{1}{2 \times 0.254} + \frac{3}{4 \times 0.1754}\right) + 0.8 = 2.7713 \qquad (5.6)$$

Table 5.3 shows the recommended standard sizes for the 4 duct sections. These are the possible upper and lower standard duct sizes. The standard duct sizes are specified as multiples of 10in. The energy and initial costs associated with each size are also shown.

After comparing the costs, the duct sizes shown in Table 5.4 were selected as the optimal duct sizes for each duct section. However, as is apparent from Table 5.5, the pressure distribution in this design is not satisfactory. The path pressure imbalance of 113.97 Pa and 97.12 Pa for paths 1 and 3 respectively are too excessive. There is, therefore, the need to change the sizes of some of the ducts to balance the pressures. This is done using the pressure and size augmentation procedures outlined in Chapter 4.

Table 5.3: Standard Duct Sizes and Associated Cost.

Duct Section	D or W		Pressure Drop (Pa)	Cost ($)		
	(in)	(m)		Initial	Energy	Total
1	9	0.2286	182	585	163	748
1	10	0.2540	142	615	127	743
2	6	0.1524	226	249	64	312
2	7	0.1778	108	290	30	320
4	9	0.2286	197	497	126	623
4	10	0.254	119	552	76	629
5	17	0.4318	135	1163	245	1408
5	18	0.4572	105	1231	190	1422

Table 5.4: Duct Sizes and Pressure Drops Before Pressure Balancing-Sample Problem I.

Duct Section	Diameter/Width		Pressure Loss (Pa)		
	(in)	(m)	Variable	Additional	Total
1	10	0.2540	141.9	25.0	166.9
2	6	0.1524	226.3	37.5	263.8
3	-	0.3300	46.90	0	46.90
4	9	0.2286	196.8	0	196.8
5	17	0.4318	134.5	37.5	172.0

Table 5.5: Path Losses Before Pressure Balancing- Sample Problem I.

Path	Sections	Pressure Loss (Pa)	Pressure Differential (Pa)
1	5-4	369.07	113.97
2	5-3-2	483.03	0
3	5-3-1	385.91	97.12

The process of pressure balancing requires the value of the duct occurrence densities. These values are shown in Table 5.6. The actual process of pressure balancing is shown in Table 5.7. This shows the duct which is changed at each iteration, the stage of the procedure (i.e. P for pressure augmentation and S for size augmentation) and the consequence of the change. The 'Decision' column indicates whether or not the design change was accepted. Table 5.8 shows the changes in the life-cycle cost of the system through the pressure balancing procedure. The rows in bold type correspond to the changes that were accepted. As is evident from Table 5.8, the life-cycle cost was successively reduced from the initial value of $3,762 to $3,626.

Table 5.6: Duct Occurrence Densities.

Section	Duct Occurrence Density
1	0.33
2	0.33
4	0.33
5	1

Table 5.7: Pressure Balancing.

Iteration Number	Stage	D or W (m)	Path Selected	Duct Selected	Path Pressures (Pa)			Max. Pressure Differential (Pa)	Decision
					1	2	3		
1	P	0.2032	1	4	519.85	483.03	385.91	133.9	Reject
2	P	0.2286	3	1	369.07	483.03	425.86	113.97	Accept
3	P	0.2032	1	4	519.85	483.03	425.86	93.98	Reject
4	P	0.2032	3	1	369.07	483.03	484.95	115.88	Reject
5	S	0.1778	2	2	369.07	364.218	425.86	61.65	Accept
6	P	0.2032	1	4	519.85	364.21	425.86	155.64	Reject
7	S	0.254	3	1	368.82	364.02	385.84	21.82	Accept

Table 5.8: Tracking of LCC of Duct System.

Iteration	Initial Cost ($)	Energy Cost ($)	Total Cost ($)
Initial Design	2883	879	3762
1	2828	946	3774
2	**2852**	**879**	**3731**
3	2797	946	3743
4	2821	883	3704
5	**2894**	**775**	**3669**
6	2838	946	3784
7	**2924**	**702**	**3626**

Table 5.9: Duct Sizes and Pressure Drops after Pressure Balancing-Sample Problem I.

Diameter/Width		Pressure Loss (Pa)		
(in)	(m)	Frictional	Additional	Total
10	0.254	141.9	25.0	166.9
7	0.1778	107.7	37.5	145.2
-	0.3300	46.90	0	46.9
9	0.2286	196.9	0	196.9
17	0.4318	134.6	37.5	172.1

The final duct sizes and sectional pressure losses are shown in Table 5.9 and the path pressure losses in Table 5.10. These are the same as that obtained in [Tsal et al. 1984b] using the T-Method which shows that this approach is capable of determining the optimal design while avoiding the tedious mathematical computations associated with the T-Method. In the T-Method, to avoid the use of an optimization algorithm like dynamic programming, to incorporate the constraint of standard duct sizes, a heuristic is used to select the standard sizes. This does not ensure that the sizes selected are optimal. The IPS-Method avoids the need for a heuristic by incorporating the constraint very early in the procedure and making a choice of standard size based on the LCC, the objective being optimized.

Table 5.10: Path Pressure Losses after Pressure Balancing-Sample Problem I.

Path	Sections	Pressure Loss (Pa)	Pressure Differential (Pa)
1	5-4	369	17
2	5-3-2	364	22
3	5-3-1	386	0

5.1.2 Sample Problem II

This problem is taken from Chapter 32 of ASHRAE [1997] and is more complicated than the one above because it does not assume a fixed value for the dynamic loss coefficients. The layout of the air duct system is shown in Figure 5.2 and the general data are given in a table. Table 5.11 gives the input parameters for each duct. The return system is made of circular ducts with the exception of duct section 4 which together with

all the supply ducts are rectangular ducts. The economic and general system parameters are also shown below. To de-couple the system during the Initial Duct Sizing stage so that each duct can be sized separately, it is assumed that the cross-sectional areas of the ducts at junctions are proportional to the flow rates of the connected duct sections.

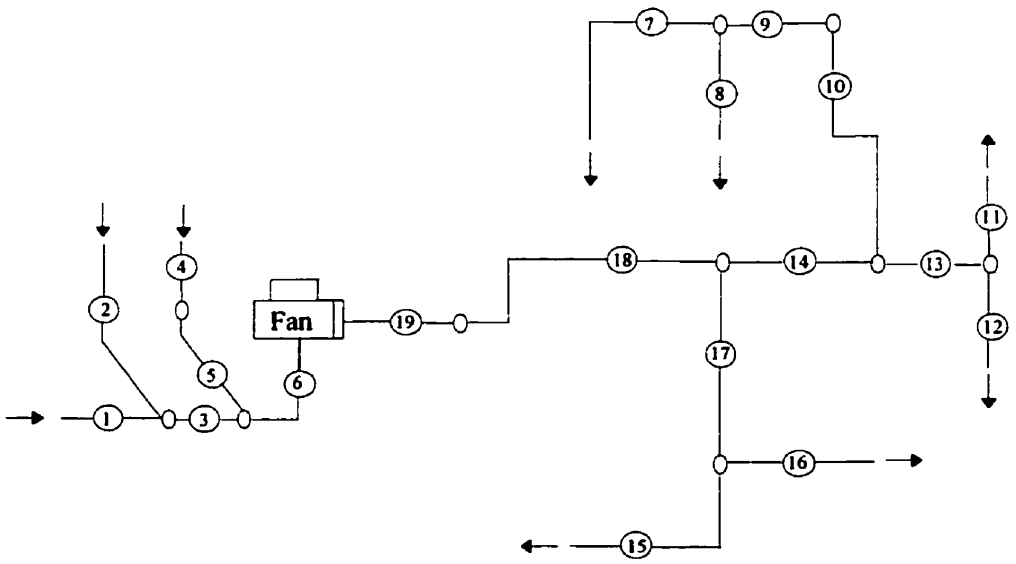

Figure 5.2: Duct Layout for Sample Problem.

Economic and General Data

Absolute roughness	0.09 mm
Air density	1.204 m^3/kg
Unit energy cost	0.06 $/kWh
Ductwork cost	43.27 $/m^2$
Fan efficiency	0.75
Motor and drive efficiency	0.8
Fan flow rate	1.9 m^3/s

Operating time	4400 hr/year
PWEF	8.61

Table 5.11: Duct Input Data.

Duct Section	Width (mm)	Length (m)	Flow Rate (m^3/s)	Fixed Extra Pressure Loss (Pa)	Fittings*
1	-	4.6	0.7	-	ED1-3,ED5-1,CD9-1
2	-	18.3	0.25	-	ED1-1,CD3-6,ED5-1, CD6-1,CD9-1
3	-	6.1	0.95	-	ED5-2,CD9-1
4	600	1.5	0.95	25	CR9-4,ER4-3
5	-	18.3	0.95	-	CD3-17,ED5-2,CD9-1
6	-	9.1	1.9	-	CD3-9,ED7-2,CD9-3
7	250	4.3	0.275	25	CR3-3,CR9-1,SR5-13
8	250	1.2	0.275	25	SR5-13,CR9-4
9	250	7.6	0.55	-	SR3-1
10	250	13.7	0.55	-	CR9-1,CR3-6,SR5-1, CR3-10
11	250	3.0	0.475	-	CR9-1,SR5-14,SR2-1
12	250	6.7	0.475	-	CR9-1,SR2-5,SR5-14
13	250	10.7	0.95	-	CR9-1,SR5-1
14	250	4.6	1.5	-	CR9-1,SR5-13
15	150	12.2	0.2	-	CR3-1,SR2-6,CR9-1, SR5-1
16	150	6.1	0.2	-	SR2-3,CR6-1,CR9-1, SR5-1
17	150	4.2	0.4	-	CR9-1,SR5-13
18	800[1]	7.0	1.9	-	CR6-4,SR4-1,CR3-17, CR3-17
19	800[1]	3.7	1.9	15	SR7-17,CR9-4

*Please see Appendix for a complete description of fittings.
[1] Width

5.1.3 Constraints for Sample Problem II

There are a number of problem specific constraints which are given below.

1. Fixed Duct Sizes

Duct section 4 was assumed to be a 600x600mm rectangular pre-sized duct. This corresponds to the size indicated in [ASHRAE 1997]. The heights (widths for ducts 18 and 19) of the supply ducts were also assumed to be equal to those in [ASHRAE 1997].

2. Wye and Tee Fittings

The sizes of the ducts to which fittings are connected were required to satisfy the following relationships:

$A_b = A_s \leq A_c$ for fitting Sr5-14,

$A_b + A_s \geq A_c$ for fitting Sr5-1,

$A_b < A_c$ and $A_s < A_c$ for fitting Sr5-13,

$A_b \leq A_c$ and $A_s \leq A_c$ for fittings Ed5-1 and Ed5-2,

where

A_t Area of duct $t = b, s, c$ (b: branch; s: straight; c: common).

3. Path Pressures

It is virtually impossible to come up with duct sizes that achieve equal path pressure losses for all the paths. A more realistic objective is to design a system to achieve a reasonable path pressure imbalance. That is, the difference between the path with the

maximum pressure losses and that with the lowest pressure should not exceed a predetermined value. For this problem, this pressure was 10 Pa.

4. Allowable Duct Sizes

It is possible from preliminary studies to place a limit on the allowable sizes of the ducts. For this problem, the sizes were limited to between 100mm and 800mm. However, the maximum permitted heights of ducts 12 and 16 were 425mm and 375mm respectively. The standard duct sizes in this range increases in steps of 25mm.

5.1.3.1 Results and Discussions

Unlike the previous problem, the algorithm discussed in Section 4.3 has been implemented in C. The dynamic loss coefficients are calculated at run time by interpolation using tables provided by ASHRAE. The pressure balancing processes for the return and supply subsystems are shown in Table 5.12 and Table 5.13 respectively. The results obtained by applying the IPS-Method to the problem are shown in Table 5.14. Table 5.15 compares the design based on the IPS-Method to that of [ASHRAE 1997]. The system pressure for this design is 479 Pa with an associated life-cycle cost of $10,897 (initial cost: $7,450, energy cost: $3,447). The ASHRAE solution has a system pressure of 679 Pa and an associated life-cycle cost of $12,054 (initial cost: $7,167, energy cost: $4887) based on the same economic factors. As can be seen, neither the supply nor return subsystems satisfied the required maximum pressure imbalance of

Table 5.12: Pressure Balancing of Return Subsystem-Sample Problem II (Standard IPS).

Iteration	Stage	Maximum Path Pressure (Pa)	Max. Pressure Differential (Pa)	Dominant Path	Initial Cost ($)	Operating Cost ($)	Total Cost ($)	Decision
Initial Design	-	180.30	110.34	-	2864	2354	5218	-
1	P	173.85	89.15	2	2848	1251	4100	Accept
2	P	163.18	56.57	2	2833	1175	4007	Accept
3	P	160.89	52.02	2	2770	1158	3929	Accept
4	P	156.76	32.49	3	2755	1128	3883	Accept
5	P	153.49	11.76	3	2693	1105	3797	Accept
6	P	188.90	50.48	1	2630	1360	3990	Reject
7	P	-	-	-	-	-	-	-*
8	P	245.84	128.81	3	2677	1770	4447	Reject
9	S	157.61	52.02	2	2708	1134	3843	Reject

*Size constraint violation

Table 5.13: Pressure Balancing of Supply Subsystem-Sample Problem II (Standard IPS).

Iteration	Stage	Maximum Path Pressure (Pa)	Max. Pressure Differential (Pa)	Dominant Path	Initial Cost ($)	Operating Cost ($)	Total Cost ($)	Decision
Initial Design	-	326.97	120.61		5026	2354	7380	-
1	P	326.97	115.87	8	5017	2354	7370	Accept
2	P	326.97	110.21	8	5007	2354	7361	Accept
3	P	326.97	103.06	8	4998	2354	7352	Accept
4	P	-	-	-	-	-	-	-*
5	P	326.97	102.52	8	4977	2354	7331	Accept
6	P	326.97	99.45	8	4968	2354	7322	Accept
7	P	327.57	92.51	8	4945	2358	7303	Reject
8	P	326.97	95.08	8	4947	2354	7301	Accept
9	P	327.57	92.51	8	4924	2358	7282	Reject
10	P	326.97	91.91	8	4926	2354	7280	Accept
11	P	326.97	89.70	8	4917	2354	7271	Accept
12	P	327.57	78.54	8	4894	2358	7252	Reject
13	P	326.97	82.95	8	4896	2354	7250	Accept

14	P	327.57	77.55	8	4873	2358	7231	Reject
15	P	326.97	76.95	8	4875	2354	7229	Accept
16	P	326.97	74.26	8	4866	2354	7220	Accept
17	P	327.57	62.72	8	4843	2358	7201	Reject
18	P	326.97	62.52	8	4845	2354	7199	Accept
19	P	327.57	56.80	8	4822	2358	7180	Reject
20	P	326.97	56.20	8	4824	2354	7178	Accept
21	P	326.97	46.28	8	4815	2354	7169	Accept
22	P	327.57	34.16	8	4792	2358	7150	Reject
23	P	326.97	30.35	8	4794	2354	7148	Accept
24	P	336.70	29.09	5	4785	2424	7209	Reject
25	P	326.97	28.05	8	4781	2354	7134	Accept
26	P	355.11	47.51	4	4772	2556	7328	Reject
27	P	326.97	19.37	8	4755	2354	7108	Accept
28	P	330.27	14.50	7	4731	2377	7109	Reject
29	P	379.00	63.24	7	4734	2728	7462	Reject
30	P	371.06	63.46	5	4745	2671	7416	Reject
31	P	341.23	33.63	4	4741	2456	7197	Reject
32	P	385.65	78.05	5	4728	2776	7504	Reject
33	S	325.49	17.88	5	4757	2343	7100	Accept
34	P	330.27	14.50	7	4734	2377	7111	Reject
35	P	379.00	63.24	7	4736	2728	7464	Reject
36	S	325.12	26.21	8	4783	2340	7124	Reject
37	S	325.12	39.77	8	4766	2340	7106	Reject

*Size constraint violation

Table 5.14: Optimal Duct Sizes and Pressure Losses-Sample Problem II (Standard IPS).

Duct Section	Size (mm)	Friction Loss (Pa)	Dynamic Loss (Pa)	Total Loss (Pa)
1	250	39.7	68.4	108.1
2	200	69.5	26.9	96.4
3	400	9.0	11.5	20.5
4	600x600	0.2	29.7	29.9
5	375	37.2	58.6	95.8
6	625	5.4	19.5	24.9
7	150x250	15.2	34.1	49.3
8	300x250	0.7	49.0	49.7
9	325x250	13.9	32.4	46.3

10	325x250	25.1	61.6	86.7
11	175x250	19.6	99.1	118.7
12	175x250	43.8	87.8	131.6
13	375x250	38.8	7.6	46.4
14	625x250	12.2	4.4	16.6
15	150x150	81.6	22.8	104.4
16	175x150	27.9	66.7	94.6
17	200x150	50.8	44.6	95.3
18	800x725	1.0	26.9	27.9
19	800x800	0.4	97.5	97.9

Table 5.15: Path Pressure Losses-Sample Problem II (Standard IPS).

Path	Ducts in Path	IPS-Method Design		ASHRAE	
		Path Loss (Pa)	Pressure Differential (Pa)	Path Loss (Pa)	Pressure Differential (Pa)
1	6-5-4	150	3	234	28
2	6-3-2	142	12	262	0
3	6-3-1	153	0	240	22
4	19-18-17-16	316	10	417	0
5	19-18-17-15	325	0	404	13
6	19-18-14-13-11	308	18	412	5
7	19-18-14-13-12	320	5	412	5
8	19-18-14-10-9-8	325	0	417	0
9	19-18-14-10-9-7	325	0	408	9

10kPa. A look at the 28^{th} and 34^{th} iterations for the supply subsystem shows that there is the possibility of achieving a better pressure imbalance albeit at a higher cost. Thus, the pressure balancing process can be repeated using the revised IPS algorithm (i.e. using Step 8A in place of Step 8 in the Pressure Augmentation Stage of the algorithm). The

pressure balancing process for this is shown in Table 5.16. This gives a maximum pressure imbalance of 10Pa which is the allowable maximum pressure differential. Although, the return subsystem also did not satisfy the pressure imbalance constraint, there was no need to apply the revised algorithm to this since the results shown in Table 5.12 do not indicate that it is possible to achieve a better pressure imbalance. The system pressure for this design is 493 Pa with an associated life-cycle cost of $10,968 (initial cost: $7,417, energy cost: $3,551). What this shows is that, from the initial duct sizes used, these are the best designs possible. It is possible that there exist a design that will give the required pressure distribution, however, the cost will be higher than the cost of the current designs.

Table 5.16: Pressure Balancing of Supply Subsystem-Sample Problem II (Revised IPS).

Iteration	Stage	Maximum Path Pressure (Pa)	Max. Pressure Differential (Pa)	Dominant Path	Initial Cost ($)	Operating Cost ($)	Total Cost ($)	Decision
Initial Design	-	326.97	120.61		5026	2354	7380	-
1	P	326.97	115.87	8	5017	2354	7370	Accept
2	P	326.97	110.21	8	5007	2354	7361	Accept
3	P	326.97	103.06	8	4998	2354	7352	Accept
4	P	-	-	-	-	-	-	-*
5	P	326.97	102.52	8	4977	2354	7331	Accept
6	P	326.97	99.45	8	4968	2354	7322	Accept
7	P	327.57	92.51	8	4945	2358	7303	Accept
8	P	327.57	88.57	8	4936	2358	7294	Accept
9	P	-	-	-	-	-	-	-*
10	P	327.57	84.07	8	4915	2358	7273	Accept
11	P	328.17	78.15	8	4892	2362	7254	Accept
12	P	328.17	69.95	8	4883	2362	7245	Accept
13	P	328.17	69.95	8	4883	2362	7245	Accept
14	P	328.17	64.26	8	4862	2362	7224	Accept
15	P	328.47	57.70	8	4839	2364	7203	Accept
16	P	328.47	46.52	8	4830	2364	7194	Accept
17	P	-	-	-	-	-	-	-*

18	P	328.47	39.15	8	4809	2364	7173	Accept
19	P	328.47	31.85	8	4785	2364	7150	Accept
20	P	336.70	24.72	5	4776	2424	7200	Accept
21	P	336.70	23.21	5	4766	2424	7190	Accept
22	P	337.22	22.00	8	4756	2427	7184	Accept
23	P	-	-	-	-	-	-	-*
24	P	337.22	12.25	8	4735	2427	7163	Accept
25	P	357.58	27.70	7	4712	2574	7286	Reject
26	P	341.68	11.81	7	4714	2459	7174	Accept
27	P	390.79	55.90	5	4705	2813	7518	Reject
28	P	355.11	20.22	4	4701	2556	7257	Reject
29	S	-	-	-	-	-	-	-*
30	S	337.08	23.72	8	4738	2426	7164	Reject
31	S	339.95	10.07	7	4724	2447	7171	Accept
32	P	390.79	60.50	5	4715	2813	7528	Reject
33	P	355.11	24.82	4	4711	2556	7267	Reject
34	S	-	-	-	-	-	-	-*
35	S	336.70	23.80	5	4748	2424	7171	Reject
36	S	338.44	12.30	7	4734	2436	7170	Reject

*Size constraint violation

Table 5.17: Optimal Duct Sizes and Pressure Losses-Sample Problem II (Revised IPS).

Duct Section	Size (mm)	Friction Loss (Pa)	Dynamic Loss (Pa)	Total Loss (Pa)
1	250	39.7	68.4	108.1
2	200	69.5	26.9	96.4
3	400	9.0	11.5	20.5
4	600x600	0.2	29.7	29.8
5	375	37.2	58.6	95.7
6	625	5.4	19.5	24.9
7	150x250	15.2	34.1	49.3
8	275x250	0.9	50.7	51.6
9	325x250	13.9	32.4	46.3
10	325x250	25.1	65.7	90.7
11	225x250	10.3	78.3	88.6
12	225x250	23.0	69.3	92.3
13	275x250	82.3	21.3	103.7
14	600x250	13.4	4.8	18.2
15	175x150	55.9	26.4	82.3

16	200x150	20.3	55.2	75.5
17	175x150	70.4	58.2	128.6
18	800x725	1.0	26.9	27.9
19	800x800	0.4	97.5	97.9

Table 5.18: Path Pressure Losses-Sample Problem II (Revised IPS).

Path	Ducts in Path	Path Loss (Pa)	Pressure Differential (Pa)
1	6-5-4	150	3
2	6-3-2	142	12
3	6-3-1	153	0
4	19-18-17-16	330	10
5	19-18-17-15	337	3
6	19-18-14-13-11	336	4
7	19-18-14-13-12	340	0
8	19-18-14-10-9-8	333	7
9	19-18-14-10-9-7	330	10

5.2 Enhanced Friction Chart

5.2.1 Sample Problem III

The use of the Enhanced Friction Chart for duct design is illustrated with the same duct design problem as the example in Section 5.1.1. Because the absolute roughness for this problem is 0.3mm instead of the value of 0.09mm used for the chart of Figure 4.5, the new chart in Figure 5.3 is used. The economic factor is equal to 0.029 m^2/kW. Using this value and the flow rates, initial duct diameters of 160mm, 220mm and 370mm are selected for duct sections 2, 4 and 5 respectively and an equivalent duct diameter of

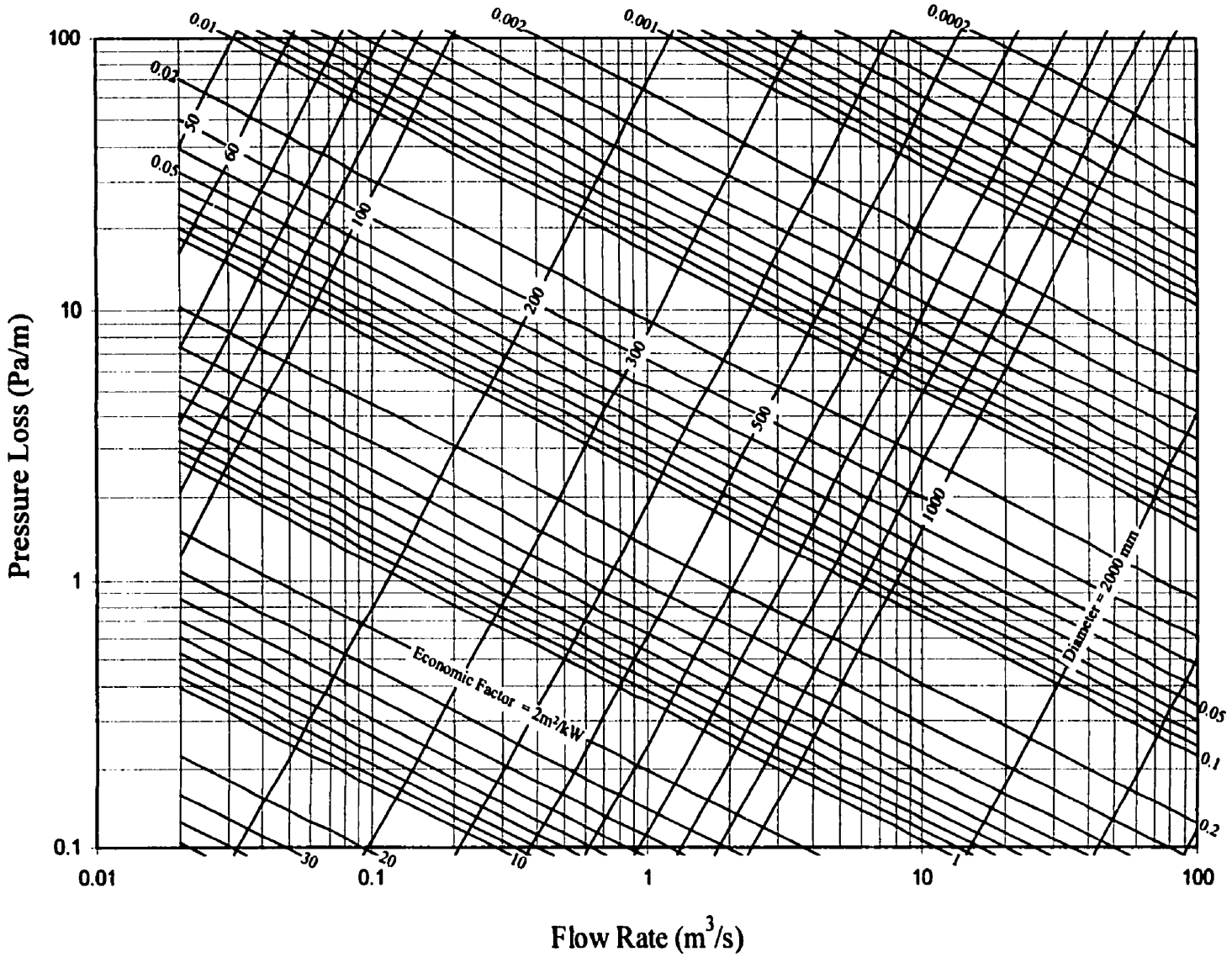

Figure 5.3: Enhanced Friction Chart (ε=0.3mm and ρ=1.2kg/m^3).

260 mm chosen for duct section 1. The corresponding width given a height of 254mm is approximately 220mm. Standardizing these sizes based on 10 inch increments gives the sizes and duct pressure drops shown in Table 5.19. The path pressures are show in Table 5.20. The final duct sizes and duct pressure drops after pressure balancing are shown in Table 5.21 and the path pressures in Table 5.22. With the exception of duct section 5, the sizes are similar to that obtained in Section 5.1.1. The smaller size in this solution increases the system pressure which results in a slightly higher cost ($3,672, a difference of $46) than that in Section 5.1.1. The pressure balancing process was the same as for the IPS-Method. In fact, the suggested procedure for pressure balancing is applicable in any duct design problem regardless of how the initial duct sizes are determined.

Table 5.19: Duct Sizes Before Pressure Balancing: Enhanced Friction Chart.

Duct Section	Diameter/Width		Pressure Loss (Pa)		
	(in)	(m)	Variable	Additional	Total
1	9	0.2286	181.85	25.0	206.85
2	6	0.1524	226.52	37.5	264.02
3	-	0.3300	46.9	0	46.9
4	9	0.2286	196.95	0	196.95
5	15	0.3810	234.60	37.5	272.10

Table 5.20: Path Losses Before Pressure Balancing: Enhanced Friction Chart.

Path	Sections	Pressure Loss (Pa)	Pressure Differential (Pa)
1	5-4	469.05	113.97
2	5-3-2	583.02	0.00
3	5-3-1	525.85	57.17

Table 5.21: Duct Sizes and Section Pressure Losses After Pressure Balancing: Enhanced Friction Chart.

Duct Section	Diameter/Width		Pressure Loss (Pa)		
	(in)	(m)	Frictional	Additional	Total
1	10	0.2032	141.89	25	166.89
2	7	0.1524	107.69	37.5	145.19
3	-	0.3300	46.90	0	46.90
4	9	0.2032	196.95	0	196.95
5	15	0.3810	234.60	37.5	272.10

Table 5.22: Path Losses After Pressure Balancing.

Path	Sections	Pressure Loss (Pa)	Pressure Differential (Pa)
1	5-4	469	17
2	5-3-2	464	22
3	5-3-1	486	0

5.3 Genetic Algorithm Approach

5.3.1 Sample Problem IV

To illustrate the use of SGA for air duct design, the duct layout from Chapter 32 of [ASHRAE 1997] is used. This is shown in Figure 5.2. The economic and general system parameters are shown below. The input duct parameters for each duct section is similar to that for Sample Problem II. Unlike the previous examples, variable time of day load demands and utility rates are considered. It is assumed that there are two different operational modes for the fan; High Volume and Low Volume. This is depicted in the daily load profile shown in Figure 5.4. The High Volume flow rates correspond to the flow rates in Table 5.11 and the Low Volume rates are half the High Volume flow rates. The system operates in the high volume mode half of the year and in the low volume mode in the remainder. Furthermore, as shown below, the electrical energy rates are higher for the peak than the non-peak periods of electricity usage. The billing policy is shown in the Figure 5.5. Thus there are a total of four flow rate/utility rate operation modes for the system. The total operating time is 6000 hrs/yr. From Figure 5.4 and Figure 5.5, it can be deduced that 2750 hours (about 91.7%) of the High Volume operation occurs during the peak utility rate period yearly and in the case of the Low Volume mode, it is 500 hours (16.7%).

Economic and General Data

Absolute roughness	0.09 mm
Air density	1.204 m^3/kg

Unit electrical energy cost	
Non-peak period	0.06 $/kWh
Peak period	0.1 $/kWh
Ductwork cost	43 $/m^2
Fan efficiency	0.75
Motor and drive efficiency	0.8
Fan flow rate	
High volume	1.9 m^3/s
Low volume	0.95 m^3/s
Total Operating time	6000 hr/year
PWEF	9.01

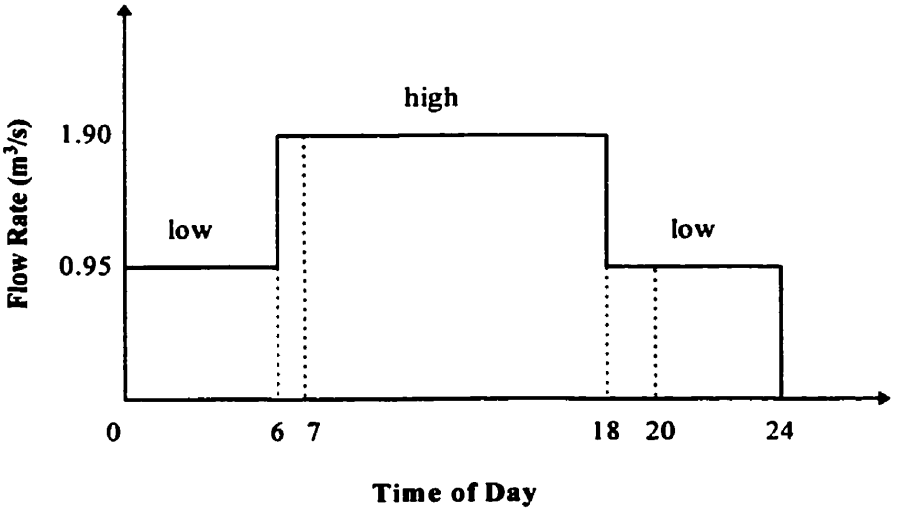

Figure 5.4: Daily Load Profile.

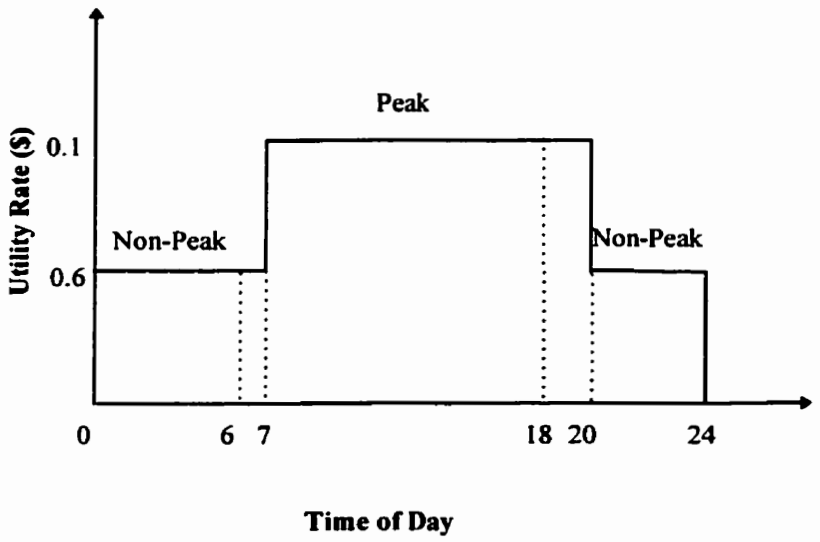

Figure 5.5: Electric Utility Billing Policy.

5.3.2 Constraints for Sample Problem III

The constraints of this particular problem are similar to that for Sample Problem II in Section 5.1.2. The only exceptions are the following.

Fixed Duct Sizes

Duct section 19 was assumed to be an 800x450mm rectangular pre-sized duct. This corresponds to the size indicated in [ASHRAE 1997].

Path Pressures

The aim was to achieve a zero pressure imbalance for this sample problem.

5.3.3 Implementation of Algorithm

The algorithm discussed in Section 4.5 has been implemented in C. A population size of 800 chromosomes and a tournament size of 5 (i.e. κ=5) were used. At each generation, a *coin toss*[1] is used to determine if a chromosome should be selected at random to undergo mutation. Mutation in the problem involved selecting a gene at random and using a *coin toss* to determine whether to increase or decrease the value by 1 (this corresponds to a size of 10mm). Figure 5.6 shows the chromosome representations for the return and supply duct subsystems separately. This was obtained using the scheme outlined in Section 4.5.1. These chromosomes contain all the duct sections with the exception of duct sections 4 and 19. However, it must be stated that it is possible to reduce the number of duct sections that are encoded in a chromosome to reduce the computation time. For example, if there is a dependency between any duct sections, only one duct needs to be sized to determine the other duct sizes. Therefore, only that particular duct section has to be included in the chromosome. The dynamic loss coefficients are calculated at run time by interpolation using tables provided by ASHRAE. The severe penalty parameter (w_1) used was 500, and the soft penalty parameter (w_2) was made equal to $1.9\left(E_d + E_c T\right)/10^3 \eta_f \eta_m$. The algorithm is stopped when 98% or more of the chromosomes have the same value for each gene.

[1] A computer implementation of a coin toss consists of generating a random number from a uniform distribution on the interval [0,1]. If a head is assumed to be the outcome of the toss when the number is less than 0.5, then a tail occurs when the number is more than or equal to 0.5.

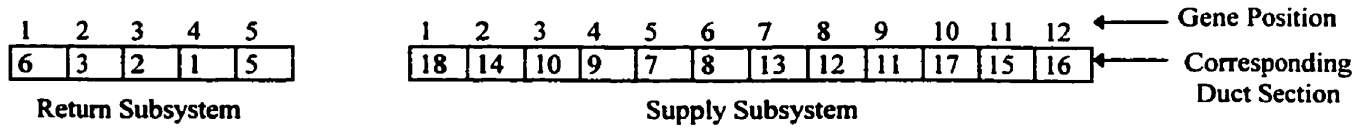

Figure 5.6: Chromosome Representation for Sample Problem.

5.3.4 Results and Discussions

The results obtained by using the segregated genetic algorithm discussed earlier are shown in Table 5.23 and Table 5.24. These are based on the best results obtained in 10 runs of the program. That is, 10 different seeds were used for the random number generator and the best solution selected. The duct sizes and associated pressure losses for both operational modes are in Table 5.23. The path pressures are indicated in Table 5.24 together with the path pressures from ASHRAE [1997]. The system total pressure for this design is 292Pa and 123Pa during the high volume and low volume operation periods respectively and has an associated cost of $11,717 (initial cost: $8,950, energy cost: $2,761). In the case of the ASHRAE Fundamentals design, the system total pressures are 679Pa and 213Pa while the total life-cycle cost would be $13,367 (initial cost: $7123, energy cost: $6,244) for the same operating conditions and utility rates shown in Figure 5.4 and Figure 5.5. For this example, the optimal design using the SGA resulted in energy costs much less than the initial cost but, for the ASHRAE design, they are nearly equal. The total cost for the ASHRAE design is 14% higher. This difference may be attributed in part to the different assumptions used for the costs and operating conditions for the two designs. The algorithm converged after 2098 generations for the

return subsystem and 3403 generations for the supply subsystem. However, as can be seen from the chart in Figure 5.7, most of the improvements were made in the earlier generations and the average and best fitness values approach each other as the algorithm progresses. Figure 5.7 shows the values for the supply subsystem and the high penalty function. The same phenomenon occurs for the return subsystem and the low penalty function.

Table 5.23: Optimal Duct Sizes and Pressure Losses.

Duct Section	Size (mm)	High Volume Operation			Low Volume Operation		
		Friction Loss (Pa)	Dynamic Loss (Pa)	Total Loss (Pa)	Friction Loss (Pa)	Dynamic Loss (Pa)	Total Loss (Pa)
1	380	4.96	7.99	12.94	1.39	2.00	3.39
2	260	19.15	-4.23	14.92	5.47	-1.06	4.41
3	390	10.23	26.69	36.91	2.83	6.67	9.50
4	600x600	0.19	28.02	28.21	0.06	25.75	25.81
5	500	9.00	13.54	22.54	2.54	3.39	5.92
6	640	4.81	17.79	22.60	1.34	4.45	5.78
7	250x250	4.18	27.56	31.74	1.20	25.64	26.84
8	410x250	0.36	31.92	32.28	0.11	26.73	26.83
9	670x250	2.72	9.82	12.54	0.78	2.46	3.24
10	580x250	6.69	29.78	36.47	1.92	7.44	9.37
11	350x250	3.53	33.80	37.32	1.00	8.45	9.45
12	350x250	7.88	30.04	37.92	2.24	7.56	9.80
13	400x250	33.42	9.14	42.55	9.22	2.28	11.51
14	760x250	7.95	3.00	10.95	2.20	0.75	2.95
15	330x150	12.92	7.93	20.85	3.71	1.98	5.69
16	350x150	5.68	14.68	20.35	1.63	3.67	5.30
17	230x150	36.45	33.82	70.27	10.08	8.45	18.53
18	800x760	0.90	28.73	29.63	0.26	7.51	7.77
19	800x450	1.80	93.90	95.71	0.50	34.73	35.23

Table 5.24: Path Pressure Losses.

Path	Ducts in Path	SGA				ASHRAE	
		High Volume		Low Volume			
		Path Loss (Pa)	Pressure Difference (Pa)	Path Loss (Pa)	Pressure Difference (Pa)	Path Loss (Pa)	Pressure Difference (Pa)
1	6-5-4	73	1	38	0	234	28
2	6-3-2	74	0	20	18	262	0
3	6-3-1	72	2	19	19	240	22
4	19-18-17-16	216	2	67	18	417	0
5	19-18-17-15	216	2	67	18	404	13
6	19-18-14-13-11	216	2	67	18	412	5
7	19-18-14-13-12	217	1	67	18	412	5
8	19-18-14-10-9-8	218	0	85	0	417	0
9	19-18-14-10-9-7	217	1	85	0	408	9

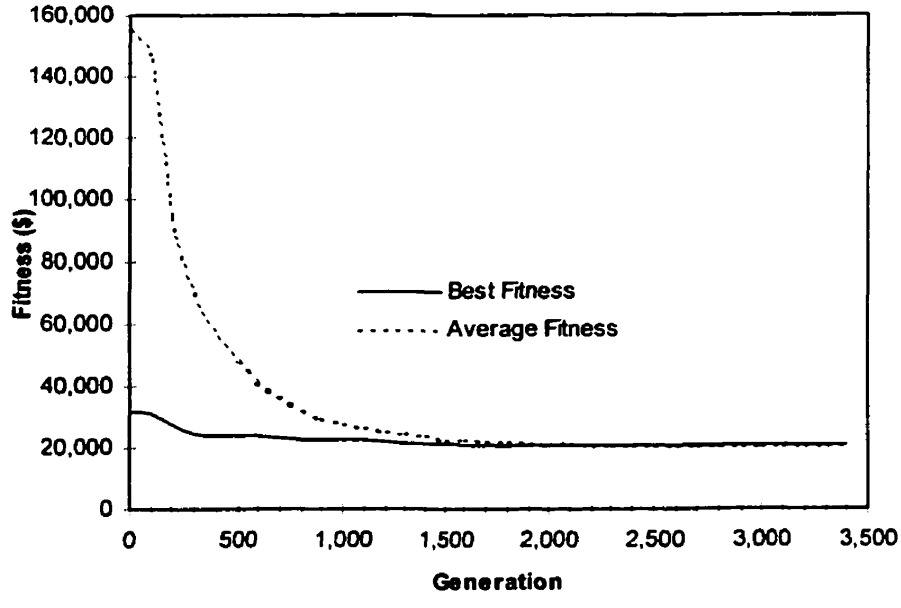

Figure 5.7: Progress of Algorithm Measured by the Average and Minimum Fitness.

As mentioned earlier, one important feature of GAs is their ability to handle complex objective functions involving variable utility rates and duty cycles for the equipment. If the problem above were to be solved using other existing duct design methodologies, it would require the simplification of the problem. This will involve using either the higher or time weighted average values of the time variable parameters. This approach will produce a design that may not be optimal in the sense of minimum LCC and performance when operated at actual operational conditions. Table 5.25 and Table 5.26 show a comparison between the SGA solution and solutions obtained using the simplifications for the return and supply subsystems respectively. All the energy cost figures are for the costs of energy under normal operation with the daily load and utility rates shown in Figure 5.4 and Figure 5.5. As can be seen, the designs based on the use of these design simplifications result in higher life-cycle costs than the design approach presented in this chapter. It is not surprising that the actual energy cost is lower when the high flow rates are used for the design. This is due to the fact that the high flow rates necessitate the selection of larger duct sizes to reduce the energy cost reflected in the higher initial cost (10.5% and 17.7% in the case of the return subsystem and 5.4% and 2.9% for the supply subsystem). Once the ducts have been over sized, the pressure losses under the actual operational conditions, which include low flow rate periods, results in a lower energy cost (35.5% and 24.5% in the case of the return subsystem and 6.3% and 3.5% for the supply subsystem) resulting in a relatively small overall increase in the total cost in the case of the return subsystem and a very small increase in the supply

Table 5.25: Comparison with Simplified Design Strategies-Return Subsystem.

Simplification Assumption	Cost ($)			Relative Change in Cost (%)		
	Initial	Energy	Total	Initial	Energy	Total
Basecase	3,379	723	4,102	-	-	-
High Flow Rate/ Peak Utility Rate	3,976	466	4,442	17.7	-35.5	8.3
High Flow Rate/ Weighted Average Utility Rate	3,733	545	4,279	10.5	-24.5	4.3
Weighted Average Flow Rate/ Peak Utility Rate	3,558	700	4,257	5.3	-3.2	3.8
Weighted Average Flow Rate/ Weighted Average Utility Rate	3,653	671	4,324	8.1	-7.2	5.4

Table 5.26: Comparison with Simplified Design Strategies-Supply Subsystem.

Simplification Assumption	Cost ($)			Relative Change in Cost (%)		
	Initial	Energy	Total	Initial	Energy	Total
Basecase	5,570	2,044	7,614	-	-	-
High Flow Rate/ Peak Utility Rate	5,872	1,916	7,788	5.4	-6.3	2.3
High Flow Rate/ Weighted Average Utility Rate	5,730	1,972	7,702	2.9	-3.5	1.2
Weighted Average Flow Rate/ Peak Utility Rate	5,321	2,395	7,717	-4.5	17.2	1.3
Weighted Average Flow Rate/ Weighted Average Utility Rate	5,462	2,183	7,645	-1.9	6.8	0.4

Table 5.27: Comparison with Simplified Design Strategies-Overall System.

Simplification Assumption	Cost ($)			Relative Change in Cost (%)		
	Initial	Energy	Total	Initial	Energy	Total
Basecase	8,950	2,767	11,717	-	-	-
High Flow Rate/ Peak Utility Rate	9,848	2,382	12,230	10	-13.9	4.4
High Flow Rate/ Weighted Average Utility Rate	9,463	2,518	11,981	5.7	-9.0	2.3
Weighted Average Flow Rate/ Peak Utility Rate	8,879	3,095	11,974	-0.8	11.9	2.2
Weighted Average Flow Rate/ Weighted Average Utility Rate	9,115	2,854	11,969	1.8	3.2	2.2

subsystem. These results however, should not be seen as supporting the use of these simplifying assumptions except for simple design problems. The results are more a reflection of the nature of this particular problem; more complex problems may give much larger differences. In the case of the weighted flow rate, the very low increase in cost with respect to the supply subsystem is achieved at the expense of greater pressure imbalance as is evident by the values in Table 5.28 and Table 5.24. Actually, the pressure distribution for both systems are inferior to the basecase design. Such large pressure imbalances would have to be adjusted by the use of additional duct dampers which are activated differently for the daytime and nighttime operating conditions if the specified flows are to be maintained.

As is apparent from the results, no one particular assumption offers the best design relative to the basecase optimal design. For the return subsystem, the most promising was based on the *Average Flow Rate/Peak Utility Rate* assumption and the least promising, on the *High Flow Rate/Peak Utility Rate* assumption. For the supply

subsystem, it was *Weighted Average Flow Rate/Weighted Average Utility Rate* and *High Flow Rate/Peak Utility Rate* respectively. This shows that designers make a leap of faith each time any of the simplifying assumptions are used, since there is no way to predict how they will perform. The segregated genetic algorithm, which does not require these assumptions, is necessary to eliminate the guess work in the design.

Table 5.28: Path Pressure Losses -Weighted Average Flow Rate/ Weighted Average Utility Rates.

Path	Ducts in Path	High Volume		Low Volume	
		Path Loss (Pa)	Pressure Difference (Pa)	Path Loss (Pa)	Pressure Difference (Pa)
1	6-5-4	51	19	32	0
2	6-3-2	70	0	19	13
3	6-3-1	70	0	18	14
4	19-18-17-16	234	0	72	13
5	19-18-17-15	233	1	72	13
6	19-18-14-13-11	233	1	71	14
7	19-18-14-13-12	234	0	72	13
8	19-18-14-10-9-8	217	17	85	0
9	19-18-14-10-9-7	217	17	85	0

Table 5.29 shows the path pressures obtained using the SGA when the system is assumed to be operating in the high volume mode and the utility rates are fixed at the peak value all the time. This illustrates the power of GA to find a good solution to the HVAC design problem by obtaining the right combination of duct sizes to achieve very good pressure balance for all the flow paths. One parameter that affects the performance of a GA is the population size. Usually, the solution improves with increasing population size as illustrated in Table 5.30 which shows the optimal LCC obtained to be sensitive to

different population sizes. However there is a population size beyond which this improvement ceases to be significant.

Table 5.29: Path Pressure Losses-High Volume Rates/ Peak Utility Rates.

Path	Ducts in Path	Path Loss (Pa)	Pressure Difference (Pa)
1	6-5-4	45.6	0.3
2	6-3-2	40.8	5.1
3	6-3-1	45.9	0.0
4	19-18-17-16	203.3	0.1
5	19-18-17-15	203.4	0.0
6	19-18-14-13-11	202.7	0.7
7	19-18-14-13-12	202.8	0.6
8	19-18-14-10-9-8	203.2	0.2
9	19-18-14-10-9-7	203.3	0.1

Table 5.30: Effect of Population Size on Performance of SGA.

Population Size	Return Subsystem Cost ($)	Supply Subsystem Cost ($)	Total Cost($)
200	4,339	7,755	12,094
400	4,173	7,697	11,870
800	4,102	7,614	11,716
1,600	4,072	7,500	11,572

5.3.5 Uncertainty in LCC

In the foregoing example, it was assumed that the parameters of the cost model, PWEF, air density, fan flow rates, ductworks cost, etc., were known with exact certainty

and were sufficient for the analysis. Although this assumption simplifies the evaluation of the costs, it is highly likely that the actual values of the parameters will not be exactly what was used for the analysis. Therefore, it is important to assess the sensitivity of each parameter on the LCC cost of the duct system. Figure 5.8 shows the percentage changes in the LCC corresponding to changes in each parameter. The changes in the parameter values is relative to the basecase values used above. The greatest changes in the LCC are due to changes in the ductwork cost and high flow rate. Changes in the fan overall efficiency (i.e. $\eta_f \cdot \eta_m$) had an equal but opposite effect on the LCC as changes in the PWEF, total yearly operating time and air density. Each of these terms are shown in Chapter 4 to have a similar effect on the LCC. The LCC is shown to be insensitive to the low flow rate and the non-peak utility rate for this particular problem.

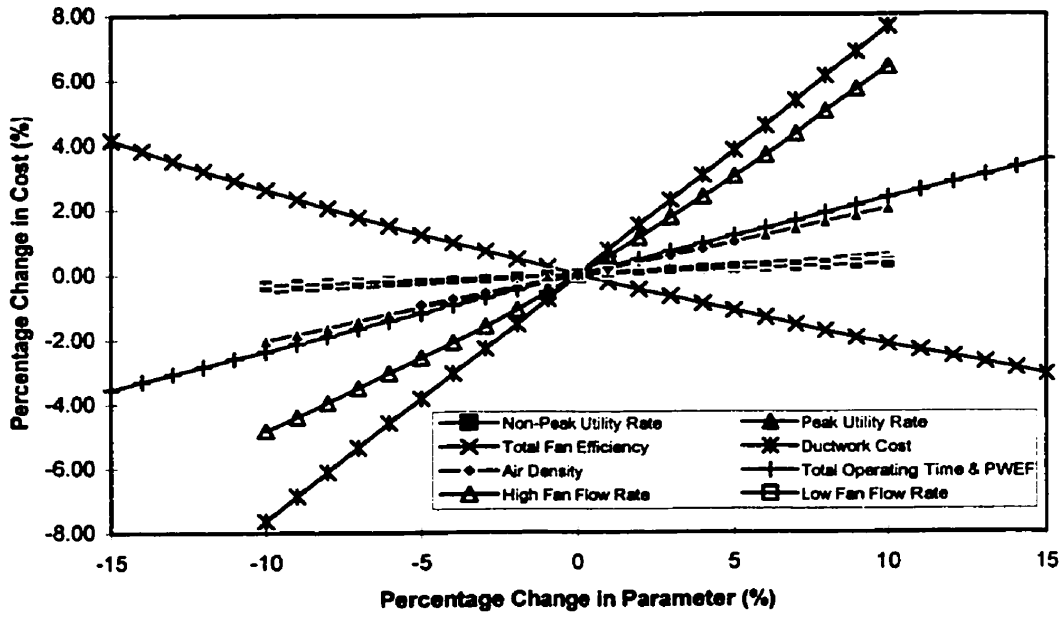

Figure 5.8: Assessing LCC Uncertainty.

This kind of uncertainty analysis considers one parameter at a time. However, in reality, it is possible to have changes in several parameters simultaneously. Furthermore, it is possible to have a parameter not vary uniformly in its assumed range. It might thus be more appropriate to represent the variation by other probability distributions. This leads to the problem of stochastic cost estimating. This was discussed in detail in Chapter 3 and in the next chapter, the stochastic cost estimating methodology would be illustrated.

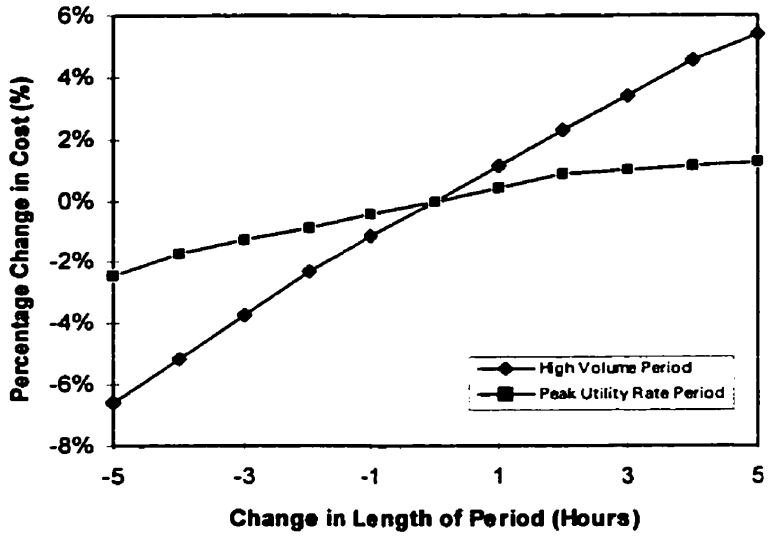

Figure 5.9: Effect of Changing Load Profile and Billing Policy.

Another consideration is the effect changes in the load profile (Figure 5.4) and billing policy (Figure 5.5) have on the LCC. Figure 5.9 shows the percentage changes in the LCC corresponding to changes in the high volume period and peak utility rates time duration (note that these changes are accompanied by corresponding changes in the low volume period and non-peak utility rate time duration respectively). A 1 hour change in

the high volume period in Figure 5.9 means that, the high volume period shown in Figure 5.4 now starts at 0530hrs and ends at 1830hrs. Similarly, a -1 hour change in the peak utility rate period in Figure 5.9 means that, the peak utility rates period shown in Figure 5.5 now starts at 0730hrs and ends at 1930hrs. As might be expected, increases in the duration of the high volume period and the peak utility rates time duration are accompanied by increases in the LCC and vice versa. The LCC is more sensitive to changes in the high volume duration than to the peak utility rates duration. For both cases, reductions in the lengths of these durations resulted in greater percentage changes in the LCC than corresponding increases.

6 Case Study: Probabilistic Cost Estimating and Optimization

6.1 Sample Applications

In the sample problems considered in the preceding chapter, it was assumed that the parameters of the cost model; PWEF, air density, fan flow rates, ductworks cost, etc., were known with exact certainty. Although this assumption simplified the evaluation of the costs and the optimization procedures, it is very likely that the actual values of the parameters will not be exactly what were used for the designs. As shown in Chapter 5, when the values of these parameters deviate from the assumed values, there is the possibility of the actual cost being significantly different from what was anticipated. To evaluate these effects, a sensitivity analysis that considered variations of the parameters one at a time was performed. However, it is likely there would be small changes in several parameters simultaneously. Furthermore, it is also possible to have a parameter not vary uniformly in its assumed range. It might thus be more appropriate to represent the variation by probability density functions that are not necessarily uniform.

Probabilistic cost estimating, like deterministic cost estimating, may be used to evaluate the cost of a system that has already be designed or is in the design process to arrive at the most cost-effective design. In probabilistic analysis, this can be with respect

to the expected LCC, minimum 95th quantile value, minimum inter-quartile range, etc. In this chapter, both applications of probabilistic cost estimating are illustrated. The first application uses the kernel estimator based simulation methodology discussed in Chapter 3 and in the second, simulation and genetic algorithm are combined in the optimal design of an HVAC air duct system. The sensitivity of the designs to variations in some physical parameters are also studied.

6.2 Cost PDF of Design for Sample Problem IV

The problem studied here is that in Sample Problem IV. The design solution obtained for that problem is shown in Table 5.23. This was based on a single value for the each parameter and had a minimum LCC of $11,717. The effect of changes in the values of the parameters on the LCC of the system was also studied taking only one parameter at a time. The interest in this section is to study the effect of simultaneous deviations from the assumed values of the parameters on the LCC of the system by considering all probable variations of the parameters in the cost model. The uncertainties considered are those in the interest rate, flow rate, escalation rate, unit energy cost, yearly operating time, overall system efficiency and unit duct cost. The distributions assigned to the parameters are shown in Table 6.1. These distributions are not based on any empirical data. They are selected just for the purposes of illustration and are assumed to be statistically independent. These distributions were chosen such that the means and/or modes were equivalent to the values assigned to these parameters in Sample Problem IV and that the range of the distributions covered the range used for the uncertainty analysis

therein. The fraction of time that the system operates in each flow rate/utility rate mode was, however, assumed fixed.

Table 6.1: Probability Density Functions of Uncertain Cost Model Input Parameters.

Cost Model Input Parameter	Distribution (Type; Parameters)
Interest Rate (i)	Triangular; Range = [2.5%,6.5%], Mode = 5%
Escalation Rate (j)	Triangular; Range = [2%,6%], Mode = 3%
Unit Electric Energy Cost (E_c)	
Non-Peak	Gamma; Mean = 0.06 \$/kWh, Variance = 0.007 \$/kWh
Peak	Gamma; Mean = 0.1 \$/kWh, Variance = 0.0117 \$/kWh
Fan Flow Rate	
High	Beta; Range [1.6 m^3/s ,2.5 m^3/s], Mean = 1.9 m^3/s %,
Low	Variance = 0.15m^3/s.
	Beta; Range [0.8 m^3/s,1.25 m^3/s], Mean = 0.95 m^3/s,
	Variance = 0.075 m^3/s.
Unit Duct Cost (S_d)	Uniform; Range = [38.7 \$/m^2, 47.3 \$/m^2]
Yearly Operating Time (T)	Normal; Mean=6000 hrs/yr, Variance = 300 hrs/yr
Total Fan Efficiency	Beta; Range [45%,70%], Mean = 60%, Variance = 4.2%.

6.2.1 Results

The application of the probabilistic cost estimating approach discussed in Chapter 3 has been implemented in C. The aim is to estimate the quantiles Ω={0.05, 0.075, ... , 0.925, 0.95} with α=0.05 and ζ set to 2% of the estimated quantile. One thousand (1,000) data points were used for the determination of b (i.e. $\bar{n}$=1000). Sampling after the preliminary analysis was done in batches of 100 data points (i.e. n=100). Figure 6.1

is the graph of b against the normalized value of $\widetilde{M}(b)$. As can be seen from the graph, 1.17 was selected as the value of b_n. Figure 6.2 is the estimated quantile function and the associated 95% confidence band. This is based on 1800 data points and the Epanechnikov kernel defined by

$$k(t) = \begin{cases} \frac{3}{4\sqrt{5}} - \frac{3t^2}{20\sqrt{5}} & for\ |t| < \sqrt{5} \\ 0 & otherwise \end{cases}. \qquad (6.1)$$

This is for the range $0.05 \leq p \leq 0.95$ and not the complete quantile function even though that could have be estimated. From Figure 6.2 or Table 6.2, it is seen that there is a 5% chance of the LCC being less than $10,592 (with a 95% confidence band of $ 10,496 and $10,654) and a 95% chance of it not exceeding $13,535 (also with a 95% confidence band of $ 13,423 and $13,658). The probability distribution function is shown in Figure 6.3.

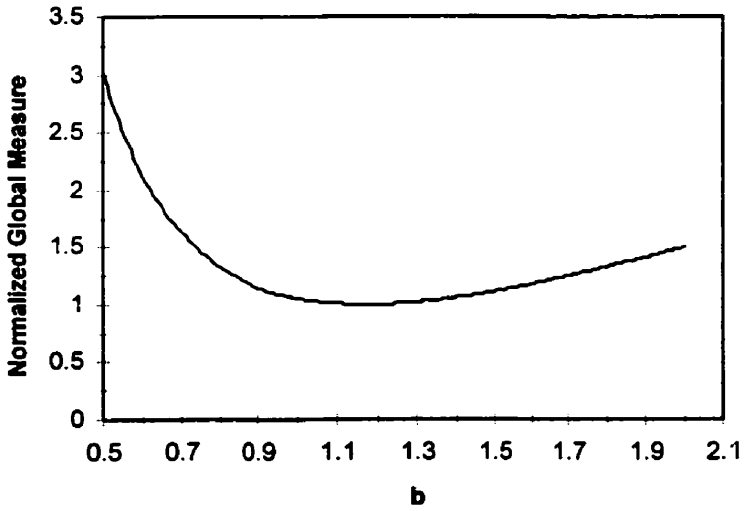

Figure 6.1: Determination of b.

For the purposes of comparison, simulations using the convergence of the sample moments were also done. The quantiles in this case were empirical estimates and are referred to as "Converged Moments Estimate" from this point on. To maintain consistency, sampling was done in batches of 100 data points and the simulations were stopped when subsequent estimates of the moments showed less than a 1% change. As stated earlier, it is difficult to translate this (1%) into the exact level of accuracy that may be achieved in the cost estimates, a disadvantage that is overcome using the approach suggested in this thesis. These quantile estimates are also shown in Figure 6.2 and required 4200 data points.

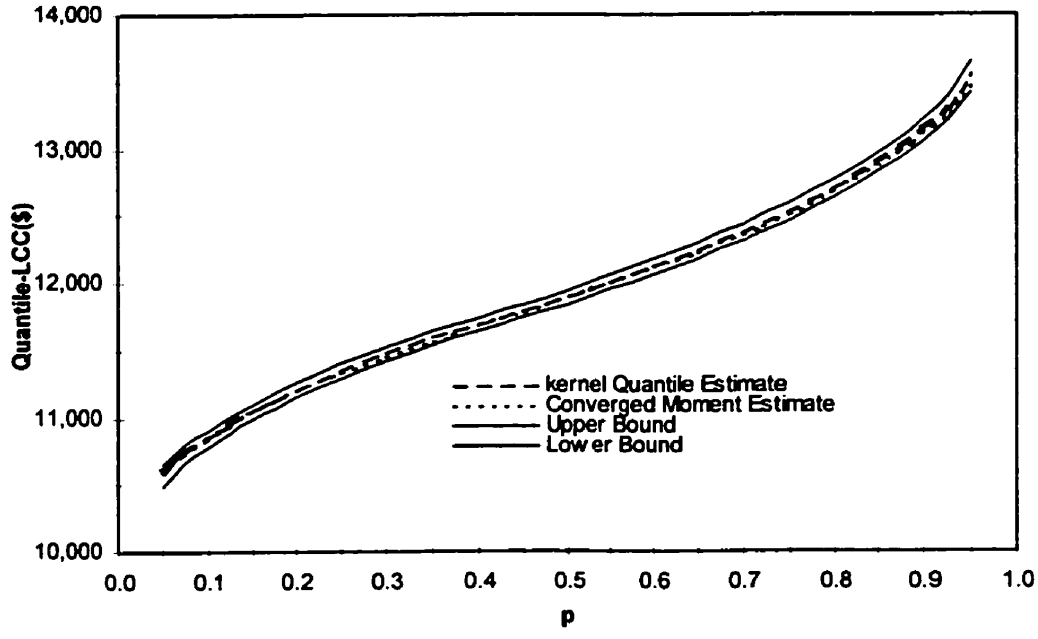

Figure 6.2: Estimated Quantile Function of the LCC of Air Duct System.

Table 6.2: Estimated Quantiles and Confidence Bounds

Quantile	Kernel Based Estimate	Converged Moments Estimate	Upper Bound	Lower Bound
0.05	10,593	10,615	10,654	10,496
0.075	10,734	10,746	10,794	10,669
0.1	10,853	10,856	10,911	10,790
0.125	10,955	10,954	11,012	10,894
0.15	11,047	11,049	11,103	10,987
0.175	11,130	11,127	11,185	11,073
0.2	11,207	11,198	11,262	11,151
0.225	11,281	11,267	11,336	11,225
0.25	11,352	11,332	11,406	11,296
0.275	11,419	11,394	11,470	11,364
0.3	11,481	11,459	11,530	11,428
0.325	11,539	11,515	11,586	11,489
0.35	11,593	11,568	11,637	11,545
0.375	11,643	11,622	11,687	11,598
0.4	11,692	11,682	11,736	11,648
0.425	11,741	11,740	11,786	11,696
0.45	11,790	11,783	11,836	11,744
0.475	11,840	11,841	11,888	11,794
0.5	11,892	11,900	11,942	11,844
0.525	11,947	11,951	11,998	11,896
0.55	12,002	12,001	12,055	11,951
0.575	12,060	12,057	12,113	12,007
0.6	12,118	12,113	12,172	12,065
0.625	12,178	12,168	12,233	12,124
0.65	12,240	12,227	12,298	12,185
0.675	12,306	12,293	12,365	12,249
0.7	12,374	12,359	12,436	12,316
0.725	12,447	12,416	12,511	12,387
0.75	12,525	12,503	12,591	12,463
0.775	12,608	12,575	12,675	12,544
0.8	12,696	12,674	12,765	12,630
0.825	12,790	12,776	12,861	12,723
0.85	12,892	12,869	12,965	12,824
0.875	13,004	12,980	13,081	12,934
0.9	13,134	13,113	13,218	13,059
0.925	13,294	13,246	13,396	13,211
0.95	13,535	13,461	13,658	13,423

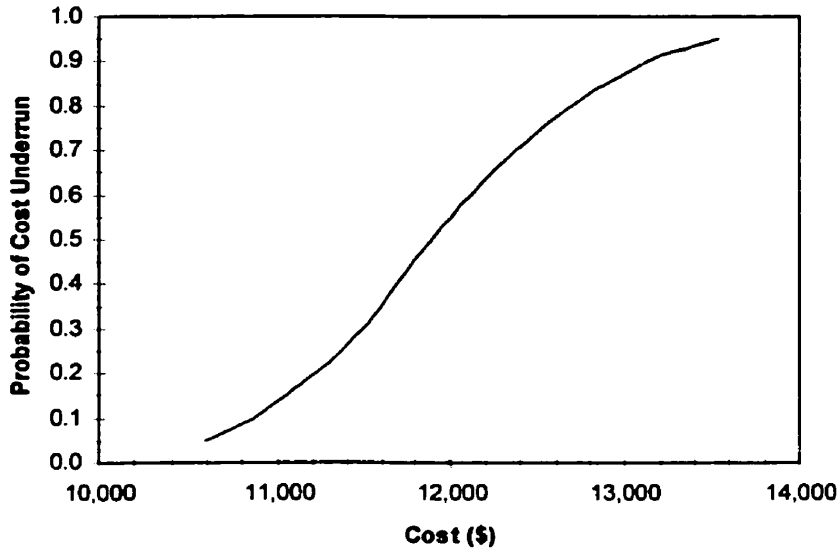

Figure 6.3: Kernel Based PDF Estimate of the LCC of the Air Duct System.

The number of data points used and the time for each estimate is shown in Table 6.3. As is apparent, the amount of data required in the new approach is far less than that for the converged moments approach and they both lie within the confidence band (Figure 6.1). With regards to computation time, the time required to sample and calculate the quantiles for the new approach was smaller. However, the exploratory studies needed for the determination of b_n required 688 secs, making the total computation time greater in the case of the suggested methodology. This is due in part to the amount of data (1000) used for that purpose. Using 100, 200 and 500 data points reduces this time to 9, 28 and 146 secs respectively. Furthermore, this time can be eliminated if the approximations mentioned in Chapter 3 are used to select a smoothing parameter. Table 6.7 shows how the choice of the size of the exploratory data influences the quantile estimate and the

estimation procedure. As expected, it does affect the value of b_n. However for this sample problem, it had very little effect on either the final size of the data sample or the quantile estimates.

As has been shown in this section, it is possible to get the same information on the estimated distribution from a significantly smaller amount of data by using the new approach. This approach also makes it easier for estimators to specify the required accuracy desired in the estimated distribution. Now that the PDF can be determined for any functional form of a CER, the logical extension is to incorporate this capability in designing the HVAC air duct system. This is studied in the next section.

Table 6.3: Number of Sample Data and Program Execution Time.

	Converged Moments Approach	New Approach
Data Size	4200	1800
Total Time (secs)	868	976
Time Without Exploratory Study (secs)	N/A	288

Table 6.4: Effect of the Size of Data for Exploratory Study.

Exploratory Data Size	Exploratory Time	Total Data Size	b_n	0.05 Quantile	0.95 Quantile
100	9	1,900	1.08	10,595	13,507
200	28	1,900	1.05	10,597	13,504
500	146	1,700	1.14	10,587	13,544
1000	688	1,800	1.17	10,593	13,535

6.3 Probabilistic Optimization of HVAC Air Duct System

This section considers the design of the HVAC air duct system when the values of the input parameters are uncertain or when a design that will be economically viable for a wide range of parameter values is desired. The adopted approach to this problem is the combination of genetic algorithm and simulation based cost estimation. As started earlier, GAs were developed independent of how the goodness or fitness of chromosomes (designs) are evaluated. It is therefore possible to use the Kernel estimator based cost estimating methodology to evaluate designs in a GA. The GA implementation does not need to be changed. The only limitation to the use of this is speed of computation. The focus is, therefore, to be on how to reduce this computation time. In dealing with probabilistic fitness functions in GAs, it is reasonable to use approximating fitness functions instead of the exact function. Thus, the first step in approximating the fitness function is to revert to the use of sample statistics for the cost estimates as an approximation to the kernel estimates. To reduce the effect of sampling variance from chromosome to chromosome, it is recommended that the same set of samples be used throughout the optimization procedure. In using GA in the deterministic case, it was realized that more than 70% of the time was used in the calculation of the dynamic loss coefficients. To reduce the computation time further, duct pressure losses are assumed to vary linearly between the pressures corresponding to the lower and upper bounds of the flow rate respectively. Thus, instead of calculating the pressure losses for each sampled flow rate, only the losses for the lower and upper bounds of the flow rates are calculated and the loss for any given flow rate approximated using a simple linear relationship.

The problem used here has the same duct layout as that for Sample Problem IV. The uncertain variables all have probability density functions similar to those assigned to them in Section 6.2. If μ and σ is the mean and standard deviation respectively of the fitness function (Equation 4.36) of the system, Design 1 is considered to be better than Design 2 when

$$\mu_1 < \mu_2 \text{ and } 1.01\mu_1 < \mu_2,$$

or

$$\mu_1 < \mu_2,\ 1.01\mu_1 > \mu_2 \text{ and } \frac{\sigma_1}{\mu_1} < \frac{\sigma_2}{\mu_2},$$

or

$$\mu_1 > \mu_2,\ \mu_1 < 1.01\mu_2 \text{ and } \frac{\sigma_1}{\mu_1} < \frac{\sigma_2}{\mu_2}.$$

That is, when the means of the cost of two designs are within 1% of each other, then the design with the smaller coefficient of variation (σ/μ) is selected. The objective of using the probabilistic objective function is to minimize the expected LCC and possibly, the dispersion (risk).

Other than the above mentioned modifications, the determination of the optimal design used the same implementation of the SGA discussed in the Chapter 4.

6.3.1 Results and Discussions

The optimal design of the system is shown in Table 6.5. The duct sizes are different from that obtained in the deterministic case discussed in Section 5.3. The cost for this system using the single fixed cost model parameters values is $12,317. This, as expected, is higher than the cost for the earlier design. The estimates of the quantiles for this design are shown in Table 6.6. This design has a lower expected LCC but, as can be

seen from Table 6.7, all the measures of dispersion were worse than those for the design from Section 5.3. This might be due to the fact that a lower premium was placed on minimizing the variance. The value of the variance only come into play when the means of two designs were within 1% of each other. This value could be increased or a fitness function that combined the weighted mean and variance could be devised if minimizing the variance is of greater importance. There is a 95% chance that the cost of this design will not be more than $13,423 as compared to $13,535 for the previous one. It is apparent that incorporating uncertainty in the fitness function help obtain a design that has a lower probability of having a high cost.

While stochastic optimization has a lot of advantages, a decision on whether to use it should be weighed against the amount of computation needed or complications introduced in doing so.

Table 6.5: Optimal Duct Sizes.

Duct Section	Size (mm)	Duct Section	Size (mm)
1	350	10	480x250
2	260	11	340x250
3	420	12	340x250
4	600x600	13	350x250
5	520	14	660x250
6	680	15	190x150
		16	210x150
7	220x250	17	260x150
8	520x250	18	800x800
9	660x250	19	800x450

Table 6.6. Estimated Quantiles.

p	Quantile	p	Quantile
0.05	10,413	0.525	11,779
0.075	10,556	0.55	11,836
0.1	10,676	0.575	11,894
0.125	10,779	0.6	11,953
0.15	10,872	0.625	12,014
0.175	10,956	0.65	12,076
0.2	11,033	0.675	12,142
0.225	11,107	0.7	12,212
0.25	11,178	0.725	12,288
0.275	11,246	0.75	12,369
0.3	11,309	0.775	12,455
0.325	11,368	0.8	12,547
0.35	11,423	0.825	12,645
0.375	11,474	0.85	12,751
0.4	11,522	0.875	12,868
0.425	11,571	0.9	13,003
0.45	11,620	0.925	13,172
0.475	11,670	0.95	13,423
0.5	11,723		

Table 6.7. Measures of Dispersion.

Statistic	Deterministic Design	Probabilistic Design
Mean	11,950	11,788
Standard Deviation	879.00	897.91
Coefficient of Deviation	0.0736	0.0762
$Q_{0.75}$-$Q_{0.25}$	1,173	1,191
$Q_{0.95}$-$Q_{0.05}$	2,932	3,010

6.4 Effect of Variations in Physical Parameters on System Performance

The duct design problems as discussed previously do not consider duct system performance variations resulting from variations in the physical parameters that will occur in a duct system due to the selection of duct materials and construction techniques

for each component and the entire system. That is, although the duct system design may show only small variations for the pressure imbalances among the various flow paths, the final installed system will likely reveal very significant deviations in the flow path pressures from those in the design or, conversely, deviations from the specified flow rate at each terminal. These deviations must be corrected before a building is finally commissioned by pressure or airflow balancing using a series of static flow control dampers in each duct flow path. This balancing of the ducting system is very complex and time consuming (e.g. for a large building this may take several technicians one or more years). It typically adds about 10% to the installed capital cost and, due to the extra pressure losses at the various dampers, a further 10% to the operating cost.

The cause of these deviations in airflow rate at each of the terminals is primarily due to variations in the dynamic loss coefficients for the various fittings and duct lengths. That is, although past, and widely used, literature suggests that a particular fitting will have a unique dynamic loss coefficient, some recent literature shows that these fitting dynamic loss coefficients will vary significantly from one supply vendor to another and they will often show some variation with inlet velocity or Reynolds number [Brooks, 1993]. This very limited literature on duct fitting dynamic loss coefficients has been confirmed by more extensive studies of dynamic loss coefficients for pipe fittings using water. For example, variations in elbow dynamic loss coefficients of 22.6% compared to the mean value of six fittings supplied by six different vendors were found and 0 to 46% compared to the standard design literature [Rahmeyer 1999a&b]. For more complex pipe fittings (e.g. Tees) these deviations in the fitting dynamic loss coefficients may be several hundred percent compared to the standard literature. Uncertainties in the

dynamic loss coefficients in the final constructed ducting system will cause the system to behave differently than the design terminal flow rates predicted and necessitate flow balancing.

A more robust duct design would reduce the cost of pressure and flow balancing in newly installed ducting systems. To illustrate the robustness of the various duct design methods, the solutions to the 19-section duct design problem were considered and a typical range of parameter variations at the 95% confidence level for the duct sizes (±2%), duct section friction factors (±5%) and duct dynamic loss coefficients (±50%) introduced. The results from the study are shown for the effect of variations in the duct diameters only in Table 6.8-Table 6.10, friction factors and dynamic loss coefficients only in Table 6.11-Table 6.13, and then all three simultaneously in Table 6.14-Table 6.16. The study was based on the high flow rates since it is similar to that for the ASHRAE design and thus provides a better basis for comparison. The "Best" and "Worst" values refer to the best and worst possible operation conditions respectively. As can be seen from the tables, the solution for Sample Problem IV based on the segregated genetic algorithm (SGA) method of duct design achieved a more robust duct design compared to the ASHRAE results with respect to the maximum pressure imbalance, average pressure imbalance, and system pressure range. This might be due in part to the fact that a design penalty function which punished designs with large pressure imbalances among the various flow paths was used.

It is possible to use a probabilistic optimization approach similar to that in Section 6.3 to ensure the design is not susceptible to the aforementioned variations. In this case, a simulation procedure is used to evaluate a design's robustness and incorporated into the

fitness. The performance of this design is shown in Table 6.8-Table 6.16, in the "Robust Design" rows. As can be seen, it outperforms all the other design solutions. This is not surprising since the robustness of the designs were explicitly treated in the optimization procedure.

Table 6.8: Maximum Path Pressure Imbalance due to Variations in Duct Sizes (Pa).

Design	Return Subsystem		Supply Subsystem	
	Best	Worst	Best	Worst
SGA	1.20	24.13	1.27	16.52
ASHRAE	4.19	110.14	7.63	30.61
Robust Design	0.05	14.11	1.53	17.01

Table 6.9: Average Path Pressure Imbalance due to Variations in Duct Sizes (Pa).

Design	Return Subsystem		Supply Subsystem	
	Best	Worst	Best	Worst
SGA	1.00	19.74	0.91	11.03
ASHRAE	2.71	90.84	4.08	21.10
Robust Design	0.04	12.17	0.89	10.30

Table 6.10: System Pressure due to Variations in Duct Sizes (Pa).

Design	Minimum	Maximum	Range
SGA	284.59	316.88	32.28
ASHRAE	631.75	775.74	143.99
Robust Design	231.83	251.80	19.97

Table 6.11: Maximum Path Pressure Imbalance due to Variations in Frictional Factors and Dynamic Loss Coefficients (Pa).

Design	Return Subsystem		Supply Subsystem	
	Best	Worst	Best	Worst
SGA	0.62	24.03	3.90	40.43
ASHRAE	7.33	97.41	12.44	70.87
Robust Design	0.33	12.18	3.81	34.67

Table 6.12: Average Path Pressure Imbalance due to Variations in Frictional Factors and Dynamic Loss Coefficients (Pa).

Design	Return Subsystem		Supply Subsystem	
	Best	Worst	Best	Worst
SGA	0.33	22.23	2.10	27.58
ASHRAE	3.69	61.99	6.50	48.62
Robust Design	0.22	10.37	2.45	19.31

Table 6.13: System Pressure due to Variations in Frictional Factors and Dynamic Loss Coefficients (Pa).

Design	Minimum	Maximum	Range
SGA	246.58	365.21	118.63
ASHRAE	556.12	830.45	274.33
Robust Design	192.46	298.49	106.03

Table 6.14: Maximum Path Pressure Imbalance due to Variations in Duct Sizes, Frictional Factors and Dynamic Loss Coefficients (Pa).

Design	Return Subsystem		Supply Subsystem	
	Best	Worst	Best	Worst
SGA	0.03	49.96	1.46	60.35
ASHRAE	0.34	184.21	4.15	111.07
Robust Design	0.02	30.28	1.29	49.74

Table 6.15: Average Path Pressure Imbalance due to Variations Duct Sizes, Frictional Factors and Dynamic Loss Coefficients(Pa).

Design	Return Subsystem		Supply Subsystem	
	Best	Worst	Best	Worst
SGA	5.45	20.14	12.09	17.81
ASHRAE	17.61	94.21	22.28	30.87
Robust Design	3.72	11.06	9.25	14.02

Table 6.16: System Pressure due to Variations in Duct Sizes, Frictional Factors and Dynamic Loss Coefficients(Pa).

Design	Minimum	Maximum	Range
SGA	222.72	405.64	182.92
ASHRAE	487.07	965.31	478.24
Robust Design	292.59	325.89	33.30

6.5 Summary

The use of the probabilistic cost estimating approach outlined in Chapter 3 has been illustrated. This approach to cost estimating provides information about the probability distribution function of cost estimates that is invaluable in decision making. As shown, it is possible to get the same level of information on the estimated distribution from a significantly smaller amount of data by using this new approach. The approach also makes it easier for estimators to specify the required accuracy desired in the estimated distribution.

Also illustrated was how the segregated genetic algorithm can be used together with probabilistic cost estimating methods to optimize an HVAC system when there are uncertain design and economic parameters. This is possible because of the flexibility of genetic algorithms. Variations in the physical parameters that occur in duct systems due to the selection of duct materials and construction techniques affect the actual performance of the duct system. It was shown that the design obtained from using SGA was less susceptible to these variations than the ASHRAE design. An even more robust design is achieved when these variations are incorporated in a probabilistic optimization procedure using SGA.

7 Conclusions and Future Work

As was discussed in Chapter 1, the objective of this thesis was to:

1. Develop methodologies for the estimation of LCC under uncertainty and the specifications of the uncertainties associated with cost estimates,
2. Investigate the development of simple life-cycle cost based design methodologies for HVAC air duct design,
3. Demonstrate the use of genetic algorithm optimization techniques in the design of complex HVAC air duct systems for minimum life-cycle cost,
4. Investigate the impact of parameter uncertainty in HVAC air duct design optimization, and
5. Show the robustness of the final design to typical variations of some key design parameters for the system components.

These issues were analyzed in the subsequent chapters. In this chapter, the final conclusions and contributions of this thesis and recommendations for future work are presented.

7.1 Summary

A review of pertinent material in the cost modeling and HVAC air duct design literature was presented in Chapter 2 of this thesis. As the literature on cost models and estimating methodologies revealed, one issue that has not been thoroughly investigated is the uncertainties in the parameters. As cost is uncertain in many aspects, it is imperative that any life-cycle model incorporate the treatment of uncertainties. Although simulation approaches to probabilistic cost estimating has been recognized as superior to analytic approaches, current work in cost estimating employing simulation often do not incorporate proper procedures for terminating the simulation and for specifying the desired accuracy in the PDF of the cost estimate.

The literature shows that current typical designs have LCC almost 30% higher than optimized designs. It can be seen from the literature on HVAC air duct design methodologies that among the three design methodologies recommended in [ASHRAE 1997], only the T-Method is a life-cycle cost optimization procedure. However, it has the shortcoming of needing the condensation and expansion of the system- a tedious procedure, and is incapable of handling complicated objective functions such as those with time varying or uncertain parameters.

In Chapter 3, a solution to the probabilistic cost estimating problem was discussed. The simulation approach employed kernel estimators and their asymptotic properties in probabilistic cost estimating. A stopping rule for the simulation procedure was proposed. Also it was suggested that the PDF be estimated by first estimating the quantile function

and then inverting it. This permits the easy specification by the estimator of the desired accuracy in the cost estimate.

The need for a design methodology that enables the design of economically efficient HVAC air duct systems can not be over emphasized. Chapter 4 discussed the methodologies and tools developed for the HVAC air duct sizing problem which are the IPS-Method, the Diameter Chart and the Enhanced Friction Chart, and the use of a Segregated Genetic Algorithm (SGA). The IPS-Method is a systematic approach to duct size selection and pressure balancing. The pressure balancing procedure can however be applied to any design problem irrespective of how the initial duct sizes are determined. The power of the IPS-Method is its simplicity and the fact that it eliminates the need to condense and expand the system; things required in the T-Method. Furthermore, it avoids the duct size rounding problem encountered in the T-Method. As a consequence of the IPS-Method, the Enhanced Friction Chart and Diameter Chart were developed. These charts can be used as guides in the sizing of duct sections. These are better tools for the selection of duct sizes to optimize LCC than the existing Friction Chart. In designing HVAC systems using the Friction Chart supplied by ASHRAE, the size selected will depend on the expertise of the designer who, to some degree, may take into consideration the economic parameters. However, different designers may arrive at different duct sizes given the same problem. The Enhanced Friction and Diameter Charts remove this inconsistency while incorporating the economic parameters explicitly in the sizing of the duct. With these charts, once the flow rate and economic factor are fixed, the size is also fixed (this is subject to minor errors caused by the reading of the diameter from the chart). For example, if a duct with a flow rate of $0.1 m^3/s$ were to be sized using

the new charts, the selected sizes would be 180mm, 150mm, and 100mm for economic factors of $1m^2/kW$, $0.2m^2/kW$ and $0.03m^2/kW$ respectively. Although these charts are meant for circular ducts, an expression for converting duct diameters to equivalent rectangular ducts was developed to enable its use for the sizing of rectangular ducts. For complex design problems where the IPS-Method and the use of the Diameter and Enhanced Friction Charts are not applicable, the use of a segregated genetic algorithm for the design of HVAC air duct systems was suggested.

In Chapters 5 and 6, case studies were used to illustrate the efficacy of the suggested approaches. Chapter 5 dealt with the air duct design methodologies and Chapter 6 discussed the probabilistic cost estimating methodology, how genetic algorithms can be used in the probabilistic optimization of the air duct system, and the sensitivity of the designs to variations in the physical parameters.

The solutions to Sample Problem I showed that the IPS-Method was capable of obtaining the same solution as the T-Method while avoiding the tedious mathematical computations associated with the T-Method. In the T-Method, to avoid the use of an optimization algorithm like dynamic programming, to incorporate the constraint of standard duct sizes, a heuristic is used to select the standard sizes. This does not ensure that the sizes selected are optimal. The IPS-Method avoids the need for a heuristic by incorporating the constraint very early in the procedure and making a choice of standard size based on the LCC, the objective being optimized. The results of the balancing procedure for both Sample Problem I and II clearly showed a progressive reduction of the LCC and path pressure imbalance.

Using the Enhanced Friction Chart, the ease in selecting the duct sizes for design problems was demonstrated. The design solution for Sample Problem III (which was the same as Sample Problem I) differed from that obtained from the IPS-Method and T-Method only in the size of one duct section and a total LCC of $46.

Sample Problem IV involved variable time-of-day operating conditions and variable time-of-day utility rates. This was solved using a segregated genetic algorithm. The optimal design using the SGA resulted in energy costs much less than the initial cost and a total cost with savings of 14% compared to the design recommended by ASHRAE [1997]. This difference may be attributed in part to the different assumptions used for the costs and operating conditions for the two designs. The illustrative examples also showed that the use of segregated genetic algorithms lead to very good pressure distribution among each of the many flow paths.

If Sample Problem IV is solved using other existing duct design methodologies, it will require the simplification of the problem by using either the higher or time weighted average values of the time variable parameters. A comparison between the solution based on SGA and solutions obtained using the simplifications for the return and supply subsystems and the overall system, showed savings of between 0.4% and 8.3%. The small savings in some of the designs should not be seen as supporting the use of these simplifying assumptions except for simple design problems. The results were more a reflection of the nature of this particular problem; more complex problems may give much larger differences. Moreover, the assumption that produced the best design relative to the basecase optimal design differed for each subsystem which shows designers can not foretell which of the simplifying assumptions would be best for a given design

problem. An approach such as the segregated genetic algorithm that does not require these assumptions is thus necessary and essential to eliminate the guess work in the design process.

Through an example, it was shown that the suggested approach to cost estimating provided information about the cost estimate that is invaluable in decision making. As the example in Chapter 6 showed, it is possible to get the same level of information on the estimated distribution from a significantly (about 57%) less amount of data by using the approach developed in this thesis as compared to the procedure that monitors the moments of the distribution. The suggested approach also makes it easier for estimators to specify the required accuracy desired in the estimated distribution. The time needed for the exploratory study to determine b_n was 688 secs for a data set of 1000. This time can be considerable reduced without adversely affecting the PDF estimate by using a smaller data set for the exploratory study.

While the IPS-Method or the enhanced friction chart, might be computationally more efficient for simple duct design problems, it is obvious that the SGA approach is less restrictive in the kind of problems it can treat as evidenced in its application to the optimization of an HVAC system when there are uncertain design and economic parameters. This is possible because of the flexibility of genetic algorithms. This design has a lower expected LCC but all the measures of dispersion were worse than those for the design from Section 5.3. This might be due to the fact that a lower premium was placed on minimizing the variance. The value of the variance only come into play when the mean of two designs were within 1% of each other. This value could be increased if minimizing the variance is of greater importance or a fitness function combining the

weighted mean and variance could be devised. There is a 95% chance that the cost of this design will not be more than $13,423 as compared to $13,535 for the previous one. It is apparent that incorporating uncertainty in the objective helps to obtain a design that has a lower probability of high cost. Variations in the physical parameters that occur in duct systems due to the selection of duct materials and construction techniques affect the actual performance of the duct system. It was shown that the design got from using SGA was less susceptible to these variations than the ASHRAE design. While the design based on SGA had the best and worst possible pressure imbalance to be 0.03Pa and 60.36Pa respectively, the ASHRAE design had corresponding values of 0.34Pa and 184.21Pa. An even more robust design is achieved when these variations are incorporated in a probabilistic optimization procedure using SGA. This has best and worst pressure imbalance of 0.02Pa and 49.74Pa respectively.

While stochastic optimization has a lot of advantages, a decision whether to use it should be weighed against the amount of computation needed or complications introduced in doing so.

7.2 Conclusions

It is concluded from this research that:

1. The IPS-Method, Enhanced Friction Chart and Diameter Chart are accurate and better design methods than existing HVAC duct design methods (including the T-Method) and should be used especially for simple duct design problems,

2. For complex duct design problems, the Segregated Genetic Algorithm (SGA) method is preferable to all other methods.
3. For duct design problems with significant uncertain parameters, the stochastic optimization method using SGA and simulation is the preferred method of design.
4. To estimate the cost of a system with uncertain parameters, combining simulation with kernel quantile estimators offers the best method.

7.3 Future Work

Two issues in cost estimating that were not treated here and are also often ignored by others is the correlation between the input parameters and the fact that the parameters can also change with time. The first problem requires the ability to generate correlated random variables and methodologies, albeit not universally applicable and accurate, exist for that purpose. The second issue can be easily incorporated into the suggested approach by dividing the life of the product into periods and specifying distributions for each uncertain parameter in each period. In both cases, the PDFs for the estimates can then be determined using the approach discussed in Chapter 3.

Although the correlation coefficient can be used to incorporate dependencies, it does have a lot of limitations. There is therefore the need to develop a better measure of association that is applicable to a wider range of multivariate distributions or to develop cost models that consist of only independent variables. The first is a statistical problem that has to be addressed by the Mathematics, Statistics and Probability research

communities. The second is a more straight forward issue. Given any CER C, with N correlated variables, it is always possible to designate N' variables as independent variables and express the remaining N- N' dependent variables in terms of the N' independent variables. Replacing these in C would give a new CER, C', which will be a function of only independent variables. This will, however, require the use of historical data.

With regards to HVAC air duct design, the segregated genetic algorithm offers an appealing way to solve a wide variety of design problems. Two avenues of further research are

1. a study of the different coding schemes possible for the chromosomes to determine the optimal coding scheme and
2. the extension of the algorithm to include the choice of the duct materials, insulation and other properties and the inclusion of leakage and the selection of the fan in the optimization.

Furthermore, although the genetic algorithm was applied to a particular air duct system, it is easy to see how this methodology can be easily extended to other ducting and piping problems. Indeed, most HVAC and R design problems with their many components and nonlinear performance factors and constraints might be best tackled using genetic algorithms to reduce life-cycle costs.

References

Alting, L., 1993, Life-Cycle Design of Products: A New Opportunity for Manufacturing Enterprises, *Concurrent Engineering: Automation, Tools, and Techniques*, ed. A. Kusiak, John Wiley & Sons, 1-17.

ASME, 1985, *ANSI/ASME PTC 19.1-1985: Measurement Uncertainty- Instruments and Apparatus*, Part 1, ASME, New York.

ASHRAE, 1997, Chapter 32: Duct Design, *ASHRAE Handbook: Fundamentals*, Atlanta, ASHRAE, Inc., SI edition.

Asiedu, Y. and Gu, P., 1998, Product Life Cycle Cost Analysis: State of the Art Review, *International Journal of Production Research*, **36** (4), 883-908.

Asiedu, Y., Besant, R. W. and Gu, P., 1999a, A Simplified Procedure for HVAC Duct Sizing, *ASHRAE Transactions*, To Appear.

Asiedu, Y., Besant, R. W. and Gu, P., 1999b, HVAC Duct System Design Using Genetic Algorithms, *HVAC&R Research*, Under Review.

Asiedu, Y., Besant, R. W. and Gu, P., 1999c, Simulation Based Cost Estimation Under Economic Uncertainty Using Kernel Estimators, *International Journal of Production Research*, Under Review.

Azzalini, A., 1981, A Note on the Estimation of a Distribution Function and Quantiles by a Kernel Method, *Biometrika*, **68** (1), 326-328.

Beasley, D., Bull, D. R., and Martin, R. R., 1993, An Overview of Genetic Algorithms: Part 1, Fundamentals, *University Computing*, **15** (2), 58-69.

Boothroyd, G., 1994, Product Design for Manufacture and Assembly, *Computer-Aided Design*, **26** (7), July, 505-520.

Boothroyd, G. and Dewhurst, P., 1983a, Design for Assembly: Selecting the Right Method, *Machine Design*, Nov. 10, 94-98.

Boothroyd, G. and Dewhurst, P., 1983b, Design for Assembly: Manual Assembly, *Machine Design*, Dec. 8, 140-145.

Boothroyd, G. and Radovanovic, P., 1989, Estimating the Cost of Machined Components During the Conceptual Design of a Product, *Annals of the CIRP*, **38**, Part 1, 157-160.

Bras, B. and Emblemsvag, J., 1995, Activity-Based Costing and Uncertainty in Designing for the Life-Cycle, *Design for X: Concurrent Engineering Imperatives*, ed. G. Q. Huang, Chapman & Hall Series on Design and Manufacture.

Brooks, P. J., 1993, New ASHRAE Local Loss Coefficients for HVAC Fittings, *ASHRAE Transactions*, **99**(2), 169-193.

Brooks, P. L., Davidson, L. J. and Palamides, J. H., 1993, Environmental Compliance: You Better Know Your ABCs, *Occupational Hazards*, Feb., 41-46.

Carriere, M., Schoenau, G. J. and Besant, R. W., 1998, A Revised Procedure for Duct Design with Minimum Life-Cycle Cost, *ASHRAE Transactions*, **104**(2), 62-67.

Chan, W-T, Chua, D. K. H., and Kannan, G., 1996, Construction Resource Scheduling with Genetic Algorithms, *Journal of Construction Engineering and Management*, **122** (2), June, 125-132.

Chapman, C. D., Saitou, K. and Jakiela, M. J., 1993, Genetic Algorithms as an Approach to Configuration and Topology Design, *Advances in Design Automation, ASME*, DE-Vol. 65-1, 485-498.

Cheng, C., 1995, Uniform Consistency of Generalized Kernel Estimators of Quantile Density, *The Annals of Statistics*, **23** (6), 2285-2291.

Cooper, D. and Chapman, C., 1987, *Risk Analysis for Large Projects-Models, Methods and Cases*, , John Wiley & Sons.

Daschbach, J. M. and Apgar, H., 1988, Design Analysis Through Techniques of Parametric Cost Estimation, *Engineering Costs and Production Economics*, **14**, 87-93.

Dean, E. B., 1989, Parametric Cost Analysis: A Design Function, *Transactions of the 33rd Annual Meeting the American Association of Cost Engineers*, San Diego, CA, USA, June.

Dean, E. B. and Unal, R., 1992, Elements of Designing for Cost, *Proceedings of AIAA 1992 Aerospace Design Conference*, Irvine, CA, USA, Feb.

Dewhurst, P., 1988, Computer-Aided Assessment of Injection Molding Cost: A Tool for DFA Analyses, *Department of Mechanical, University of Rhode Island, Report #24*, April.

Dewhurst, P. and Blum, C., 1989, Supporting Analyses for the Economic Assessment of Diecasting in Product Design, *Annals of the CIRP*, **38**, Part 1, 161-164.

Dewhurst, P. and Boothroyd, G., 1984a, Design for Assembly: Automatic Assembly, *Machine Design*, Jan. 26, 87-92.

Dewhurst, P. and Boothroyd, G., 1984b, Design for Assembly: Robots, *Machine Design*, Feb. 23, 72-76.

Dewhurst, P. and Boothroyd, G., 1988, Early Cost Estimating in Product Design, *Journal of Manufacturing Systems*, **7** (3), 183-191.

Dixon, J. R. and Poli, C., 1995, *Engineering Design and Design for Manufacturing: A Structured Approach*, Field Stone Publishers.

Dowlatshahi, S., 1992, Product Design in a Concurrent Engineering Environment: An Optimization Approach, *International Journal of Production Research*, **30** (8), 1803-1818.

Ehrlenspiel, K., 1987, Reduction of Product Costs in West Germany, *International Conference on Engineering Design, ICED '87*, Aug., 796-806.

Emblemsvag, J. and Bras, B., 1994, Activity-Based Costing for Product Retirement, *Advances in Design Automation, ASME*, DE-Vol. 69-2, 351-361.

Fabrycky, W. J., 1987, Designing for the Life Cycle, *Mechanical Engineering*, Jan., 72-74.

Fabrycky, W. J. and Blanchard, W. J., 1991, *Life-Cycle Cost and Economic Analysis*, Prentice Hall.

Fad, B. E. and Summers, R. M., 1988, Parametric Estimating for New Business Ventures, *Engineering Costs and Production Economics*, **14**, 165-176.

Fleischer, G. A. and Khoshnevis, B., 1986, Incorporating Economic Impact Assessment into Computer-Aided Design, *1986 International Industrial Engineering Conference Proceedings*, 163-174.

Flood, I., 1997, Modeling Uncertainty in Cost Estimates: A Universal Extension of the Central Limit Theorem, *Proceedings of the 1997 4th Congress on Computing in Civil Engineering*, New York, Jun 16-18, 551-558.

French, M. J., 1990, Function Costing: Potential Aid to Designers, *Journal of Engineering Design*, **1** (1), 47-53.

Gershenson, J. and Ishii, K., 1993, Life-Cycle Design for Serviceability, *Concurrent Engineering: Automation, Tools, and Techniques*, ed. A. Kusiak, John Wiley & Sons, 363-384.

Gibbons J. D., 1993, *Nonparametric Measures of Association*, Sage University Paper Series on Quantitative Applications in the Social Sciences, (07-091), Sage, Newbury Park, CA,USA.

Greves, D., and Schreiber, B., 1993, Engineering Costing Techniques in ESA, *URL-http://esapub.esriu.esa.it/pointtobullet/greves1.html*,.

Grimm, N. R., 1990, Duct Sizing, *HVAC Systems and Components Handbook*, ed. Grimm, N. R. and Rosaler, R. C., 2nd Edition, McGraw-Hill, New York, 3.2.1-3.2.4

Gupta, Y. P., 1983, Life Cycle Cost Models and Associated Uncertainties, *Electronics Systems Effectiveness and Life Cycle Costing*, NATO ASI Series, Vol. F, ed. J. K. Skwirzynski, Springer-Verlag, Berlin, 535-549.

Gupta, Y. and Chow, W. S., 1985, Twenty-Five Years of Life Cycle Costing - Theory and Application: A Survey, *The International Journal of Quality and Reliability Management*, **2**, 51-76.

Harr, M. E., 1989, Probabilistic Estimates for Multivariate Analyses, *Applied Mathematical Modelling*, **13**, May, 313-318.

Heiselberg, P., 1996, Room Air and Contaminant Distribution in Mixing Ventilation, *ASHRAE Transactions*, **102** (2), 332-339.

Herbert, M. B., 1990, Conceptual and Preliminary Design, *HVAC Systems and Components Handbook* ed. Grimm, N. R. and Rosaler, R. C., 2nd Edition, McGraw-Hill, New York, 1.1.5-1.1.19.

Huthwaite, B., 1989, The Link Between Design and Activity-Based Accounting, *Manufacturing Systems*, Oct., 44-47.

Irwin, D., Simonson, C. J., Saw, K. and Besant, R. W., 1998, Contaminant and Heat Removal Effectiveness and Air-to-Air Heat/Energy Recovery for a Contaminated Air Space, *ASHRAE Transactions*, **104** (2), 433-447.

Ishii, K., 1995, Life-Cycle Engineering Design, *Design for Manufacturability, ASME*, DE-Vol. 81, 39-45.

Jelen, F. C. and Black, J. H., 1983, *Cost and Optimization Engineering*, 2nd Edition, McGraw Hill.

Johnson, V. S., 1990, Minimizing Life Cycle Cost for Subsonic Commercial Aircraft, *Journal of Aircraft*, **27** (2), Feb., 139-145.

Kaplan, R. S., 1989, Management Accounting for Advanced Technological Environments, *Science*, **245** (25), Aug., 819-823.

Kendall, M. G., and Stuart, A., 1961, *The Advanced Theory of Statistics-Volume 2*, Charles Griffin & Company, London,.

Keys, L. K., 1990, System Life Cycle Engineering and DF'X', *IEEE Transactions on Components, Hybrids and Manufacturing Technology*, **13** (1), March, 83-93.

Kirkpatrick, A. T. and Elleson, J. S., 1996, *Cold Air Distribution System Design Guide*, Atlanta , ASHRAE Inc.

Knight, W. A., 1991, Design for Manufacture Analysis: Early Estimates of Tool Costs for Sintered Parts, *Annals of the CIRP*, **40**, Part 1, 131-134.

Kriwet, A., Zussman, E. and Seliger, G., 1995, Systematic Integration of Design for Recycling into Product Design, *International Journal of Production Economics*, **38**, 15-22.

Lind, N. C., 1983, Modelling of Uncertainty in Discrete Dynamical Systems, *Applied Mathematical Modelling*, **7**, June, 146-152.

Lurie, P. M. and Goldberg, M. S., 1998, An Approximate Method for Sampling Correlated Random Variables from Partially-Specified Distributions, *Management Science*, **44** (2), Feb., 203-218

Marks, M. D., Eubanks, C. F. and Ishii, K., 1993, Life-Cycle Clumping of Product Design for Ownership and Retirement, *Design Theory and Methodology, ASME*, DE-Vol. 53, 83-90.

McNichols, G. R., 1983, Uncertainties of LCC Predictions, *Electronics Systems Effectiveness and Life Cycle Costing*, NATO ASI Series, **F**, ed. J. K. Skwirzynski, Springer-Verlag, Berlin, 583-594.

Michalewicz, Z., Dipankar, D., Le Riche, R. G. and Schoenauer, M., 1996, Evolutionary Algorithms for Constrained Engineering Problems, *Computers in Industrial Engineering*, **30** (4), 851-870.

Noble, J. S. and Tanchoco, J. M. A., 1990, Concurrent Design and Economic Justification in Developing a Product, *International Journal of Production Research*, **28** (7), 1225-1238.

Ostwald, P. F., 1974, *Cost Estimating for Engineering and Management*, Prentice Hall.

Panchalingam, G. and Harr, M. E., 1994, Modelling of Many Correlated and Skewed Random Variables, *Applied Mathematical Modelling*, **18**, Nov., 635-640.

Pugh, S., 1974, Manufacturing Cost Information-The Needs of the Engineering Designer, *Information Systems for Designers*, Southampton, UK, Paper 12, 1-8

Rahmeyer, W. J., 1999a, Pressure Loss coefficients of Threaded and Forged Weld Pipe Fittings for Ells, Reducing Ells, and Pipe Reducers, *ASHRAE Transactions*, **105**(2).

Rahmeyer, W. J., 1999, Pressure Loss Coefficients of Pipe Fittings for Threaded and Forged Weld Pipe Tees, *ASHRAE Transactions*, **105**(2).

Ralescu, S. S. and Sun, S., 1993, Necessary and Sufficient Conditions for the Asymptotic Normality of Perturbed Sample Quantiles, *Journal of Statistical Planning and Inference*, **35**, 55-64.

Ravindran, A., Phillips, D. T., and Solberg, J. J., 1987, *Operations Research-Principles and Practice*, 2nd Edition, John Wiley & Sons.

Rosenblueth, E., 1975, Point Estimates for Probability Moments, *Proceedings of the National Academy of Science*, **72** (10), Oct., 3812-3814.

Sheather, S. J. and Marron, J. S. 1990 Kernel Quantile Estimators, *Journal of the American Statistical Association*, **85** (410), 410-416.

Shields, M. D. and Young, S. M., 1991, Managing Product Life Cycle Costs: An Organizational Model, *Cost Management*, Fall, 39-52.

Tsal, R. J., Behls, H.F. and Mangel, R., 1988a, T-Method Duct Design, Part I: Optimization Theory, *ASHRAE Transactions*, **94** (2), 90-111.

Tsal, R. J., Behls, H.F. and Mangel, R., 1988b, T-Method Duct Design, Part II: Calculation Procedure and Economic Analysis, *ASHRAE Transactions*, **94** (2), 112-150.

Tzemos, S. and Dippold, D., 1986, Stochastic Cost Estimating in Repository Life-Cycle Cost Analysis, *Proceedings of the Annual Meeting of the Nuclear Materials Management*, New Orleans, LA, USA, **15**, June, 279-290.

Uher, T. E., 1996, A Probabilistic Cost Estimating Model, *Cost Engineering*, **38** (1), 33-40.

Weirda, L. S., 1988, Product Cost-Estimation by the Designer, *Engineering Costs and Production Economics*, **13**, 189-198.

Wilson, R. L., 1986, Operations and Support Cost Model for New Product Concept Development, *Proceedings of the 8th Annual Conference on Components and Industrial Engineering*, 128-131.

Winter, B. B., 1973, Strong Uniform Consistency of Integrals of Density Estimator, *The Canadian Journal of Statistics*, **1** (2), 247-253.

Yang, S-S., 1995, A Smooth Nonparametric Estimator of a Quantile Function, *Journal of the American Statistical Association*, **80** (392), 1004-1011.

Zelterman, D., 1990, Smooth Nonparametric Estimation of the Quantile Function, *Journal of Statistical Planning and Inference*, **26**, 339-352.

Zenger, D., Dewhurst, P., 1988, Early Assessment of Tooling Costs in the Design of Sheet Metal Parts, *Department of Mechanical, University of Rhode Island, Report #29*, Aug.

Zhi, H., 1993, Simulation Analysis in Project Life Cycle Cost, *Cost Engineering*, **35** (12), 33-40.

Appendix A

A.1 Calculation of the Friction Factor

The fan pressure depends on the duct pressure drops ΔP, which is calculated using the Darcy-Weisbach equation,

$$\Delta P = \left(\frac{fL}{D_h} + \sum C \right) \frac{\rho V^2}{2} \qquad \text{(A.1)}$$

where

f Friction factor

D_h Hydraulic diameter (m)

$\sum C$ Summation of dynamic friction loss coefficient for duct fittings within the duct section

ρ Air density(kg/m^3)

V Air flow velocity in duct (m/sec).

The equation used to find the dimensionless friction factor was developed by Altshul and modified by Tsal [ASHRAE 1997] to

$$f' = 0.11 \left(\frac{\varepsilon}{D_h} + \frac{68}{\mathrm{Re}} \right)^{0.25}, \qquad \text{(A.2)}$$

$$f = \begin{cases} f' & \text{if } 0.018 \le f' \\ 0.85f' + 0.0028 & \text{otherwise} \end{cases} \tag{A.3}$$

where

ε Absolute roughness factor

Re Reynolds number.

The Reynolds number can be calculated using

$$\text{Re} = \frac{D_h V}{\upsilon} \tag{A.4}$$

where

υ Kinematic viscosity of the air.

For standard air, the Reynolds number can be calculated using

$$\text{Re} = 66400 D_h V \,. \tag{A.5}$$

Appendix B

B.1 Determination of Equivalent Optimal Rectangular Duct

Let us consider two ducts with no fittings, one rectangular and the other circular with the same flow rate, Q and length, L.

The optimal diameter and width (assuming the height is fixed) are given be Equations (B.1) and (B.2) respectively.

$$D^6 = \frac{40 \times \rho}{\pi^3}\left(\frac{Z}{10^3 S_d}\right) Q^3 f_C \tag{B.1}$$

$$W^4 = \frac{\rho}{2}\left(\frac{Z}{10^3 S_d}\right)\frac{Q^3 f_R (2W + 3H)}{4H^3} \tag{B.2}$$

It is reasonable to expect that the cost of transporting a given amount of air from on point to another to be similar for both the circular and the rectangular duct. This was the principle behind the suggestion in [Carriere et al. 1998] to assess the performance of a duct based on the *Cost Factor*. Thus the optimal duct diameter given by Equation (B.1) and the optimal width given by Equations (B.1) and (B.2) should give the same cost providing the predetermined height of the rectangular duct satisfies

$$D >> 2H/\pi . \tag{B.3}$$

From Equations (B.1) and (B.2),

$$\frac{8W^4H^3}{(2W+3H)f_R} = \rho\frac{Z}{10^3 S_d}Q^3, \tag{B.4}$$

and

$$\frac{\pi^3 D^6}{40 f_C} = \rho\frac{Z}{10^3 S_d}Q^3. \tag{B.5}$$

Combining Equations (B.4) and (B.5) gives

$$\frac{8W^4H^3}{(2W+3H)f_R} = \frac{\pi^3 D^6}{40 f_C},$$

$$\Rightarrow D = 1.476\left(\frac{8W^4H^3}{2W+3H}\cdot\frac{f_C}{f_R}\right)^{1/6}. \tag{B.6}$$

For the circular duct, assuming standard conditions gives,

$$f_C' = 0.11\left(\frac{\varepsilon}{D}+\frac{1.024}{DV_C}\right)^{0.25}$$

and for the rectangular duct,

$$f_R' = 0.11\left(\frac{\varepsilon}{D_h}+\frac{1.024}{D_hV_R}\right)^{0.25}.$$

If the two ducts have the same frictional factor, then

$$\frac{\varepsilon}{D}+\frac{1.024}{DV_C} = \frac{\varepsilon}{D_h}+\frac{1.024}{D_hV_R},$$

which will imply that

$$D = D_h \Rightarrow D = \frac{2HW}{H+W} \tag{B.7}$$

and

$$V_C = V_R \Rightarrow \frac{\pi D^2}{4} = HW \Rightarrow D = 1.1284\sqrt{HW} = D_v. \quad \text{(B.8)}$$

If Equations (B.7) and (B.8) hold, then

$$D = \frac{\pi D^2}{2(H+W)} \Rightarrow D = \frac{2(H+W)}{\pi} = D_c. \quad \text{(B.9)}$$

Thus a circular duct will have the same frictional factor as a rectangular duct for a give flow rate if the hydraulic (D_h), equivalent-by-cost (D_c) and equivalent-by-velocity (D_v) diameters of the rectangular duct and the diameter of the circular duct are all equal (i.e. $D_h=D_c=D_v=D$). That is, the two ducts will have the same frictional pressure losses. In other words, a rectangular duct will have the same energy and material costs and subsequently, similar life-cycle costs as a circular duct with the same flow rates if their frictional factors are the same. If the initial assumption holds then, $f_C=f_R$, and Equation (B.5) reduces to

$$D = 1.476\left(\frac{8W^4H^3}{2W+3H}\right)^{1/6}. \quad \text{(B.10)}$$

Hence, once a round duct has been selected from the Enhanced Friction Chart, it is reasonable to select a rectangular duct which will satisfy Equation (B.10).

Appendix C

C.1 Genetic Algorithm

Genetic Algorithms (GAs) are an optimization strategy in which points or states in the design space are analogous to organisms in a process of evolution by natural selection [Chapman et al. 1993]. Each candidate solution or state in the optimization problem is represented by a coded representation of design attributes that is analogous to a *chromosome*. Thus a chromosome completely defines one functional design. The goodness of an individual chromosome as a solution to the problem is evaluated as its *fitness*. Initially, GAs use problem knowledge to randomly generate a *population* of functional designs or chromosomes. Operations such as *selection*, *crossover* and *mutation* are then performed on the chromosomes to produce the next generation of designs with improved fitness. This process of creating new designs for a new generation is analogous to biological reproduction. The population of design alternatives evolves over a series of generations until a terminal criterion is met (i.e. until a good solution is obtained). Unlike most optimization algorithms, GAs work with a collection of design solutions rather that with a single solution with the search proceeding along different paths simultaneously. In this way, GAs can find optimal or relatively good sub-optimal solutions in a short computation time.

A schematic for a very simple HVAC air duct system is shown in Figure C.1 (the flow rates are not indicated). This system has four duct sections or elements numbered 1 through 4 and 2 airflow paths comprised of sections (4 and 3), and (4, 2 and 1). Duct elements 4, 3 and 1 are specified round ducts and duct 2 is rectangular. This duct system design problem is used below to explain some of the terminology introduced above and illustrate the genetic algorithm method of design.

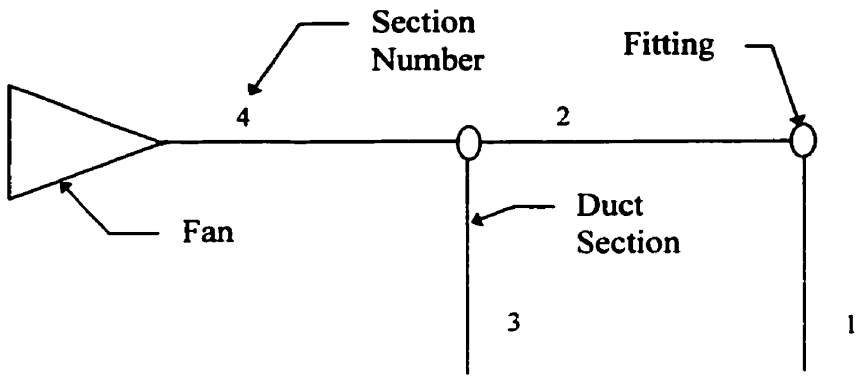

Figure C.1: A Simple Duct System.

C.2 Chromosome

Each design or chromosome is comprised of a string or set of *genes*, which may be visualized as boxes arranged in a linear fashion as shown in Figure C.2. The position of each gene is called the *locus* of the gene and its value, the parameter being optimized, is called the *allele*. The five gene values (alleles) in this example correspond to the diameter or sizes of each of the four duct elements and because duct element number 2 is rectangular, it requires two genes to specify its size (height and width), giving a total of

five genes. This value can be any real number (integers are used in Figure C.2); however, GA traditionalist insist on a binary representation. Thus, Figure C.2 can also be represented as in Figure C.3 where each parameter is now represented by 4 binary digits, one group of four genes.

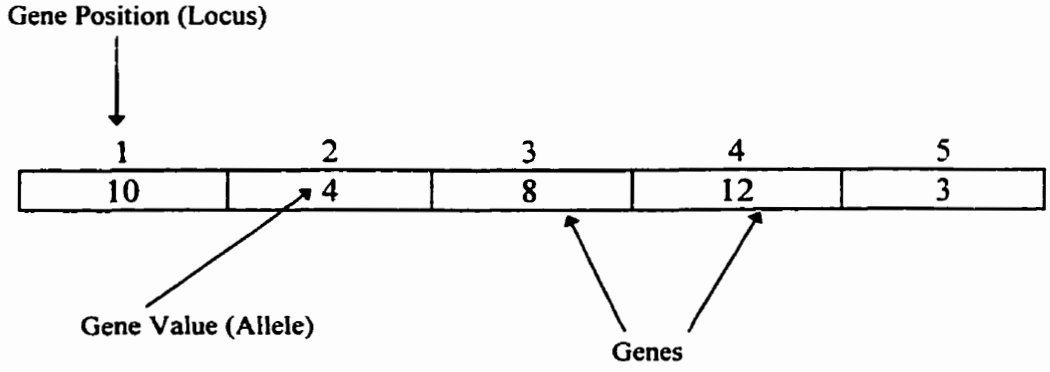

Figure C.2: Chromosome Representation as a String.

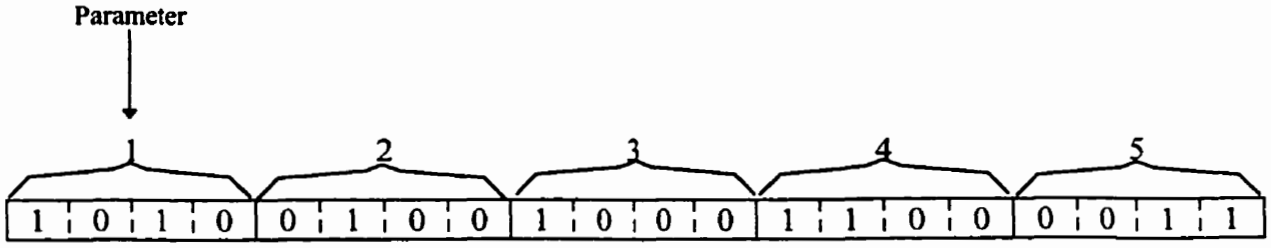

Figure C.3: Binary Representation of the Allele for the Genes of the Chromosome in Figure C.2.

In this simple air duct design, the issues of material and fan selection are not treated. A chromosome should thus represent the specification of the duct sizes and must be of size equal to the number of sizes to be determined. If it is assumed that the height of the rectangular duct is predetermined by architectural constraints, then the set of genes in each chromosome is defined to be equal to the total number of duct sections with each gene value representing the size of that duct section. It is not necessary that the gene position correspond to the duct section number as was seen in the design problem in Chapter 5. The next question that needs to be addressed is the allele or value of each gene. This value should represent the true duct size in some manner. A couple of representations are proposed. The first maps numbers onto a table containing the duct sizes. For the duct system in Figure C.1, a table of acceptable duct sizes for round ducts (Table C.1) and rectangular ducts (Table C.2) are developed with each duct in each table having a unique index (ducts in different tables can have the same index).

Table C.1: Available Round Duct Sizes

Index	1	2	3	4
Diameter(m)	0.100	0.125	0.150	0.175

Table C.2: Available Rectangular Duct Sizes

Index	1	2	3	4
Width(m)*	0.150	0.175	0.200	0.225

*Assuming that the height of the duct section is predetermined.

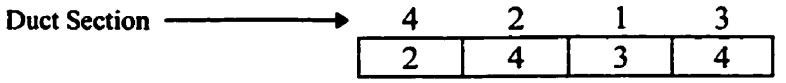

Figure C.4: Sample Chromosome.

Now, if the alleles represent these indices, then given any chromosome, the duct size is uniquely determined by the tables. For the chromosome shown in Figure C.4, the duct sizes are, Duct 4, 0.125m; Duct 3, 0.175m; Duct 2, 0.225m; and Duct 1, 0.150m. It should be noted that the gene positions do not correspond to the duct numbers. The second representation deals with the case where the duct sizes are in a given interval and increase by jumps of a constant value at the end of each interval. In this case, the tabular representation is not needed since a gene value can be transformed to a corresponding duct size by Equation (C.1). This is the representation adopted in the implementation of GA for the duct design problem in this thesis.

$$Duct\ Size = Lower\ Limit + (Size\ Jump \times Gene\ Value) \qquad (C.1)$$

Using this representation, and assuming that the *Lower Limit* equals 0.1m and the *Size Jump* equals 0.025m, the chromosome corresponding to the same sizes as that of Figure C.4 is as shown in Figure C.5.

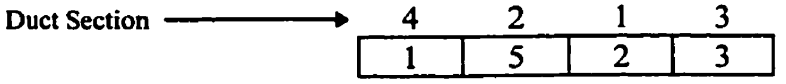

Figure C.5: Sample Chromosome Based on Equation (C.1).

In the foregoing, it was assumed that the design decision in this case was just the duct sizes, however, material selection could also have been included. In that case, two four-gene chromosomes end-to-end are used with the first set of genes dedicated to the duct sizes and the other to the materials. Given that 1, 2, 3 and 4 represent aluminum, fiber glass, galvanized steel and PVC plastic pipe respectively, then the chromosome in Figure C.6 represents a design with the following specifications: Duct 4, 0.125m aluminum duct; Duct 3, 0.175m PVC plastic pipe duct; Duct 2, 0.225m fiber glass duct; and Duct 1, 0.150m fiber glass duct. Likewise, the chromosome can be expanded to incorporate other attributes of the duct section such as external insulation.

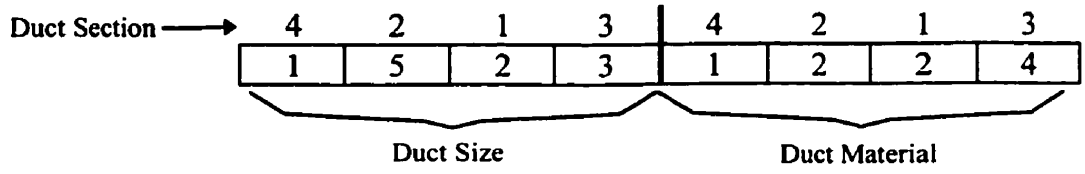

Figure C.6: Sample Two-Parameter Chromosome.

C.3 Fitness Function

The fitness is an expression of how well a particular chromosome satisfies the constraints of a problem and the designer's requirements. The fitness is used to screen the chromosomes in one generation set and decide which ones will proceed to the next generation and which ones will be used for crossover (breeding) and gene mutation. In

most instances, the value of the objective function is a good measure of the fitness of the chromosomes. Unfortunately the objective function value of a chromosome alone is not always useful for guiding a genetic search. For example, in combinatorial optimization problems, where there are many constraints, most points in the search space often represent invalid chromosomes and hence have zero "real" value. For a GA to be effective in this case, a fitness function where the fitness of an invalid chromosome is viewed in terms of its potential to lead to a valid chromosome must be invented [Beasley et al. 1993].

C.4 Selection, Crossover and Mutation

In GAs, as in life, design solutions (organisms) are generated and tested in succeeding generations with offspring designs arising from parent designs. Individuals for the next generation are selected according to their fitness values and the next generation is generated through the processes of crossover and mutation. An individual may persist across several generations (and experience longevity) or be replaced in the very next generation (and experience early death) depending on the generation-gap policy effected by the modeler [Chan et al. 1996]. That is, the choice of killing off or retaining members of one generation in the succeeding generation depends on the designer. Crossover is an operation in which two chromosomes are combined to produce one or two new offspring chromosomes. This allows offspring chromosomes or designs to retain traits from parent designs. A crossover operation is shown in Figure C.7. Table C.3 shows the

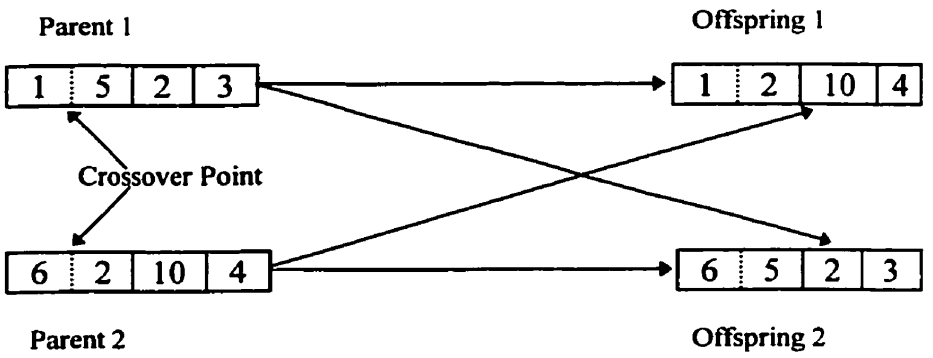

Figure C.7: The Crossover Operation on Chromosomes.

Table C.3: Duct Sizes Corresponding to Crossover Operation.

Duct Section	Duct Sizes			
	Parent 1	Parent 2	Offspring 1	Offspring 2
1	0.150	0.350	0.350	0.150
2	0.225	0.150	0.150	0.225
3	0.175	0.200	0.200	0.175
4	0.125	0.250	0.125	0.250

corresponding duct sizes of the two parents and two offspring designs. The two original designs (parents) in this crossover would have come from a population of size say, 10 (i.e. 10 designs). As already mentioned, the choice (selection) of a chromosome to undergo these operations depend on its fitness. Generally, the fitter the chromosome, the higher the chances it will be selected. However, lesser fit chromosomes are sometimes kept to ensure some of their desirable properties are maintained in the population pool. Since the total number of designs should be maintained through each generation, the two

new designs (offspring) will have to replace (1) both parents, (2) one parent and one of the other 8 designs, or (3) two of the other 8 designs.

Figure C.8 depicts the mutation operation. Mutation involves randomly changing one or more alleles of a chromosome. This is less frequent than crossover but has the potential to yield radically improved designs over parent designs and also to allow the search to escape from points that may be local optimums but not necessarily a global optimum. In this case, a new design is obtained by changing the size of duct section 1 from 0.150m to 0.175m.

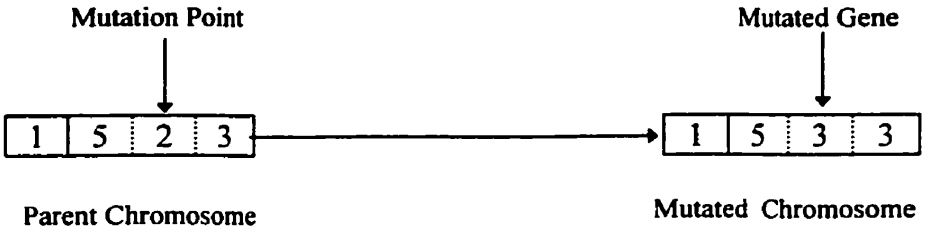

Figure C.8: The Mutation Operation on a Chromosome.

Appendix D

D.1 Duct Fittings

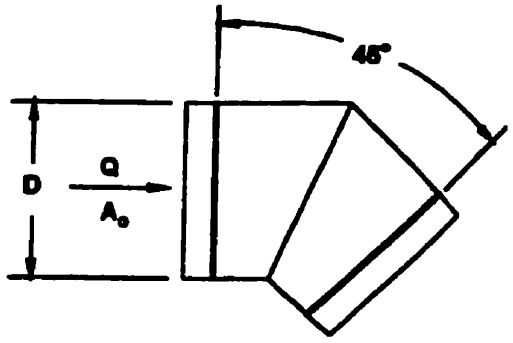

CD3-17 Elbow, Mitered, 45 Degree

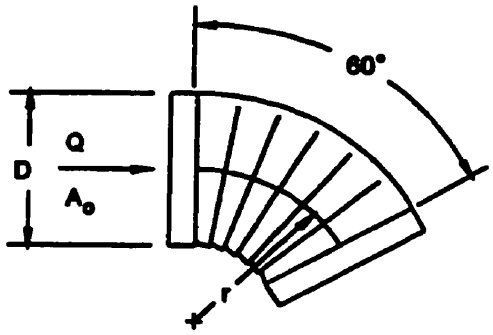

CD3-6 Elbow, Pleated, 60 Degree, r/D = 1.5

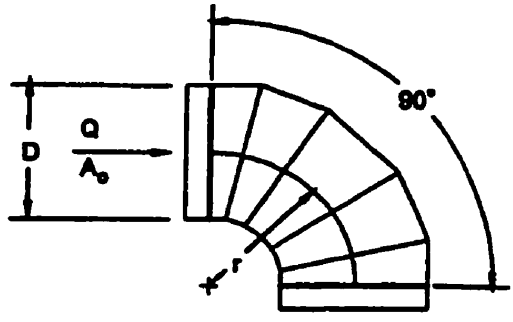

CD3-9 Elbow, 5 Gore, 90 Degree, r/D = 1.5

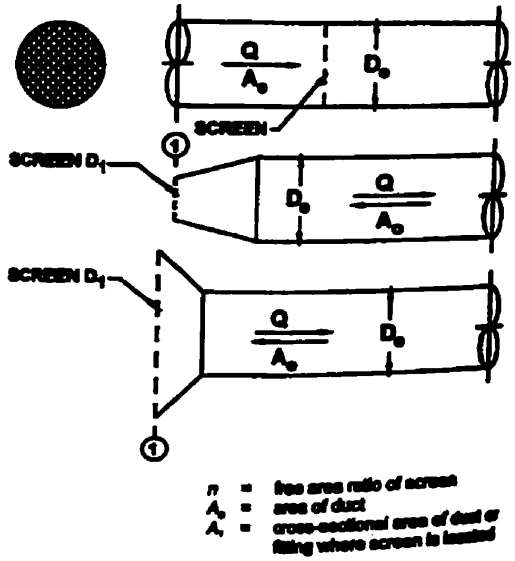

CD6-1 Screen (Only)

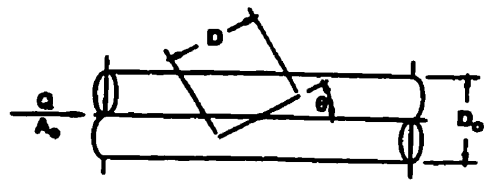

CD9-1 Damper, Butterfly

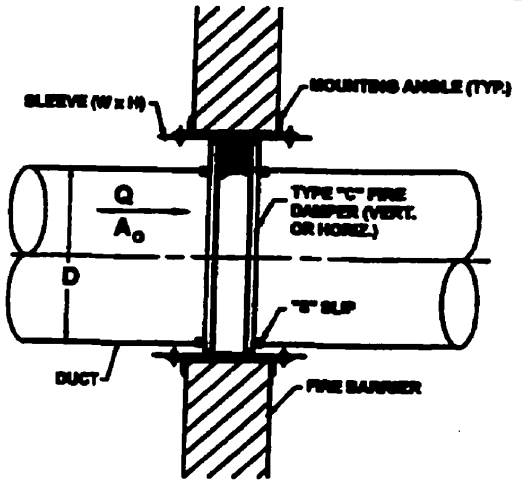

CD9-3 Fire Damper, Curtain Type, Type C

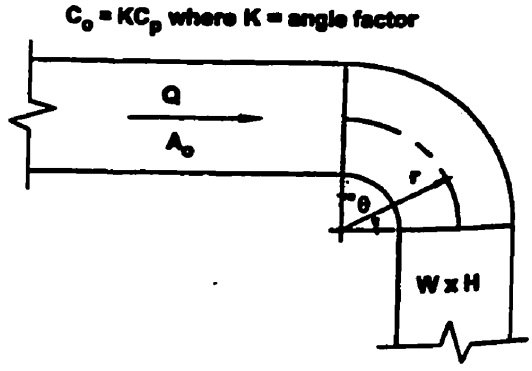

CR3-1 Elbow, Smooth Radius, without Vanes

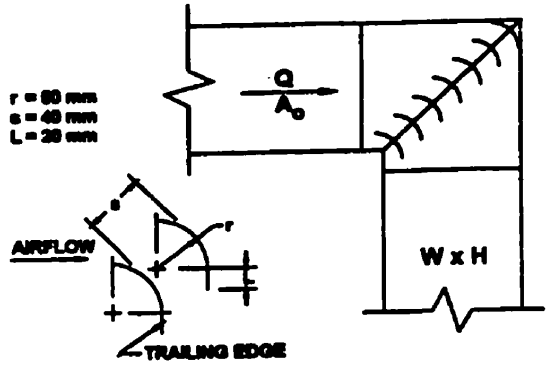

CR3-10 Elbow, Mitered, 90 Degree, Single-Thickness Vanes (Design 2)

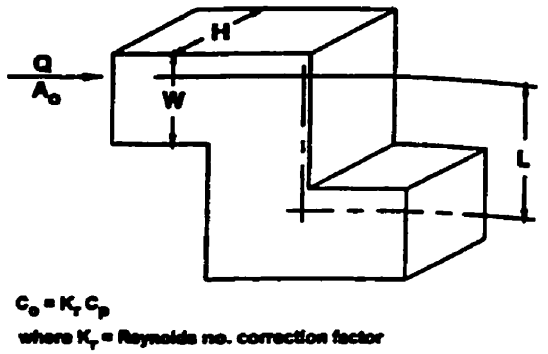

CR3-17 Elbow, Z Shaped

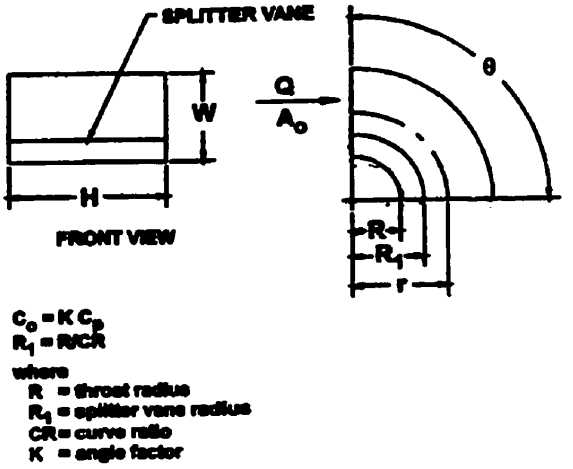

CR3-3 Elbow, Smooth Radius, One Splitter Vane Throat Radius/Width Ratio, R/W

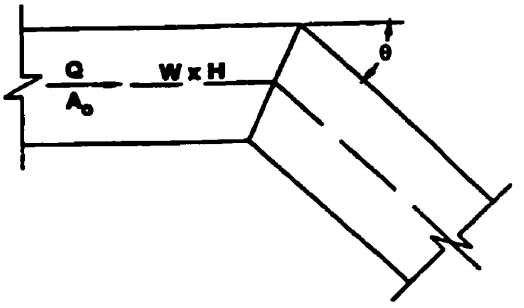

CR3-6 Elbow, Mitered

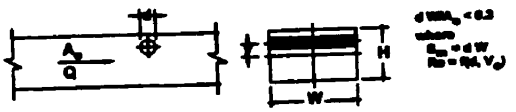

CR6-4 Obstruction, Smooth Cylinder in Rectangular Duct

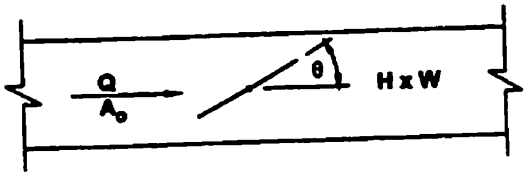

CR9-1 Damper, Butterfly

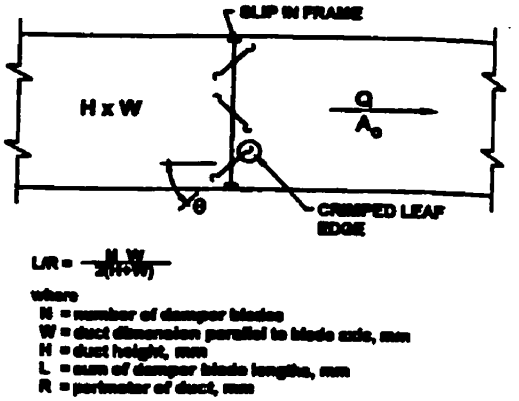

CR9-4 Damper, Opposed Blades

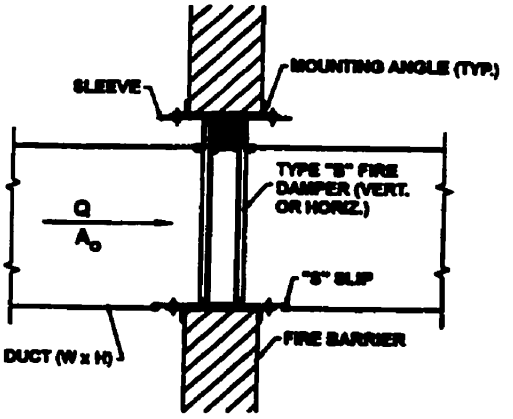

CR9-6 Fire Damper, Curtain Type, Type B

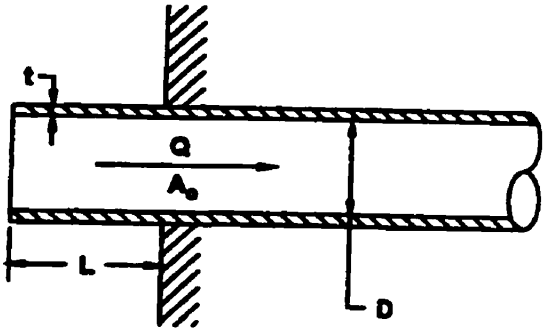

ED1-1 Duct Mounted in Wall

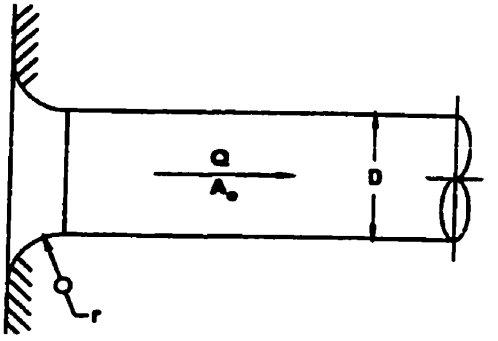

ED1-3 Bellmouth, with Wall

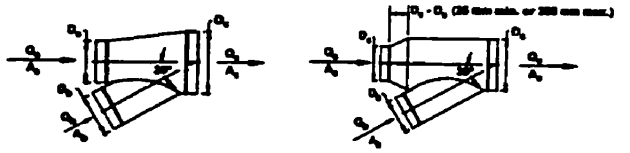

ED5-1 Wye, 30 Degree, Converging

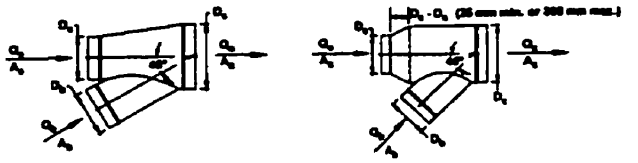

ED5-2 Wye, 45 Degree, Converging

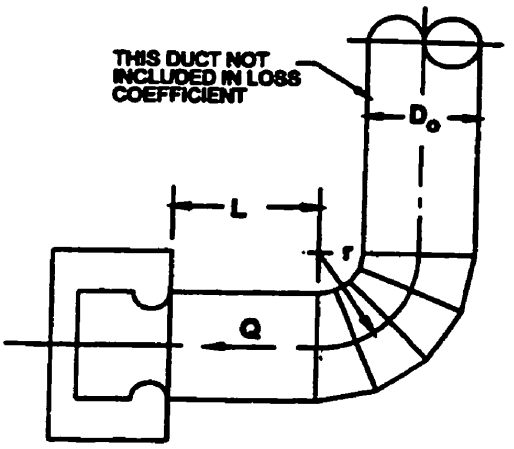

ED7-2 Fan Inlet, Centrifugal, SWSI, with 4-Gore Elbow

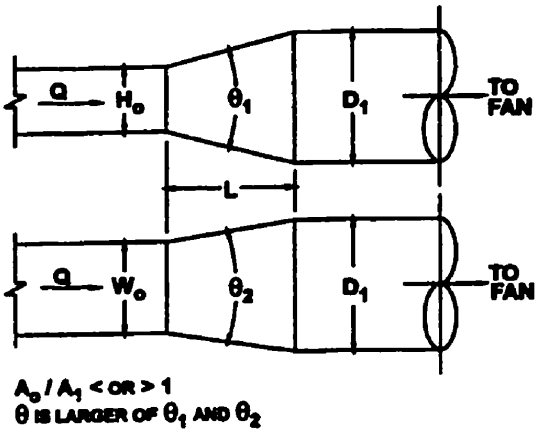

ER4-3 Transition, Rectangular to Round, Exhaust/Return Systems

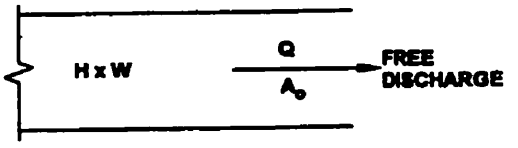

SR2-1 Abrupt Exit

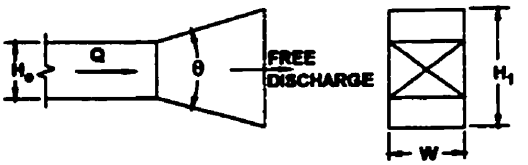

SR2-3 Plain Diffuser (Two Sides Parallel), Free Discharge

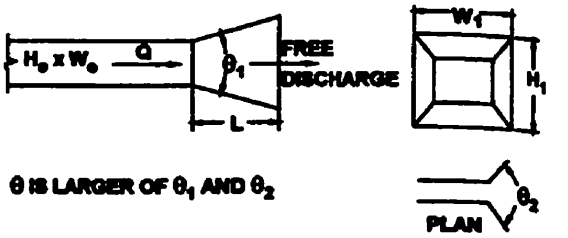

SR2-5 Pyramidal Diffuser, Free Discharge

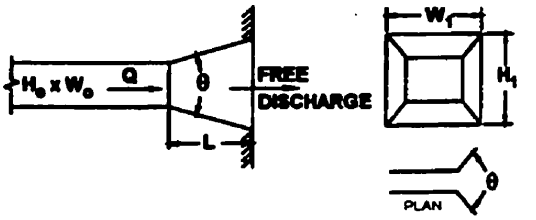

SR2-6 Pyramidal Diffuser, with Wall

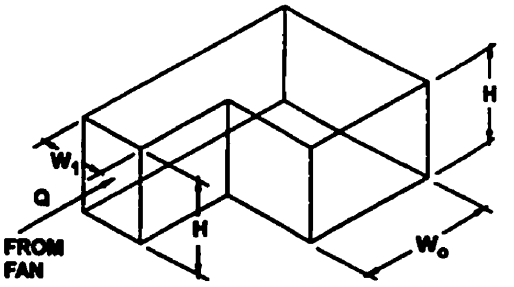

SR3-1 Elbow, 90 Degree, Variable Inlet/Outlet Areas, Supply Air Systems

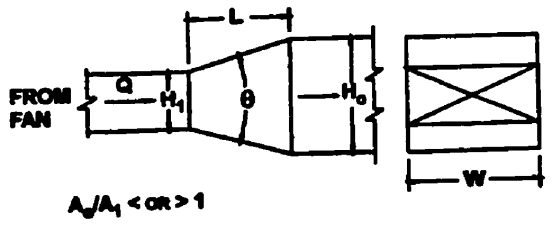

SR4-1 Transition, Rectangular, Two Sides Parallel, Symmetrical, Supply Air Systems

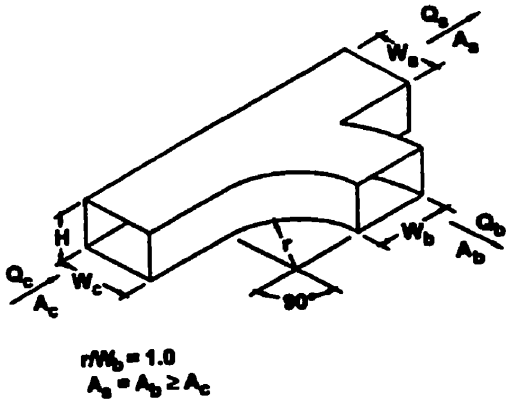

SR5-1 Smooth Radius Wye of the Type As + Ab > or = Ac, Branch 90 Degrees to Main, Diverging

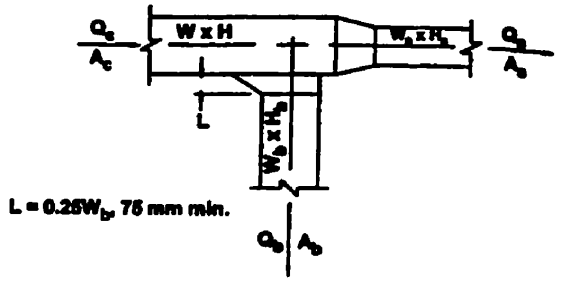

SR5-13 Tee, 45 Degree Entry Branch, Diverging

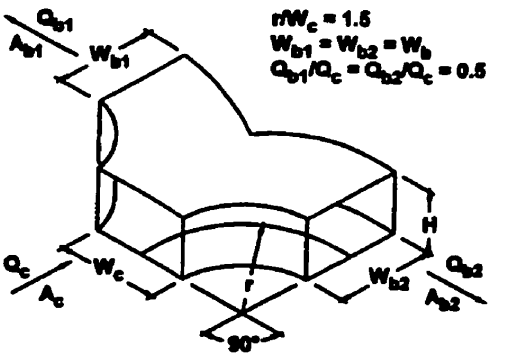

SR5-14 Wye, Symmetrical, Dovetail, Qb/Qc = 0.5, Diverging

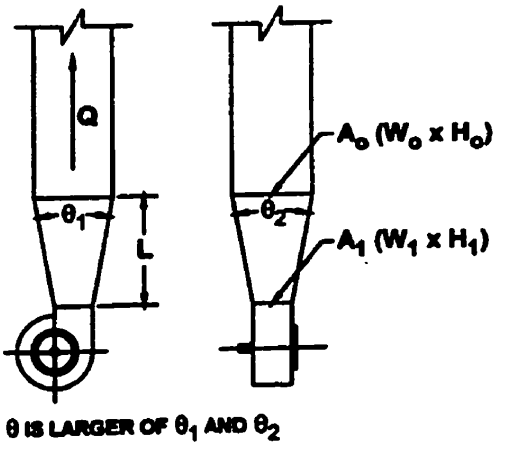

SR7-17 Pyramidal Diffuser at Centrifugal Fan Outlet with Ductwork